NASA TECHNICAL MEMORANDUM

NASA TM X-2581

NASA TM X-2581

SUPERSONIC AERODYNAMIC CHARACTERISTICS OF A LIFTING-BODY ORBITER MODEL WITH A BLUNTED DELTA PLANFORM AT MACH 2.30 TO 4.60

by A. B. Blair, Jr.

Langley Research Center
Hampton, Va. 23365

NATIONAL AERONAUTICS AND SPACE ADMINISTRATION • WASHINGTON, D. C. • SEPTEMBER 1972

1. Report No.	2. Government Accession No.	3. Recipient's Catalog No.
NASA TM X-2581		

4. Title and Subtitle	5. Report Date
SUPERSONIC AERODYNAMIC CHARACTERISTICS OF A LIFTING-BODY ORBITER MODEL WITH A BLUNTED DELTA PLANFORM AT MACH 2.30 TO 4.60	September 1972
	6. Performing Organization Code

7. Author(s)	8. Performing Organization Report No.
A. B. Blair, Jr.	L-8366
	10. Work Unit No.
9. Performing Organization Name and Address	502-37-01-01
NASA Langley Research Center Hampton, Va. 23365	11. Contract or Grant No.
	13. Type of Report and Period Covered
12. Sponsoring Agency Name and Address	Technical Memorandum
National Aeronautics and Space Administration Washington, D.C. 20546	14. Sponsoring Agency Code

15. Supplementary Notes

16. Abstract

An investigation has been made in the Langley Unitary Plan wind tunnel to determine the aerodynamic characteristics of a lifting-body orbiter model with a blunted delta planform.

The model was tested at Mach numbers from 2.30 to 4.60, at nominal angles of attack from -4^{o} to 60^{o} and angles of sideslip from -4^{o} to 10^{o}, and at a Reynolds number of 8.2×10^{6} per meter (2.5×10^{6} per foot).

17. Key Words (Suggested by Author(s))	18. Distribution Statement
Space shuttle vehicle Blunted delta planform	Unclassified – Unlimited

19. Security Classif. (of this report)	20. Security Classif. (of this page)	21. No. of Pages	22. Price*
Unclassified	Unclassified	93	$3.00

*For sale by the National Technical Information Service, Springfield, Virginia 22151

SUPERSONIC AERODYNAMIC CHARACTERISTICS OF A LIFTING-BODY ORBITER MODEL WITH A BLUNTED DELTA PLANFORM AT MACH 2.30 TO 4.60

By A. B. Blair, Jr.
Langley Research Center

SUMMARY

An investigation has been made in the Langley Unitary Plan wind tunnel to determine the aerodynamic characteristics of a lifting-body orbiter model with a blunted delta planform. The model was tested at Mach numbers from 2.30 to 4.60, at nominal angles of attack from -4° to 60° and angles of sideslip from -4° to 10°, and at a Reynolds number of 8.2×10^6 per meter (2.5×10^6 per foot).

For the moment-center location of the model, the data indicate some regions of static instability and nonlinear aerodynamic characteristics. The longitudinal aerodynamics are strongly influenced by the basic body alone, which is highly unstable and nonlinear with increasing lift coefficient or angle of attack. In addition, because of the negative values of pitching moment at zero lift for the model with controls neutral, stable trim points were not obtainable with either the upper or lower flaps except at low angles of attack at the lower test Mach numbers. The model is directionally unstable except for some small regions of marginal stability at high angles of attack.

INTRODUCTION

The National Aeronautics and Space Administration is currently developing a reusable space shuttle system capable of economically placing large payloads in near-earth orbit. As part of this general effort, the Langley Research Center has conducted a wind-tunnel investigation to determine the supersonic aerodynamic characteristics of a lifting-body orbiter model with a blunted delta planform.

The investigation was conducted in the Langley Unitary Plan wind tunnel at Mach numbers from 2.30 to 4.60, at nominal angles of attack from -4° to 60° and angles of sideslip from -4° to 10°, and at a Reynolds number of 8.2×10^6 per meter (2.5×10^6 per foot).

SYMBOLS

The results of this investigation are presented as force and moment coefficients, with the longitudinal characteristics referred to the stability-axis system and the lateral characteristics referred to the body-axis system. The moment reference point is located at 78 percent of the reference length. Values are given in both the International System of Units (SI) and U.S. Customary Units. The measurements and calculations were made in U.S. Customary Units. The symbols are defined as follows:

C_D drag coefficient, $\frac{\text{Drag}}{qS}$

$C_{D,b}$ base drag coefficient, $\frac{\text{Base drag}}{qS}$

$C_{D,c}$ balance-chamber drag coefficient, $\frac{\text{Chamber drag}}{qS}$

$C_{D,o}$ drag coefficient at zero lift

C_L lift coefficient, $\frac{\text{Lift}}{qS}$

C_{L_α} lift-curve slope near $\alpha = 0^o$, per degree

C_l rolling-moment coefficient, $\frac{\text{Rolling moment}}{qSl}$

C_{l_β} effective-dihedral parameter, $\left(\frac{\Delta C_l}{\Delta \beta}\right)_{\beta=0^o,4^o}$, per degree

C_m pitching-moment coefficient, $\frac{\text{Pitching moment}}{qSl}$

$C_{m_{C_L}}$ longitudinal-stability parameter

$C_{m_{\delta_E}}$ pitching-moment effectiveness of lower flap at $\alpha = 0^o$, per degree

C_n yawing-moment coefficient, $\frac{\text{Yawing moment}}{qSl}$

C_{n_β} directional-stability parameter, $\left(\frac{\Delta C_n}{\Delta \beta}\right)_{\beta=0^o,4^o}$, per degree

C_Y side-force coefficient, $\frac{\text{Side force}}{qS}$

C_{Y_β} side-force parameter, $\left(\frac{\Delta C_Y}{\Delta \beta}\right)_{\beta=0^o,4^o}$, per degree

L/D lift-drag ratio

l reference length, 44.50 centimeters (17.52 inches)

M Mach number

q free-stream dynamic pressure

S reference planform area, 0.0429 meter^2 (0.4621 foot^2)

α angle of attack measured with respect to the zero water line of the model, degrees

β angle of sideslip, degrees

δ_E deflection of the lower flap (positive when trailing edge is down), degrees

δ_F deflection of the upper flaps (negative when trailing edge is up), degrees

δ_R deflection of the rudders, positive with trailing edge left, degrees

Subscripts:

L left

max maximum

R right

Abbreviations:

BL buttock line

MS model station

WL water line

Model components:

B_4 blunted delta planform body

E_3 lower trailing-edge trim flap

F_{16} fin

APPARATUS AND TESTS

Tunnel

Tests were conducted in the high Mach number test section of the Langley Unitary Plan wind tunnel, which is a variable-pressure, continuous-flow facility. The test section is about 2.13 meters (7 feet) long and 1.22 meters (4 feet) square. The nozzle leading to the test section is of the asymmetric sliding-block type which permits a continuous variation in test-section Mach number from about 2.3 to 4.7.

Model

Details of the 0.01-scale orbiter model are shown in figure 1 and table I. Photographs of the model are shown in figure 2. The model consisted of a lifting body having a blunted delta planform with a flat lower surface (B_4) and a set of aft-mounted contoured fins. The model had upper and lower body flaps for pitch control. The upper flaps (two panels) were located between the fins and were deflected in only one direction (trailing edge up). When undeflected they faired smoothly into the upper body surface. The lower trailing-edge trim flap (E_3) was hinged 1.22 cm (0.48 in.) aft of the base of the lower body surface. Each of the two fins (F_{16}) has a movable upper rear portion which was used for rudder control.

Unless otherwise noted model components of all configurations in the present report were designated $B_4F_{16}E_3$ with the left and right rudders deflected (trailing edges inboard 20^o).

Test Conditions

Tests were performed at a Reynolds number of 8.2×10^6 per meter (2.5×10^6 per foot) at the following tunnel conditions:

M	Stagnation temperature		Stagnation pressure	
	K	^{o}F	kN/m^2	psfa
2.30	339	150	91.69	1915
2.96	339	150	129.80	2711
3.95	353	175	231.21	4829
4.60	353	175	311.56	6507

The dewpoint temperature measured at stagnation pressure was maintained below 239 K (-30^{o} F) to assure negligible condensation effects. No transition trips were placed on the model because it was believed that the bluntness of the model would assure a turbulent boundary layer. Schlieren photographs of the model at various Mach numbers are presented as figure 3.

Measurements

Aerodynamic forces and moments were measured by means of an internally mounted six-component electrical strain-gage balance. The balance was rigidly fastened to a sting-support system. Pressure measurements were made within the fuselage balance chamber and at the model base.

Corrections

Angles of attack have been corrected for tunnel-flow misalinement. Angles of attack and sideslip have been corrected for deflection of the sting and balance due to aerodynamic loads. The drag data have not been adjusted to account for the pressures acting over the model base, and therefore represent total drag values. Typical values of the measured base and chamber drag coefficients are presented in figure 4.

PRESENTATION OF RESULTS

DISCUSSION

For the moment center location of the model, the data indicate some regions of static instability and nonlinear aerodynamic characteristics. The longitudinal aerodynamics are strongly influenced by the basic body alone, which is highly unstable and nonlinear with increasing C_L or α. (See fig. 12.) The addition of the lower surface flap (which adds area aft) improves the inherently poor body-alone longitudinal characteristics, and the addition of the fins (which also add aft planform area) provides some further longitudinal-stability improvement. The configuration is directionally unstable, except for some small regions of marginal stability at high angles of attack, and this unstable trait is also a result of the basic instability of the body. (See fig. 17.)

The longitudinal control requirements are complicated by a negative value of C_m at zero lift attributable to the aerodynamics of the basic model with controls neutral. The lower flap is effective in producing pitching moments but the variation of C_m with flap deflections is very nonlinear and is manifested as an increase in effectiveness with increasing C_L or α. However, for the moment center location of the model, no stable trim points were obtainable except at some low angles of attack with $\delta_F = -40^o$ (figs. 5 to 7). The upper surface flap deflection produces an increment of C_m at low α but the effectiveness diminishes rapidly with increasing M and C_L or α, and under some conditions the deflection is completely ineffective. Because of the initial negative values of C_m, stable trim points were not obtainable with the upper flap control except at some low values of α at the lower test Mach numbers.

SUMMARY OF RESULTS

A wind-tunnel investigation has been conducted at Mach numbers from 2.30 to 4.60, at nominal angles of attack from -4° to 60° and angles of sideslip from -4° to 10°, to determine the static aerodynamic characteristics of a lifting-body orbiter model with a blunted delta planform.

For the moment-center location of the model, the data indicate some regions of static instability and nonlinear aerodynamic characteristics. The longitudinal aerodynamics are strongly influenced by the basic body alone, which is highly unstable and nonlinear with increasing lift coefficient or angle of attack. In addition, because of the negative values of pitching moment at zero lift for the model with controls neutral, stable trim points were not obtainable with either the upper or lower flaps except at low angles of attack at the lower test Mach numbers. The model is directionally unstable except for some small regions of marginal stability at high angles of attack.

Langley Research Center,
National Aeronautics and Space Administration,
Hampton, Va., August 24, 1972.

TABLE I.- GEOMETRIC CHARACTERISTICS OF COMPONENTS OF MODEL (0.01 SCALE)

Body, B_4 (blunted delta planform; nose, 2:1 ellipsoid)		
Length, cm (in.)	39.42	(15.52)
Maximum width, cm (in.)	20.47	(8.06)
Maximum depth, cm (in.)	6.93	(2.73)
Area:		
Reference planform, m^2 (ft^2)	0.0429	(0.4621)
Base, m^2 (ft^2)	0.0106	(0.1137)
Leading-edge sweep, deg	78	
Leading-edge radius:		
Forward, cm (in.)	1.22	(0.48)
Aft, cm (in.)	0.91	(0.36)
Overall length (includes lower flap), cm (in.)	46.28	(18.22)
Maximum width (includes fins), cm (in.)	28.14	(11.08)
Maximum depth (includes fins), cm (in.)	11.13	(4.38)
Reference length, cm (in.)	44.50	(17.52)
Split upper-surface flap		
Area, m^2 (ft^2)	0.0064	(0.0693)
Span (equivalent):		
Leading edge, cm (in.)	13.11	(5.16)
Trailing edge, cm (in.)	15.65	(6.16)
Sweep angle:		
Leading edge, deg	-28	
Trailing edge, deg	0	
Hinge line, deg	-28	
Chord:		
Inboard, cm (in.)	2.34	(0.92)
Outboard, cm (in.)	5.79	(2.28)
Lower trailing-edge flap, E_3		
Area, m^2 (ft^2)	0.0101	(0.1086)
Span (equivalent):		
Leading edge, cm (in.)	15.70	(6.18)
Trailing edge, cm (in.)	14.48	(5.70)

TABLE I.- GEOMETRIC CHARACTERISTICS OF COMPONENTS OF MODEL (0.01 SCALE) – Concluded

Sweepback angle:	
Leading edge, deg	0
Trailing edge, deg	0
Hinge line, deg	0
Chord, cm (in.)	6.81 (2.68)
Hinge line, MS, cm (in.)	45.72 (18.00)
Aft-mounted contoured fins, F_{16}	
Area (per fin), m^2 (ft^2)	0.0058 (0.0624)
Span (equivalent), both fins, cm (in.)	15.24 (6.00)
Aspect ratio	2.0
Taper ratio	0.5
Roll-out angle, deg	30
Toe-in angle:	
Root, deg	4
Tip, deg	0
Sweep angle:	
Leading edge, deg	39
Trailing edge, deg	9
0.25 chord, deg	33
Chords:	
Root, cm (in.)	10.16 (4.00)
Tip, cm (in.)	5.08 (2.00)
M.A.C., cm (in.)	7.93 (3.12)
Aerodynamic twist, deg	-4
Rudders	
Area (per panel), m^2 (ft^2)	0.0022 (0.0237)
Span (equivalent), cm (in.)	7.62 (3.00)
Sweepback angle:	
Leading edge, deg	14
Trailing edge, deg	9
Hinge line, deg	14
Chord:	
Inboard, cm (in.)	3.30 (1.30)
Outboard, cm (in.)	2.49 (0.98)

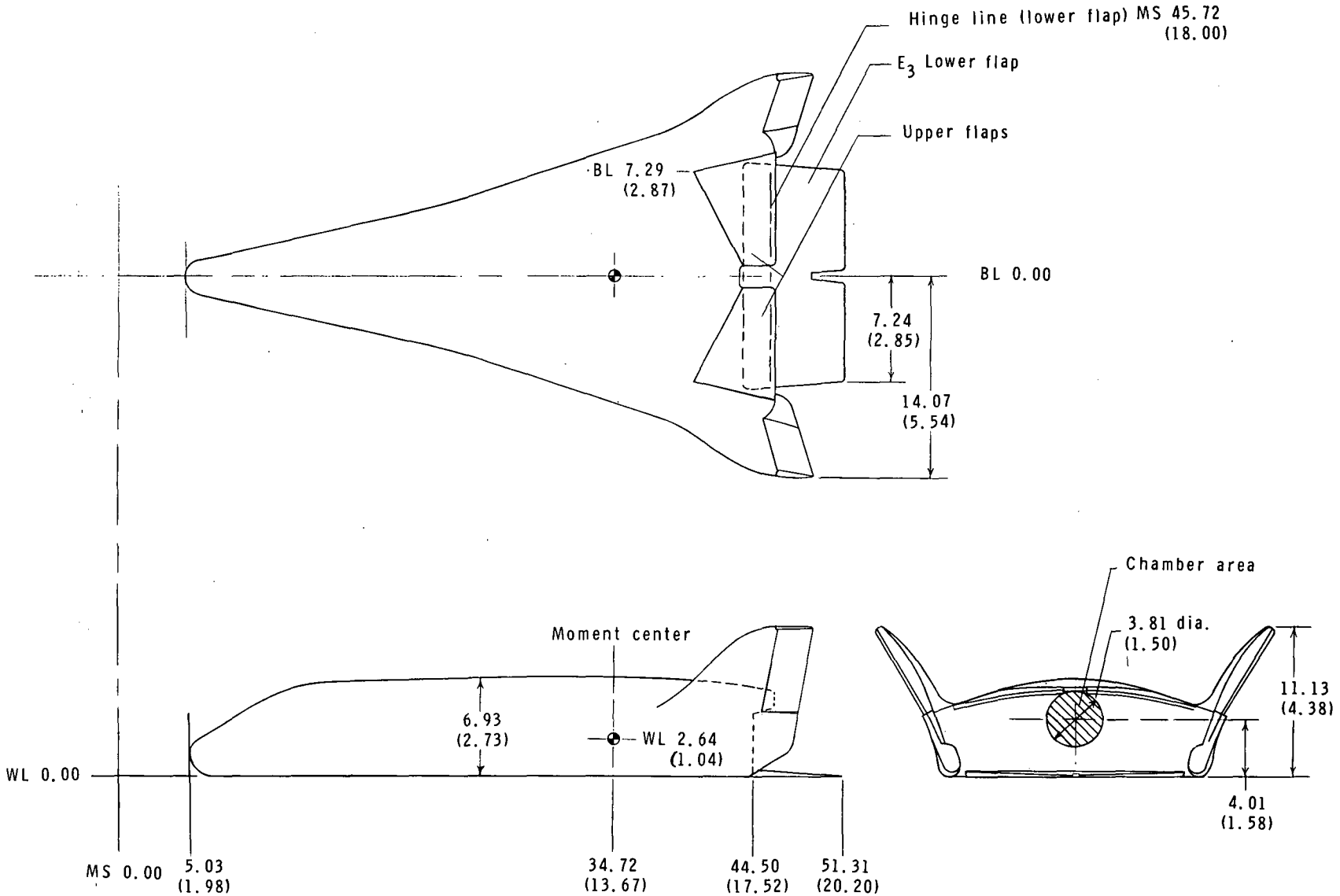

Figure 1.- Details of model. All dimensions are given in centimeters and parenthetically in inches.

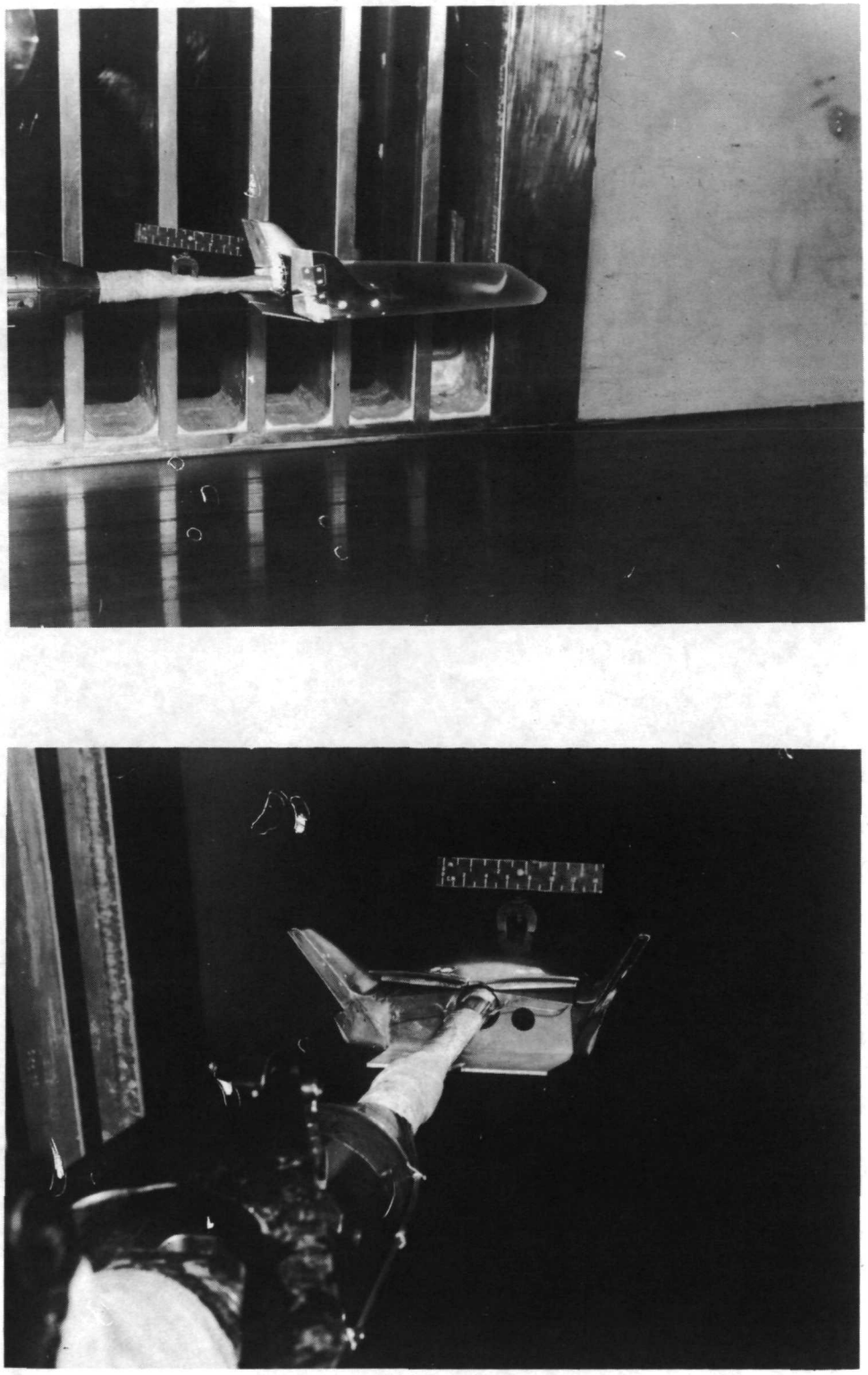

L-72-2486

Figure 2.- Photographs of model.

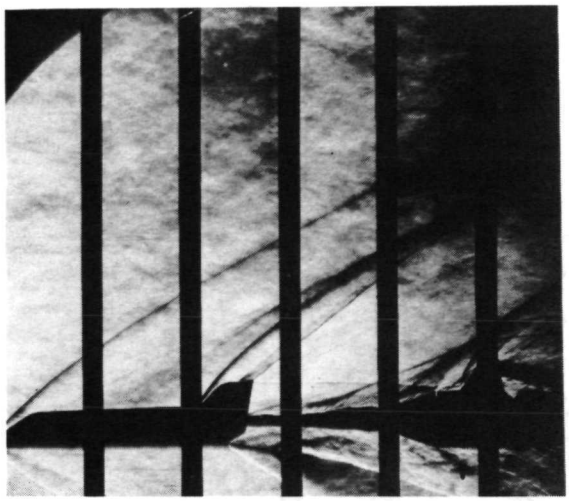

α = -0.3°.

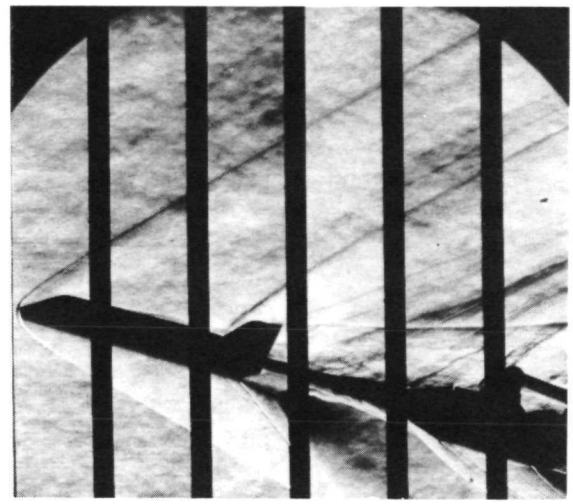

α = 16.6°

α = 33.7°

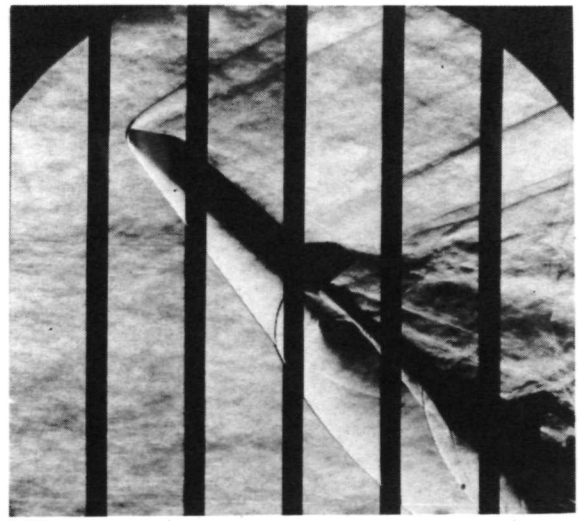

α = 42.3°

(a) M = 2.30.

Figure 3.- Schlieren photographs of the model. $\delta_E = 10^o$; $\delta_F = -20^o$.

α = -0.3°

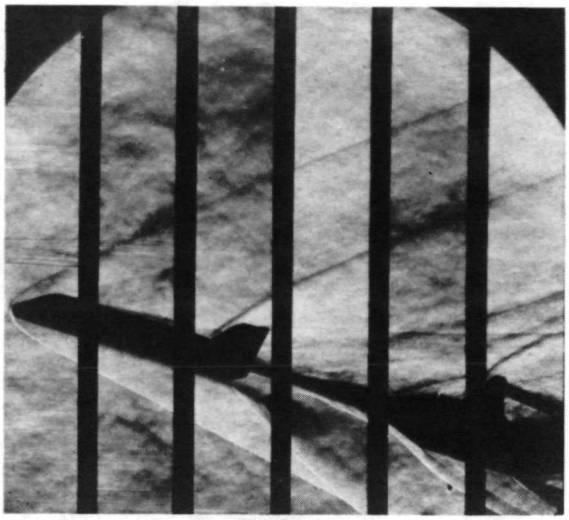

α = 16.4°

α = 33.2°

α = 47.0°

(b) M = 2.96.

Figure 3.- Continued.

α = 0.1°

α = 20.7°

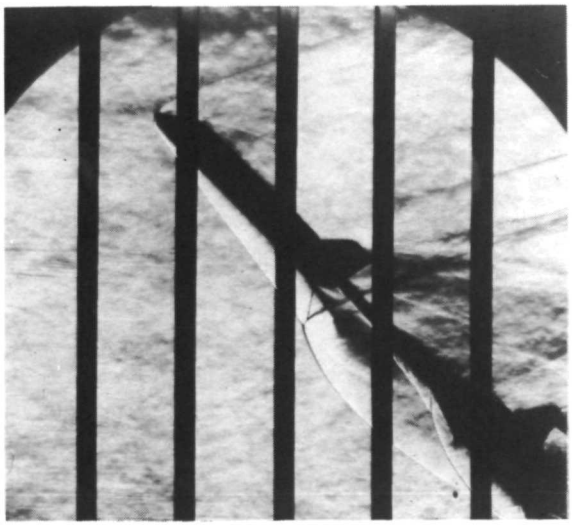

α = 46.6°

α = 61.3°

(c) M = 3.95.

Figure 3.- Continued.

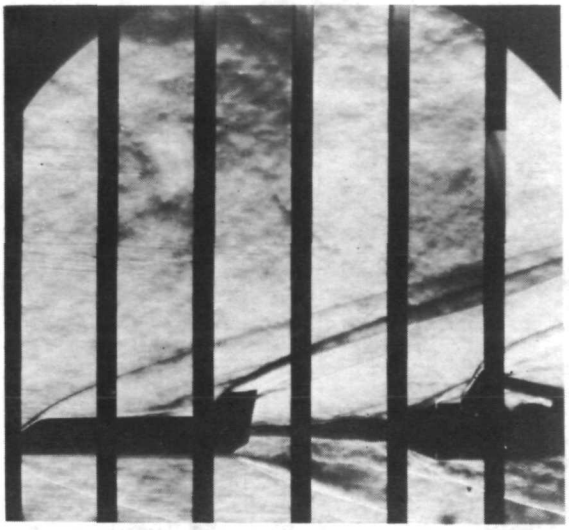

α = 0.2°

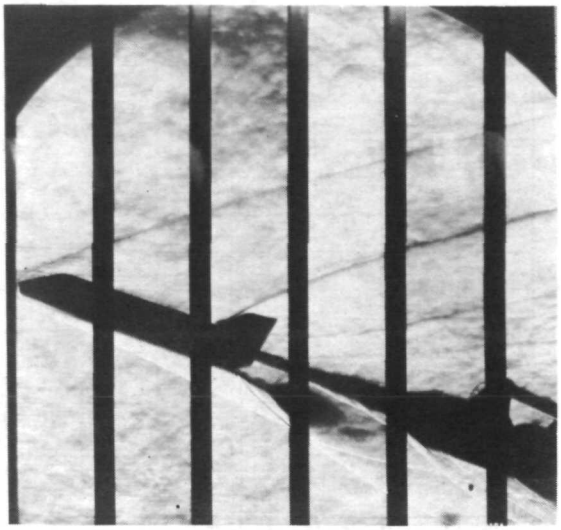

α = 20.7°

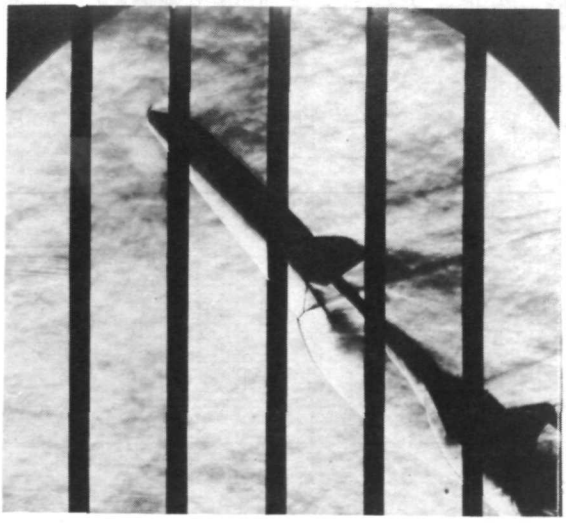

α = 46.6°

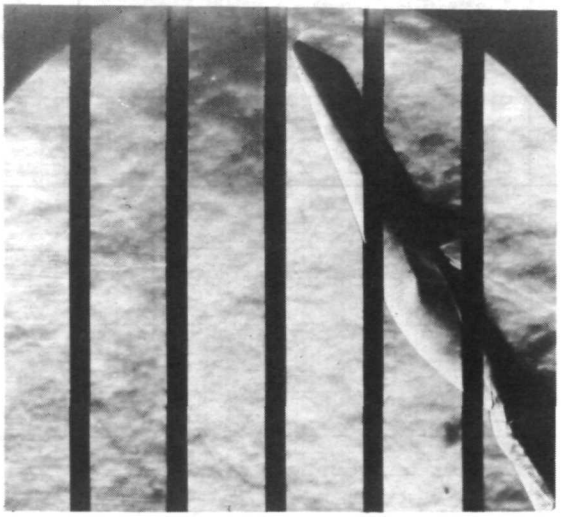

α = 60.7°

(d) M = 4.60.

Figure 3.- Concluded.

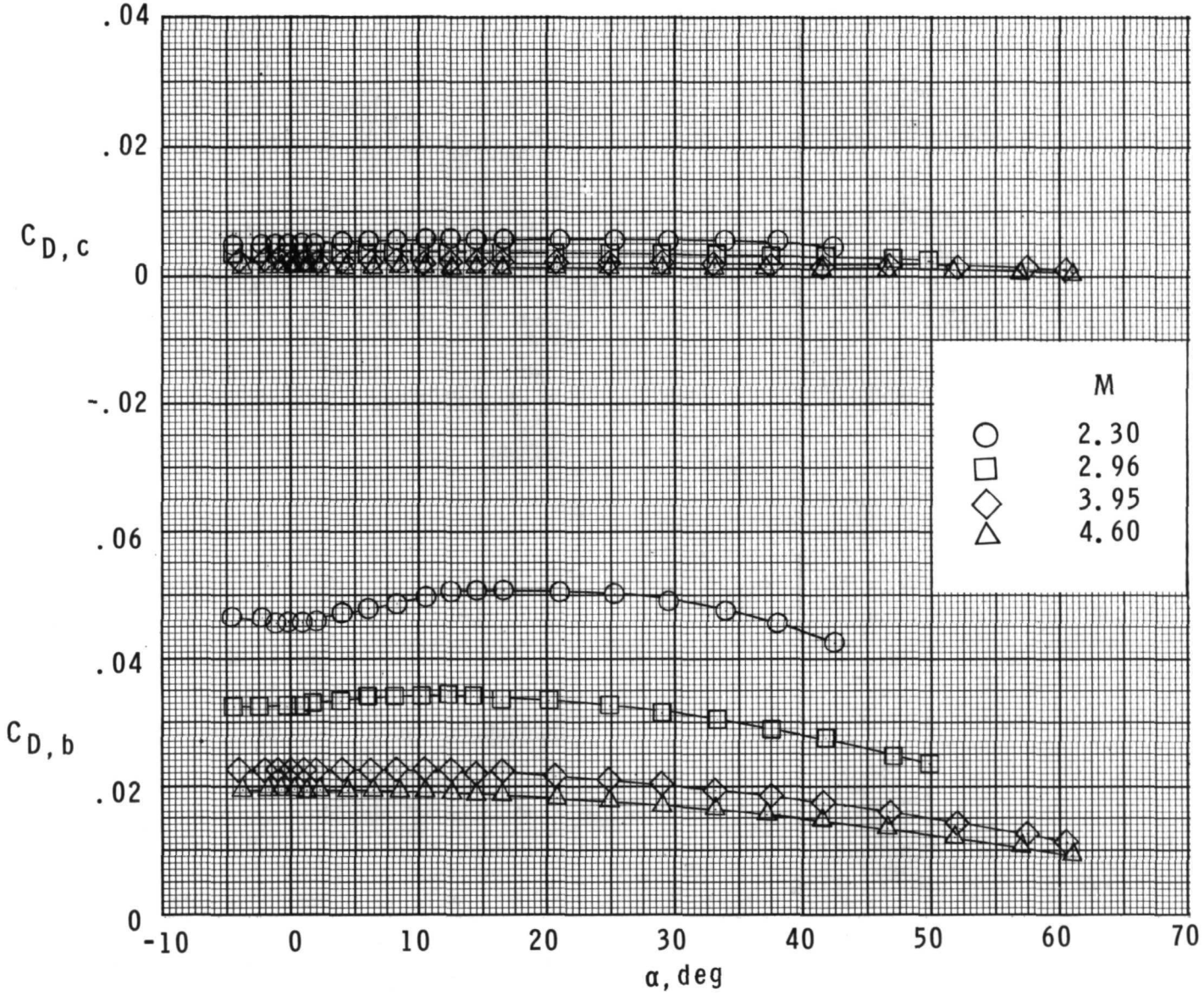

Figure 4.- Typical values of the base and chamber drag coefficients.

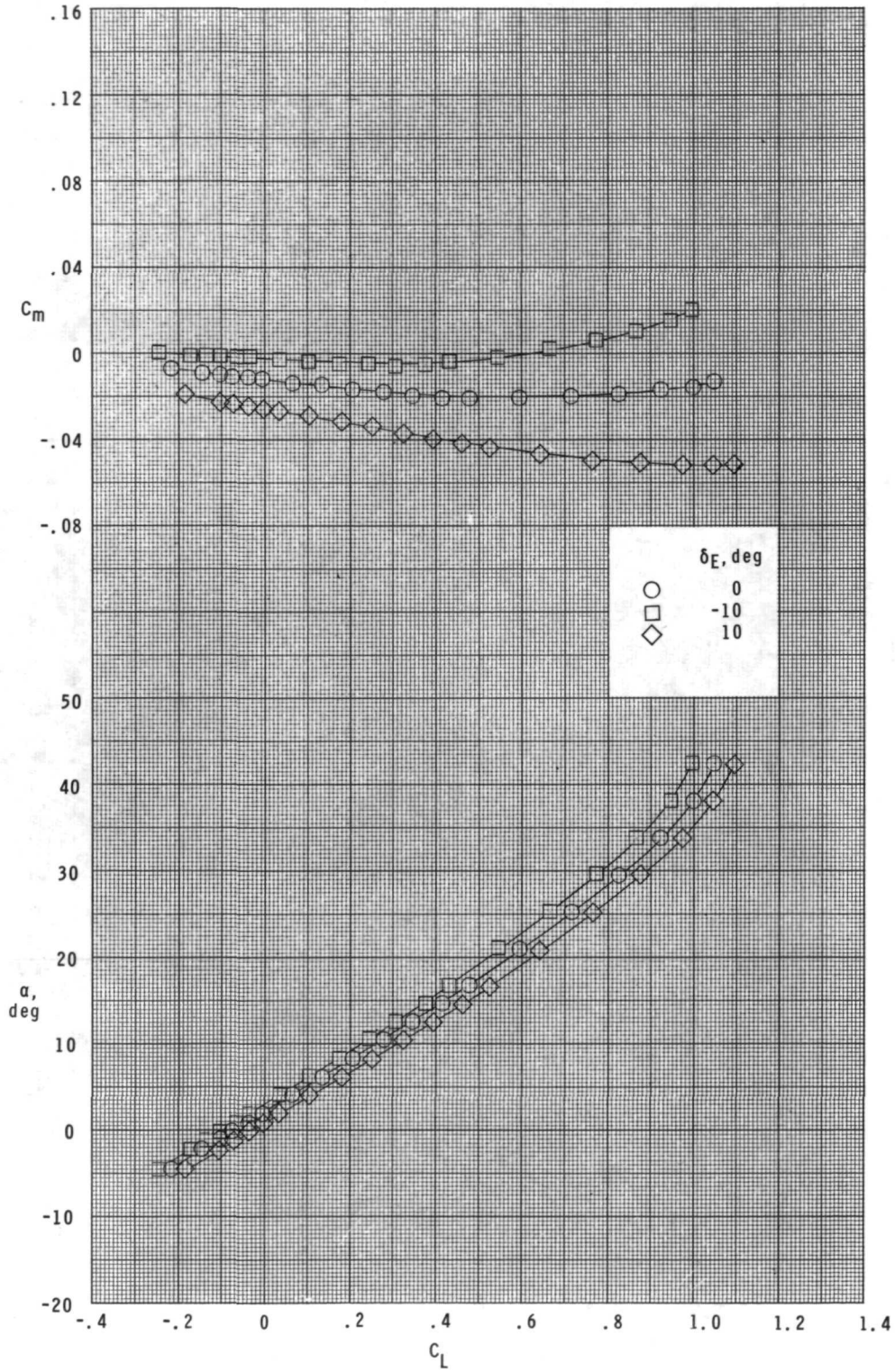

(a) M = 2.30.

Figure 5.- Effect of lower flap deflection on pitch characteristics. $\delta_F = -20^o$; $\delta_{R,L} = -20^o$; $\delta_{R,R} = +20^o$.

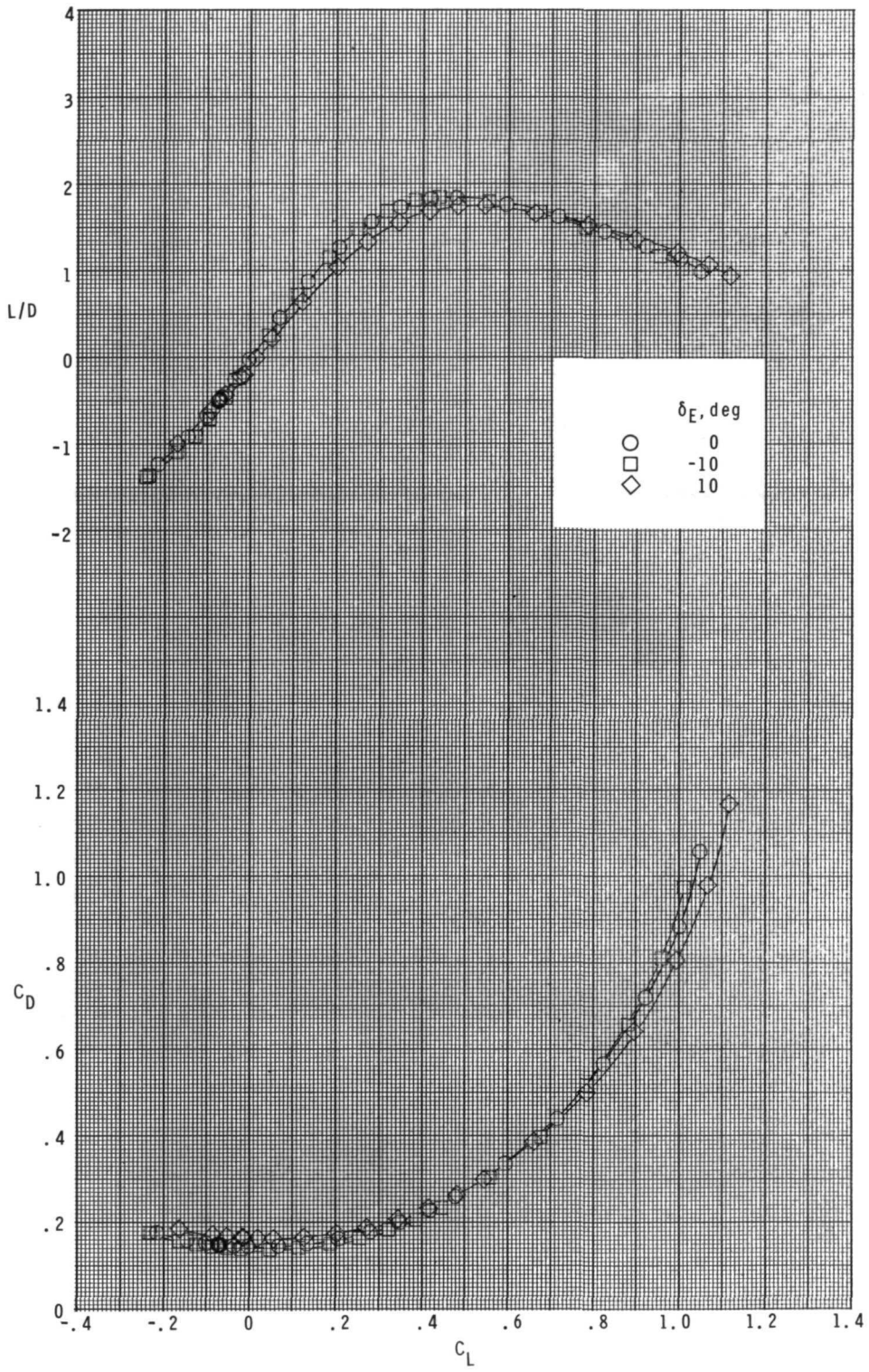

(a) Concluded.

Figure 5.- Continued.

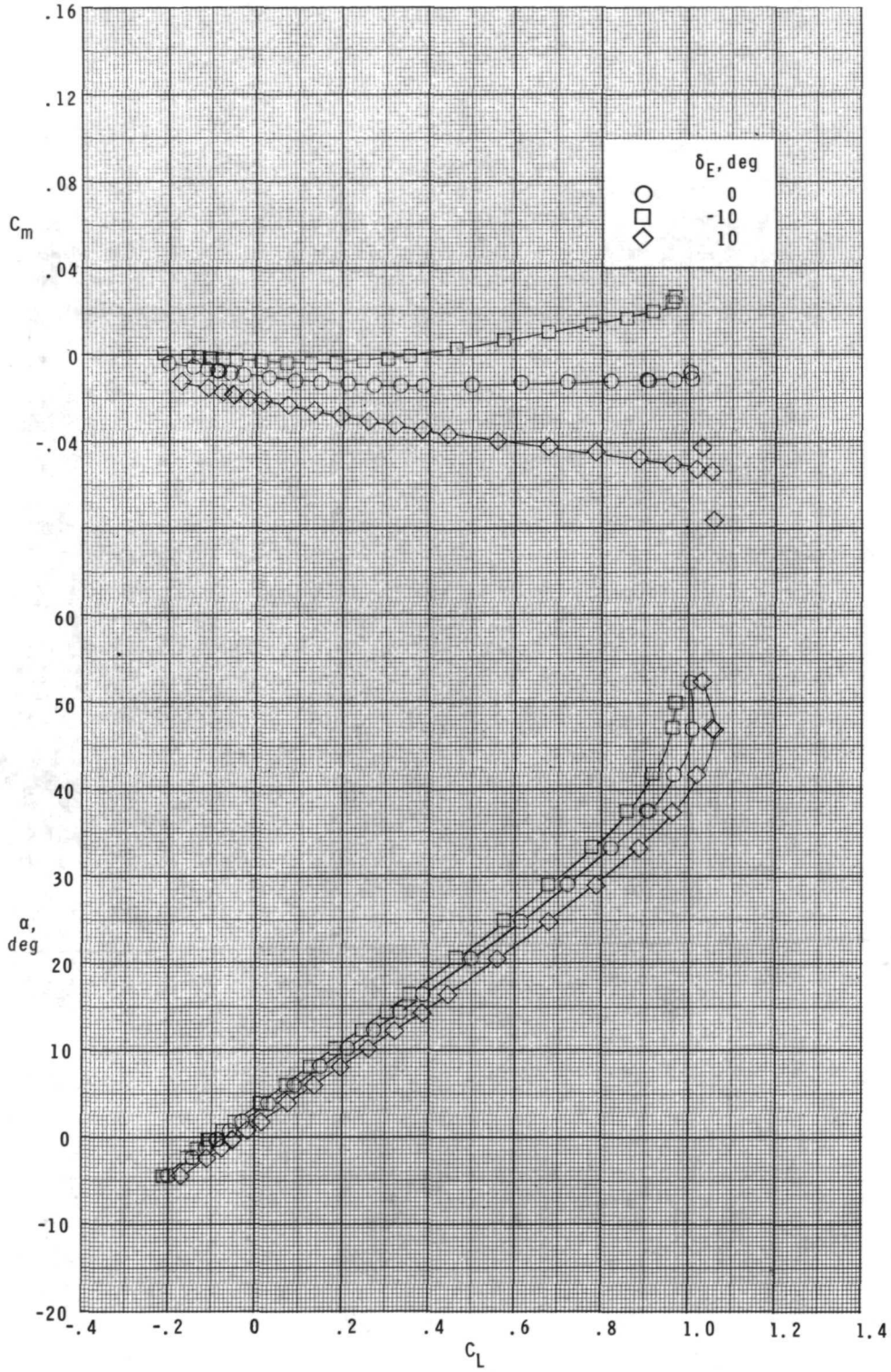

(b) M = 2.96.

Figure 5.- Continued.

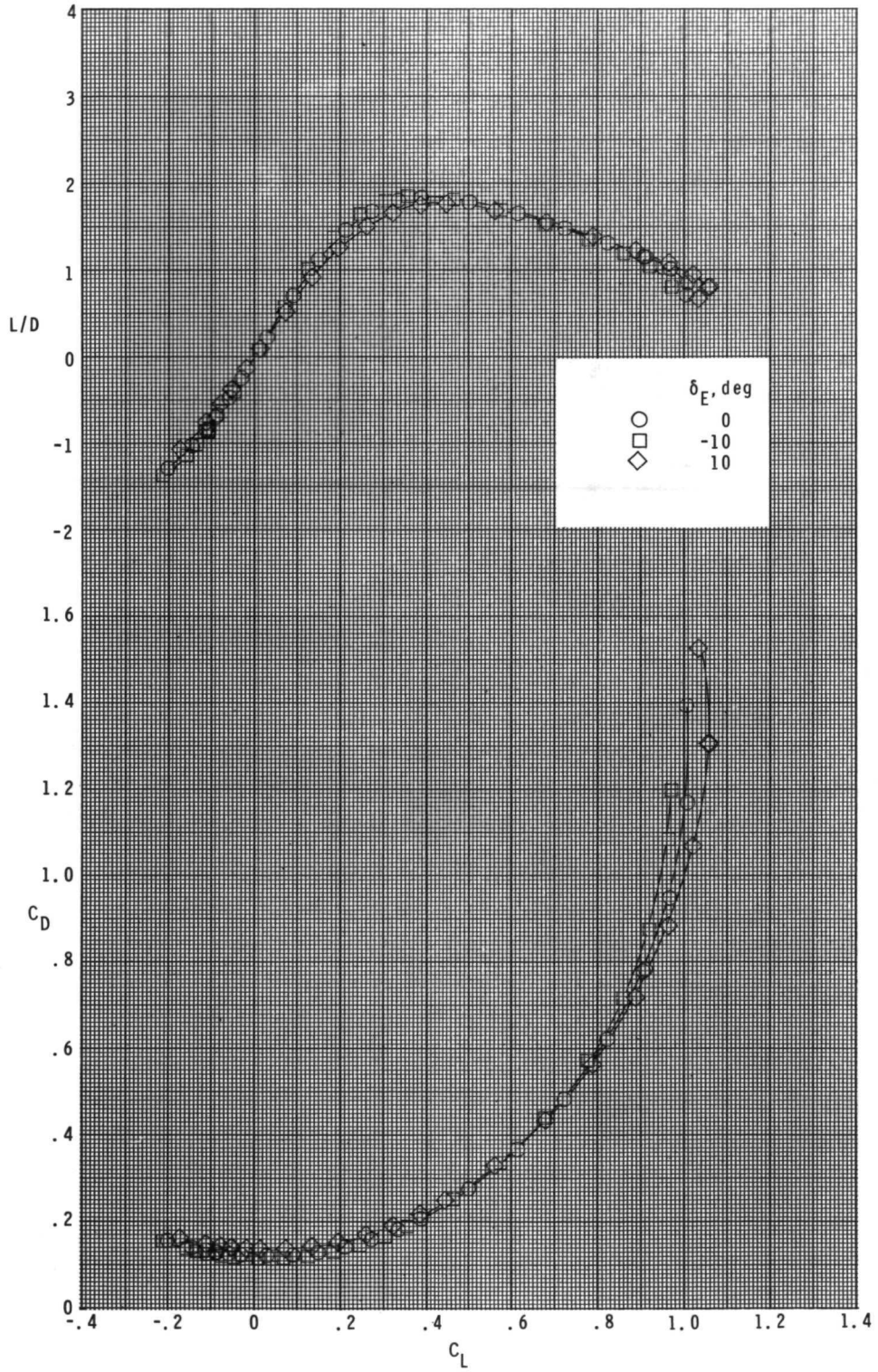

(b) Concluded.

Figure 5.- Continued.

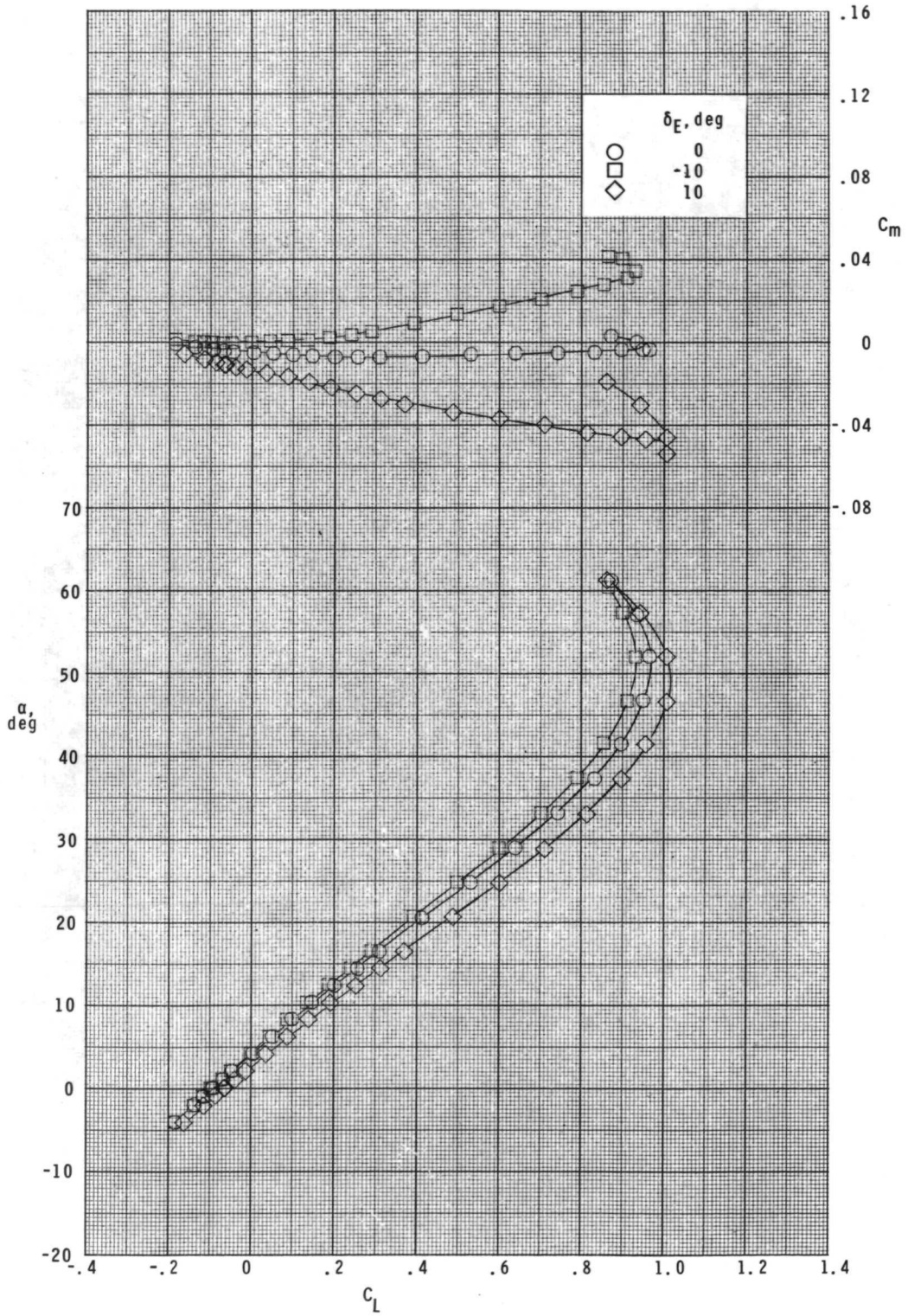

(c) M = 3.95.

Figure 5.- Continued.

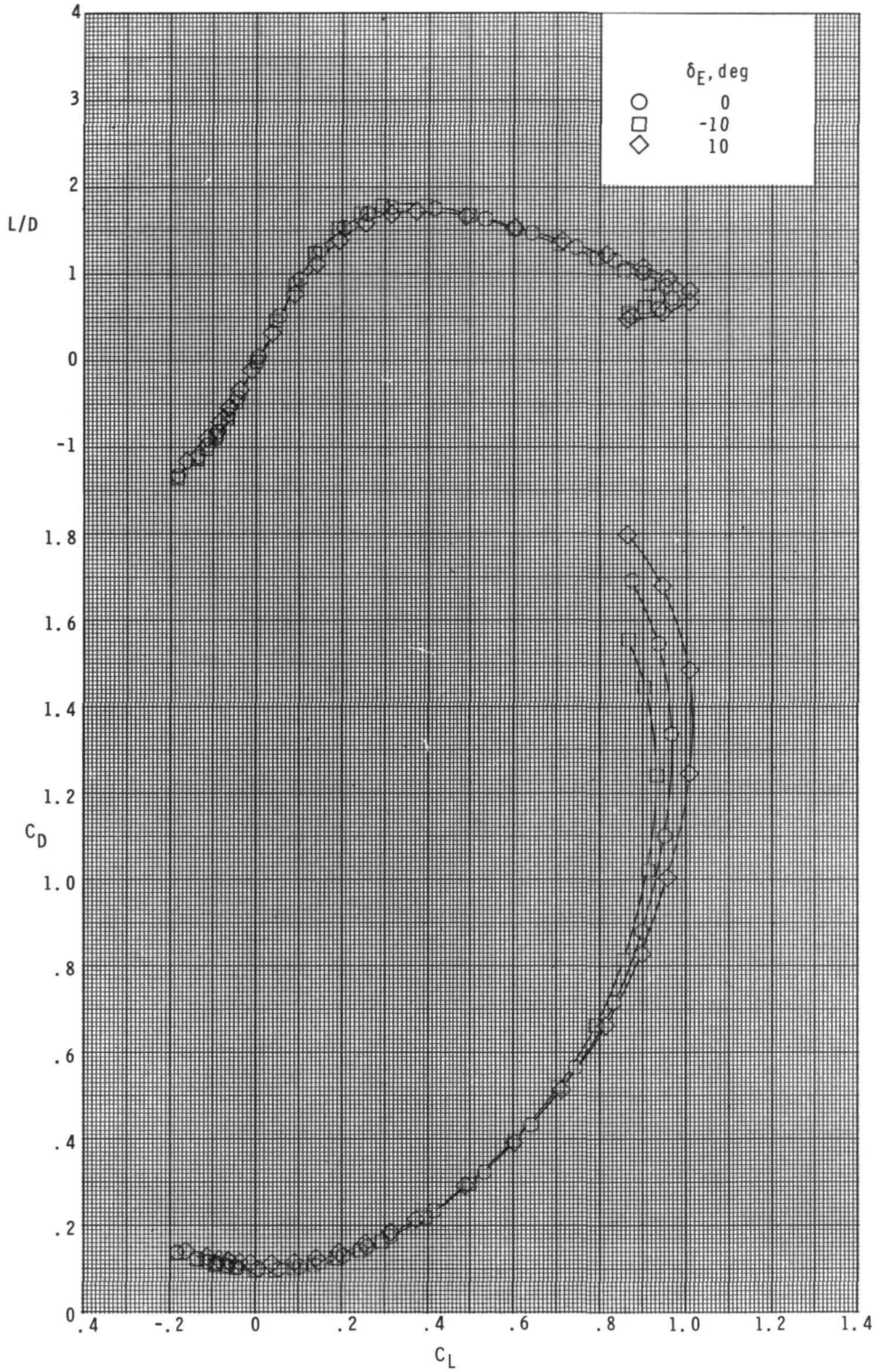

(c) Concluded.

Figure 5.- Continued.

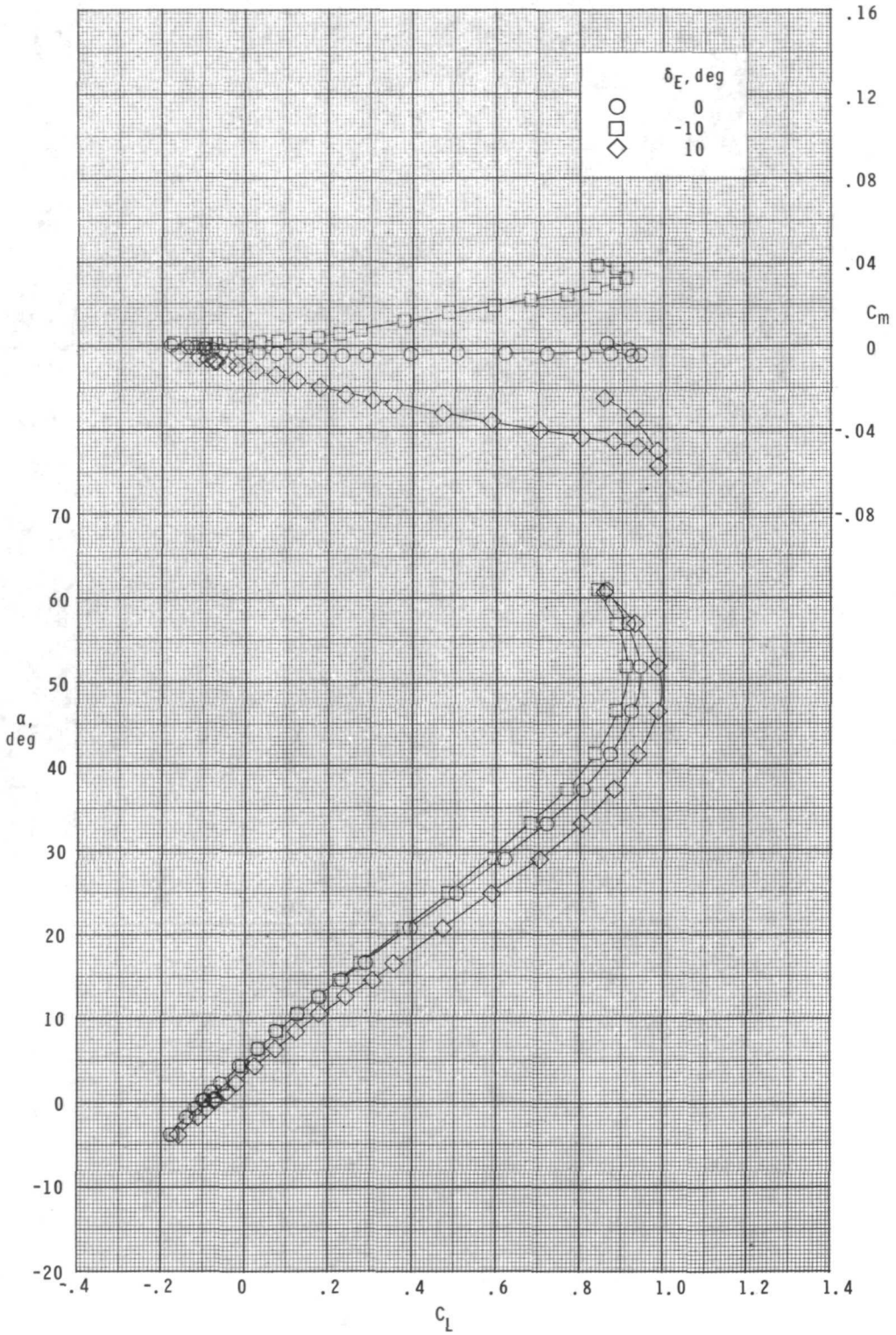

(d) M = 4.60.

Figure 5.- Continued.

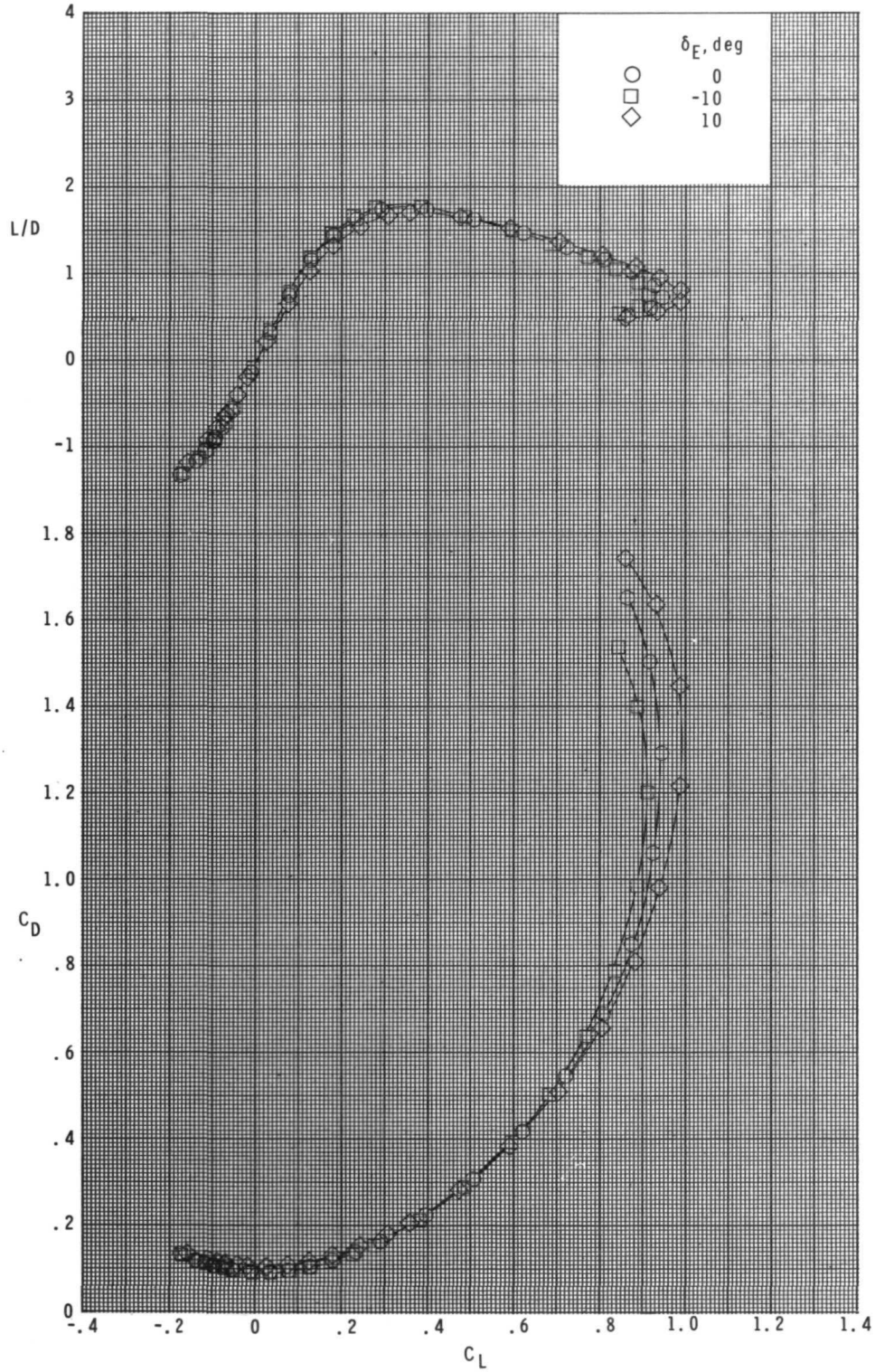

(d) Concluded.

Figure 5.- Concluded.

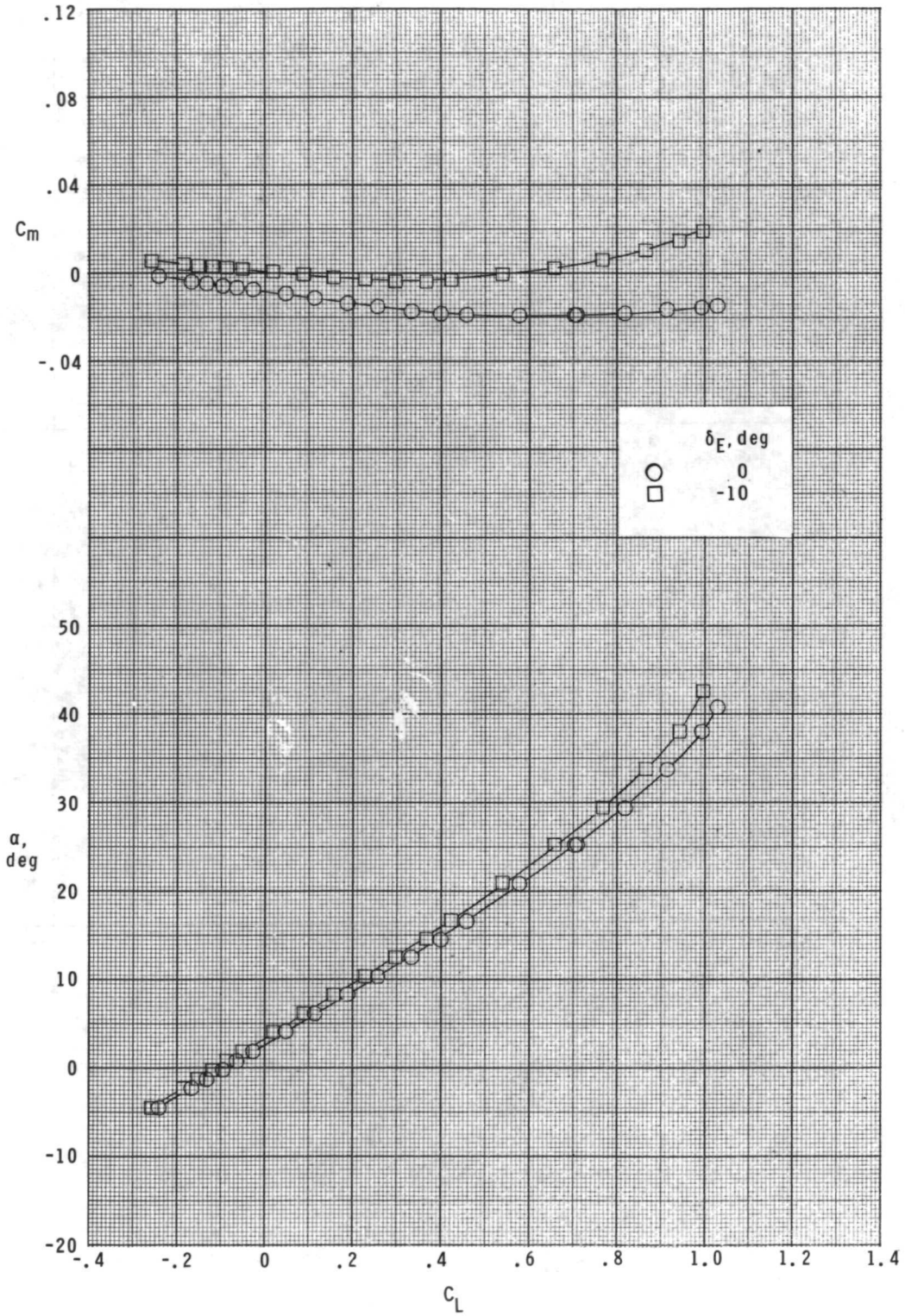

(a) M = 2.30.

Figure 6.- Effect of lower flap deflection on pitch characteristics. $\delta_F = -30^o$; $\delta_{R,L} = -20^o$; $\delta_{R,R} = +20^o$.

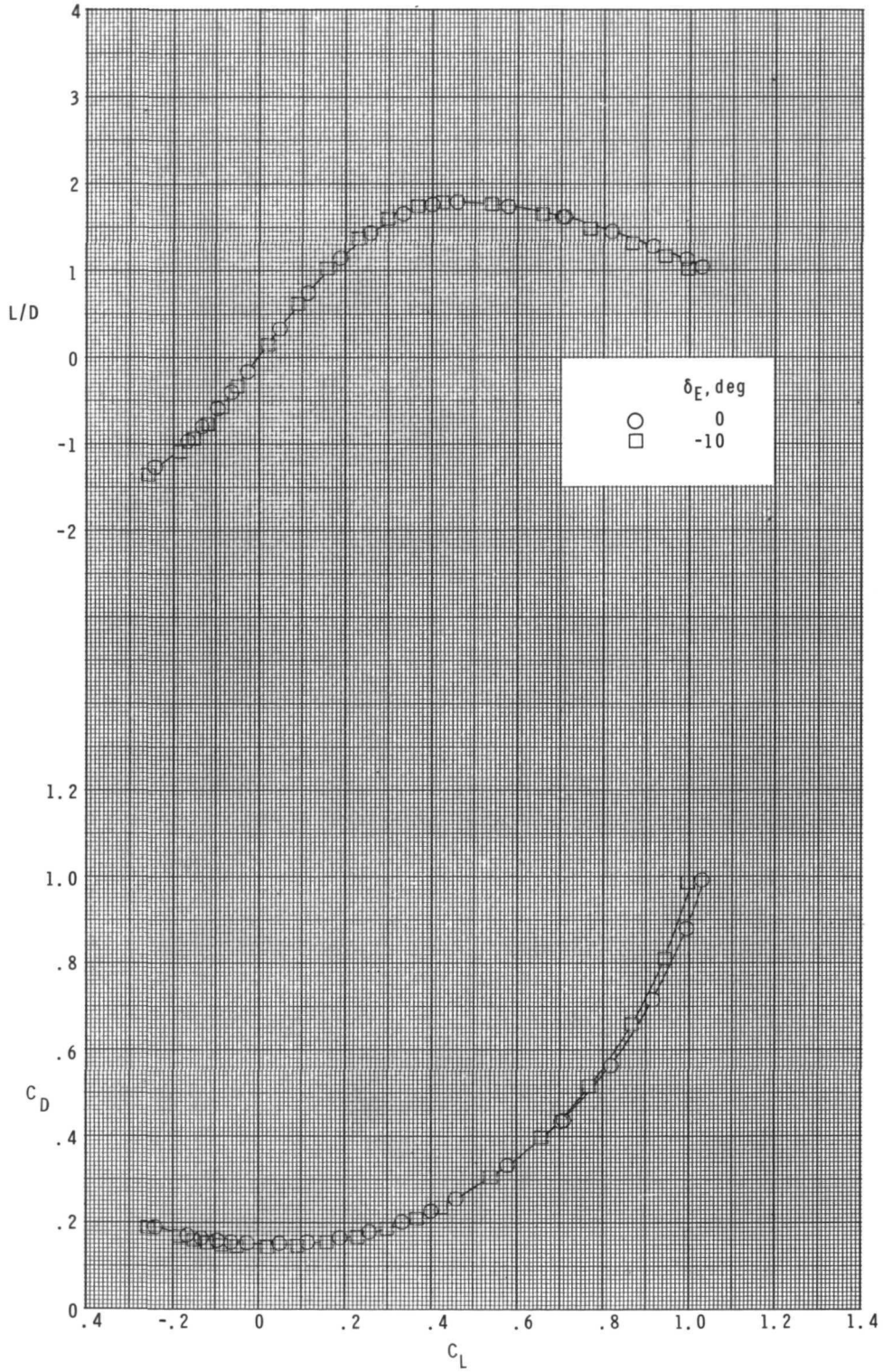

(a) Concluded.

Figure 6.- Continued.

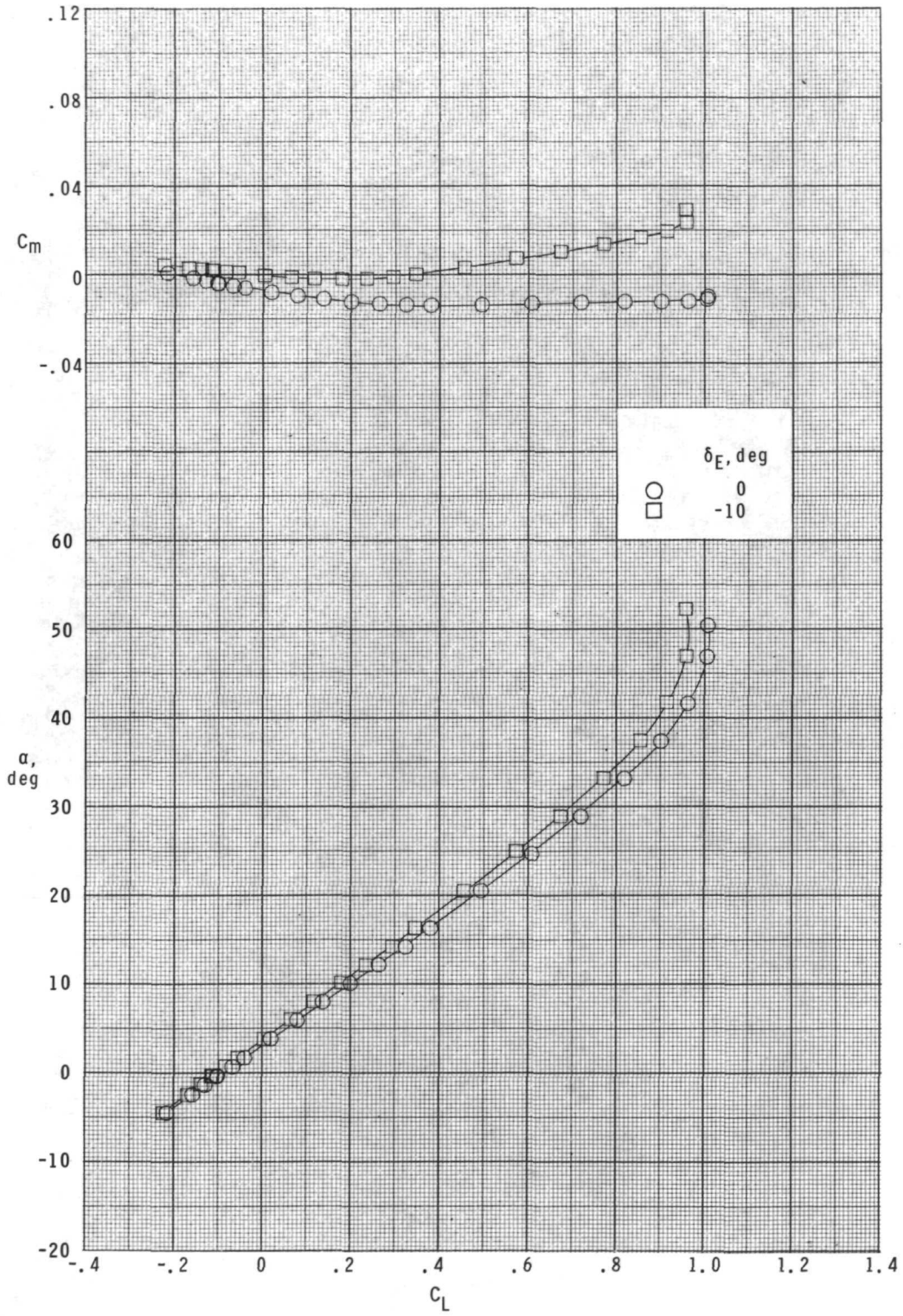

(b) M = 2.96.

Figure 6.- Continued.

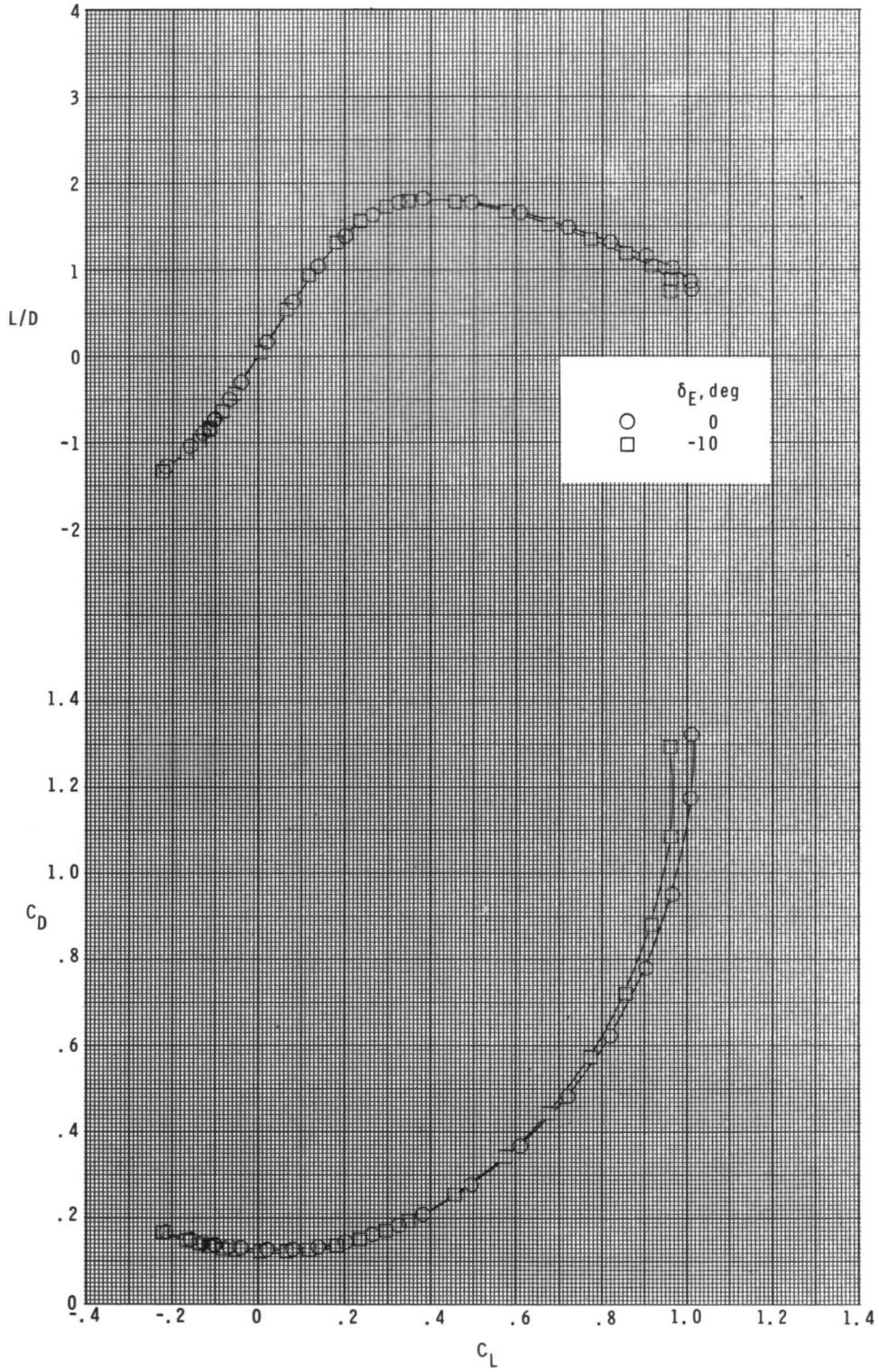

(b) Concluded.

Figure 6.- Continued.

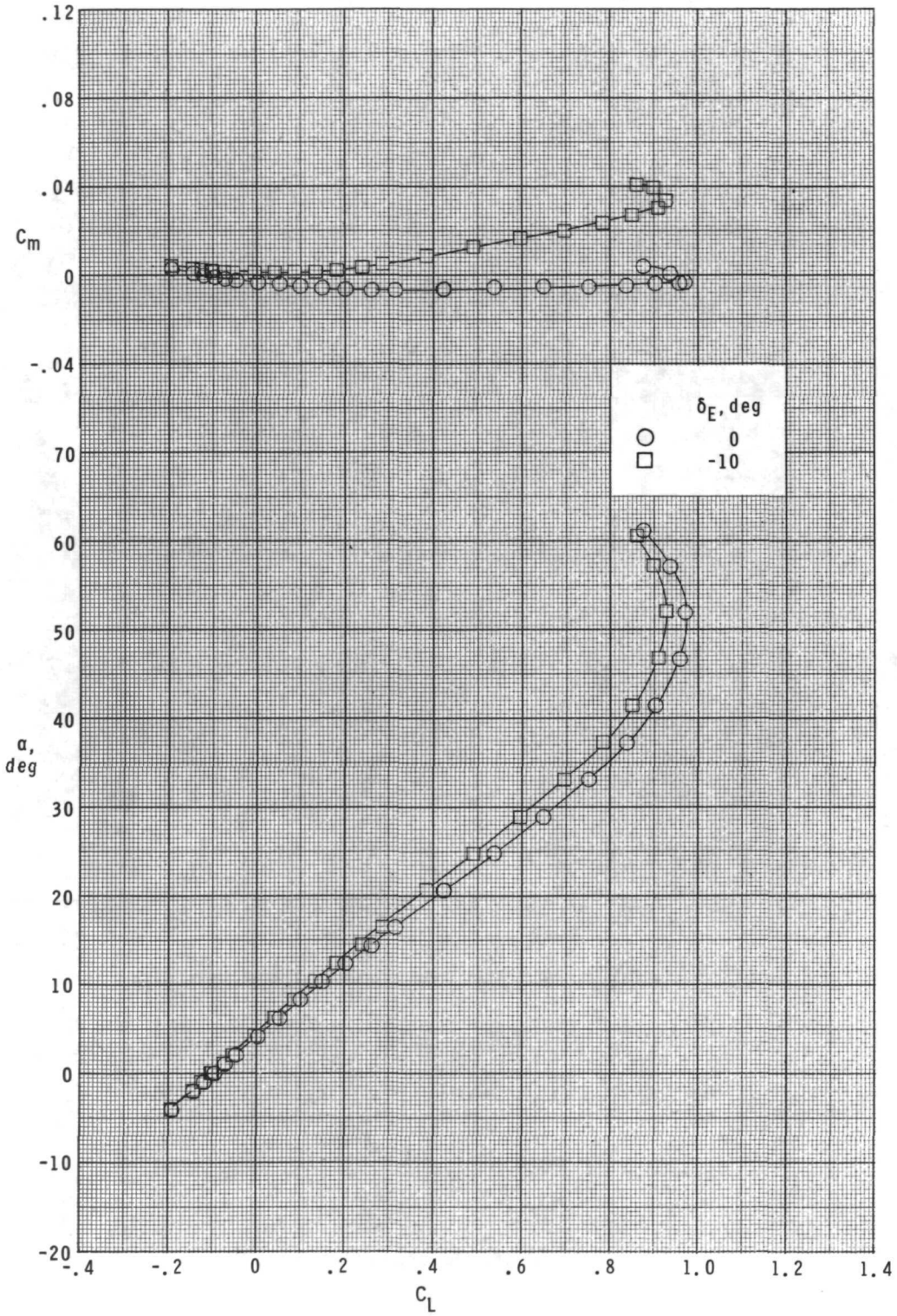

(c) M = 3.95.

Figure 6.- Continued.

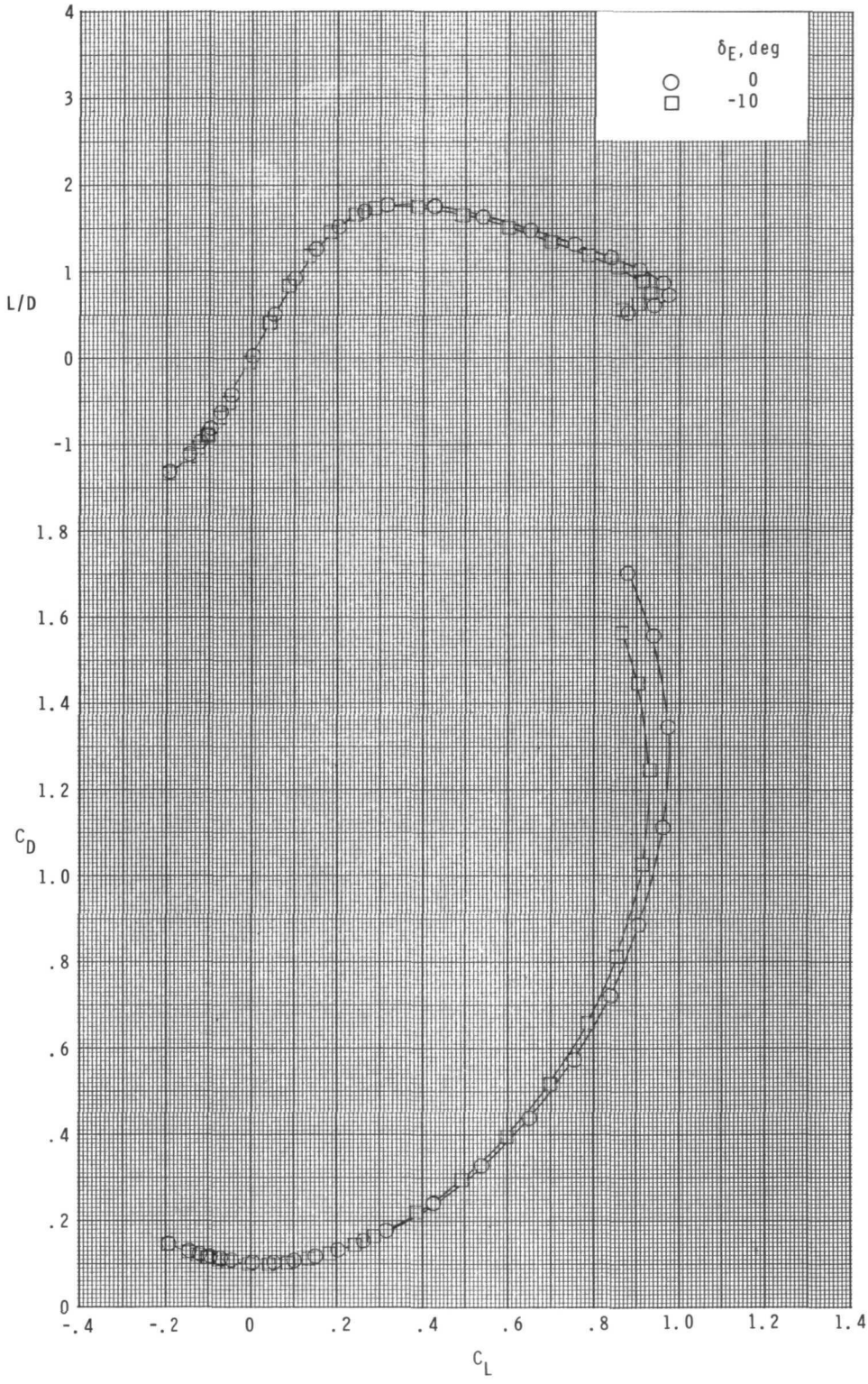

(c) Concluded.

Figure 6.- Continued.

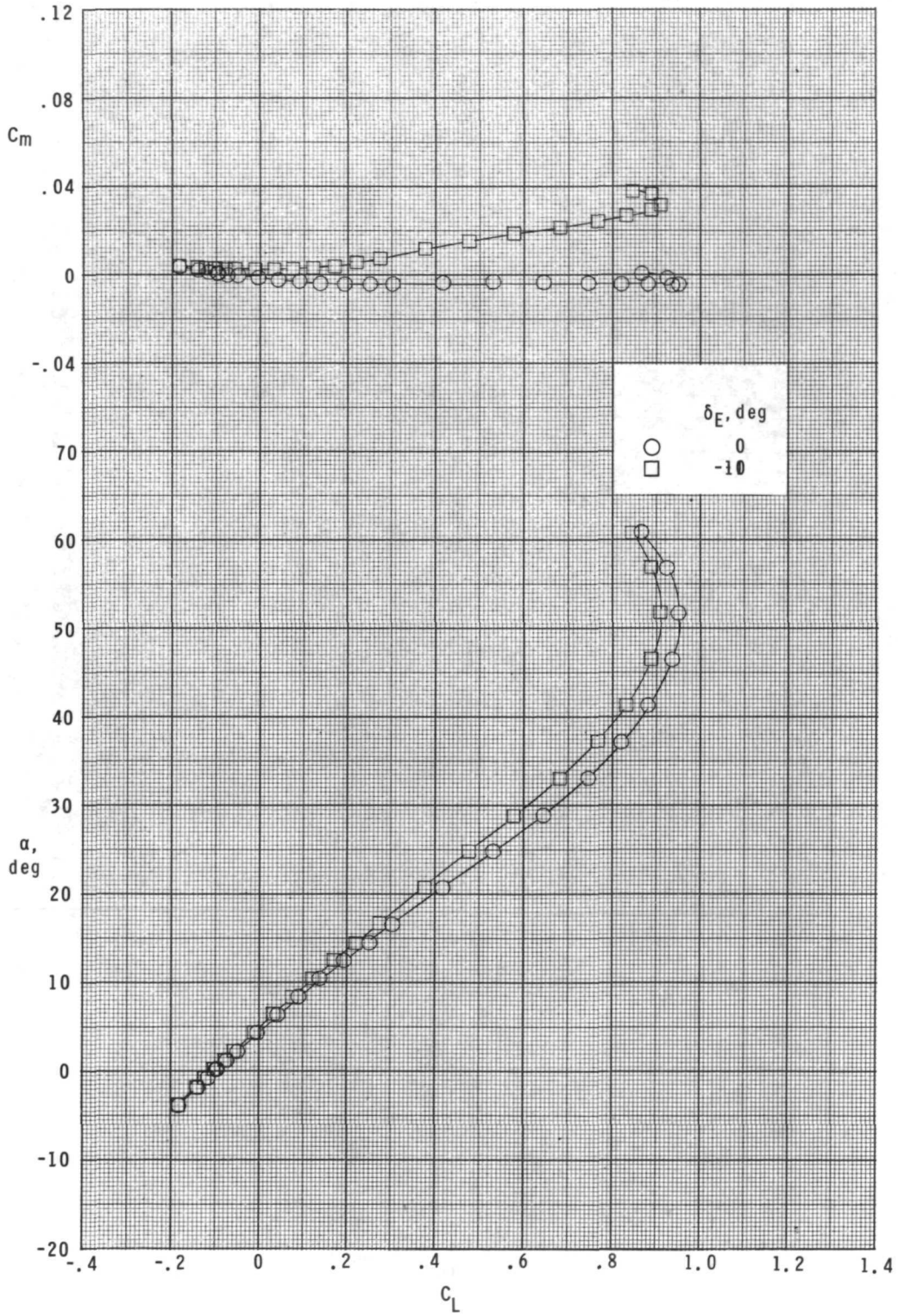

(d) M = 4.60.

Figure 6.- Continued.

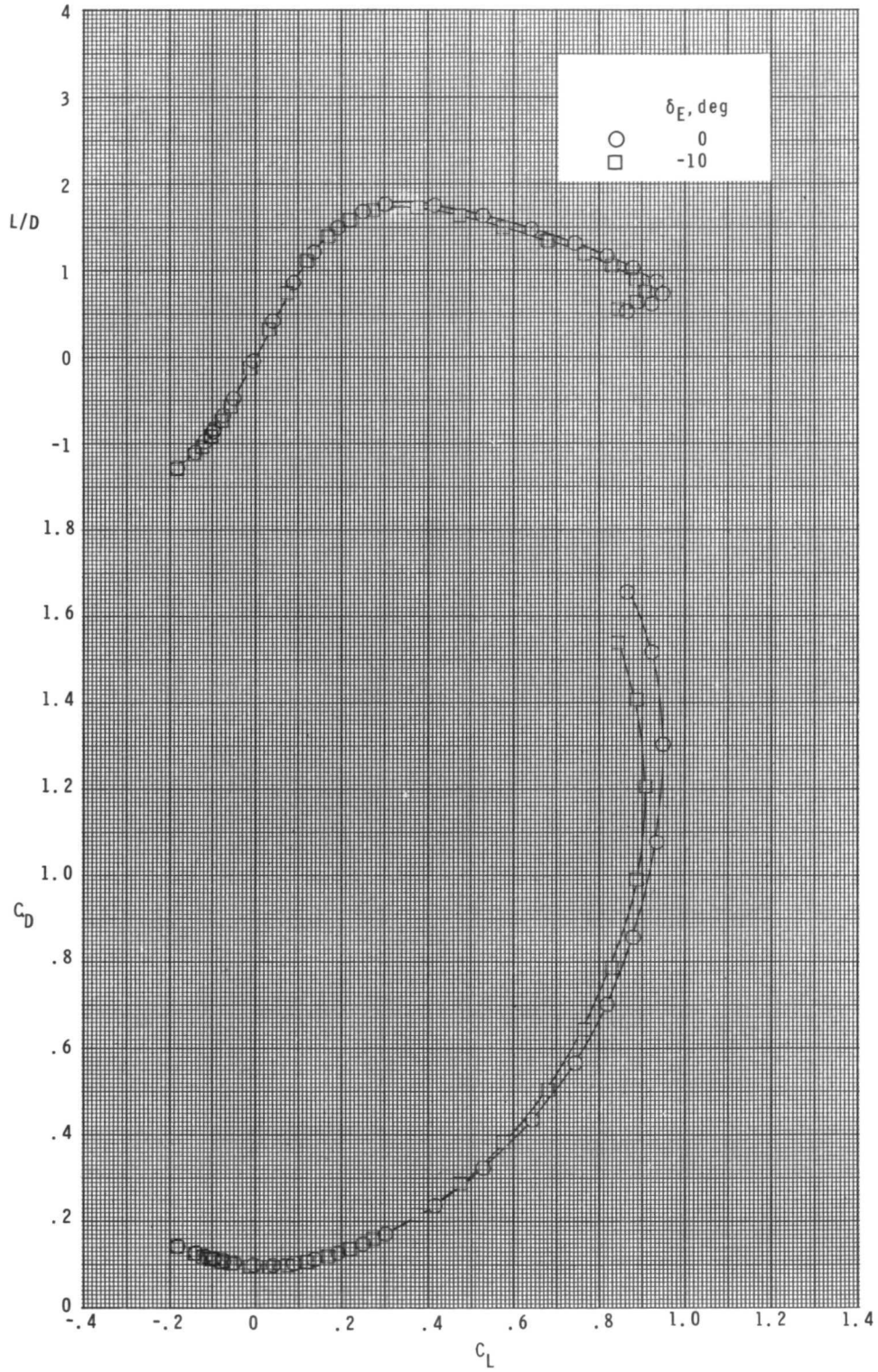

(d) Concluded.

Figure 6.- Concluded.

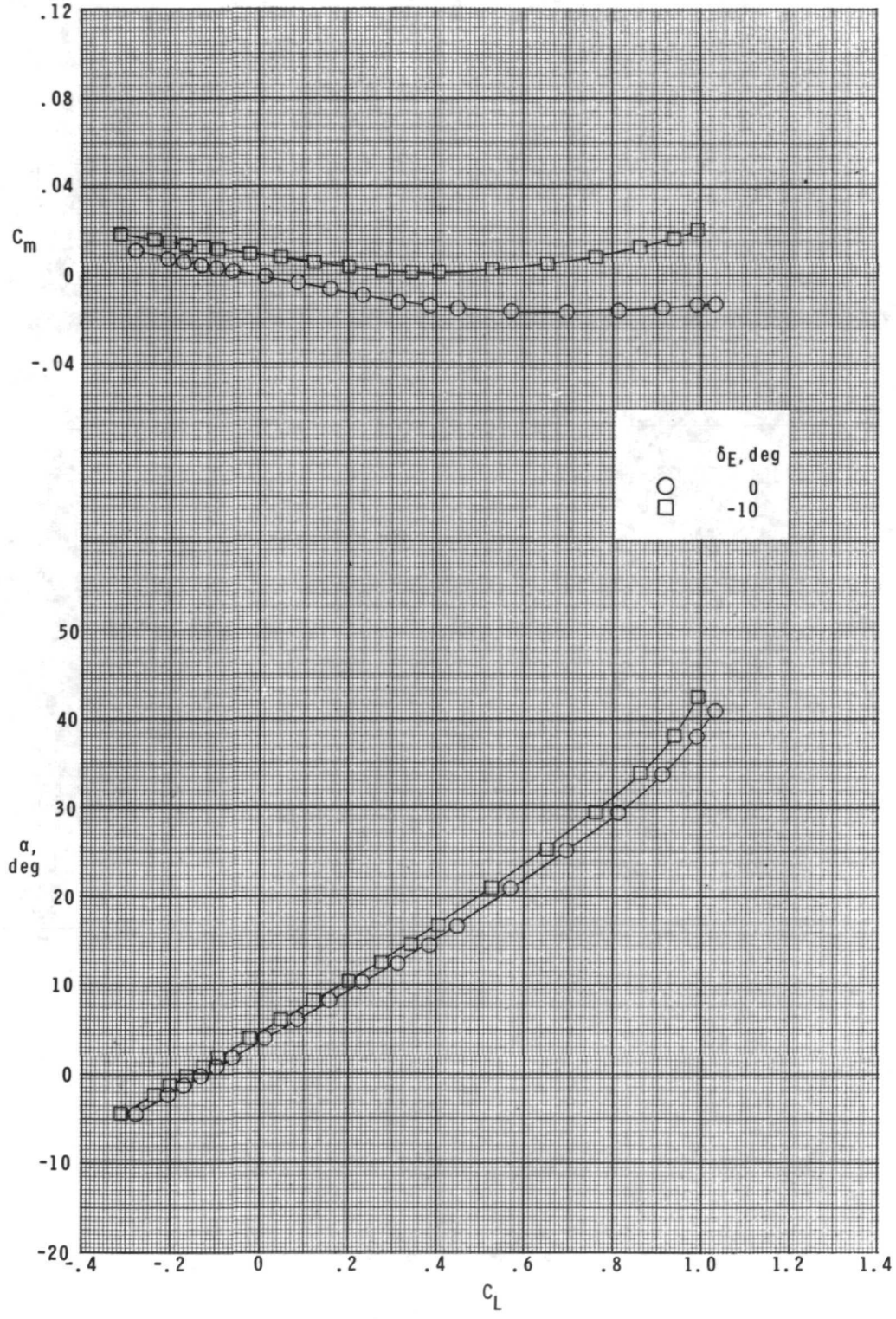

(a) M = 2.30.

Figure 7.- Effect of lower flap deflection on pitch characteristics. $\delta_F = -40^o$; $\delta_{R,L} = -20^o$; $\delta_{R,R} = +20^o$.

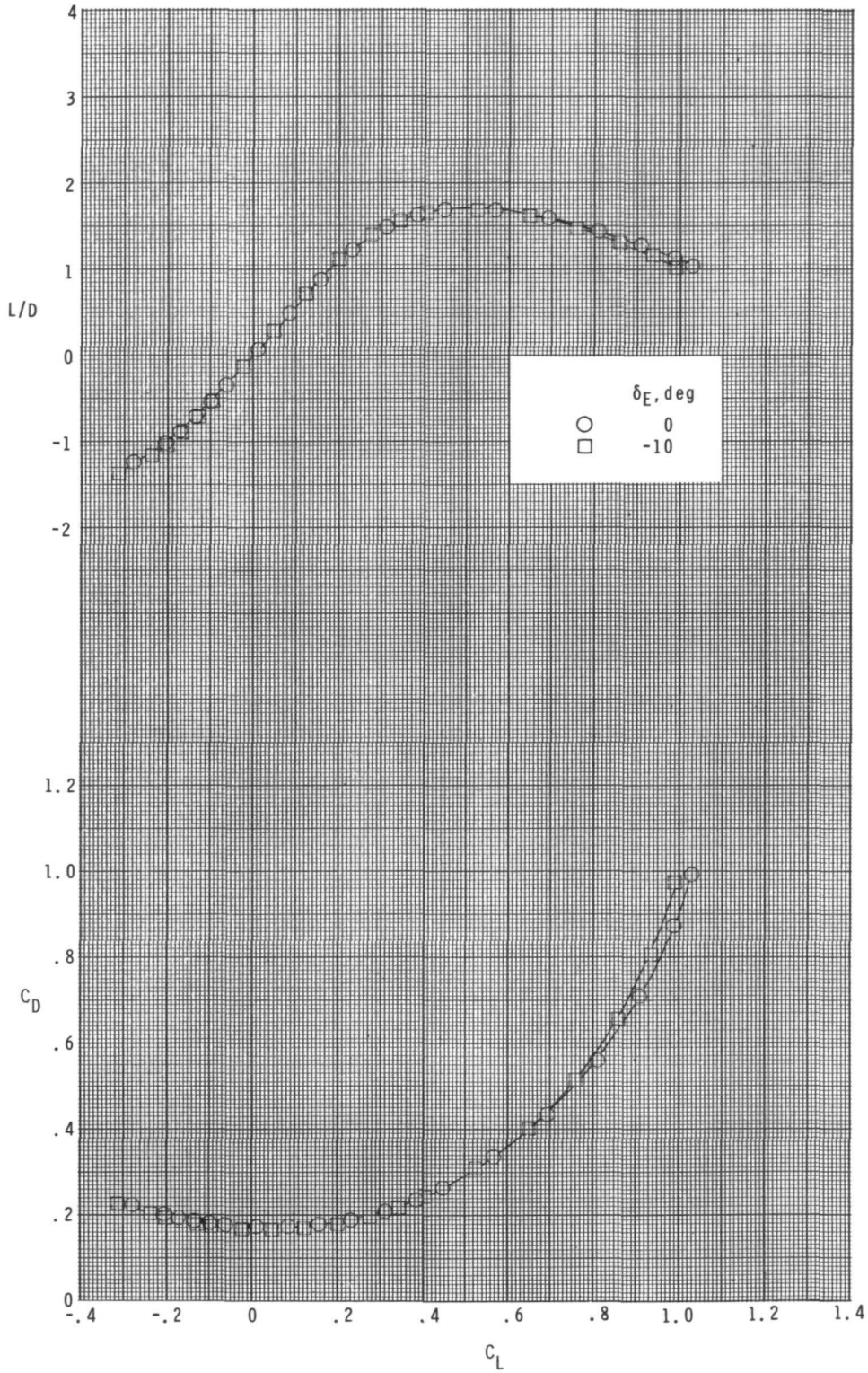

(a) Concluded.

Figure 7.- Continued.

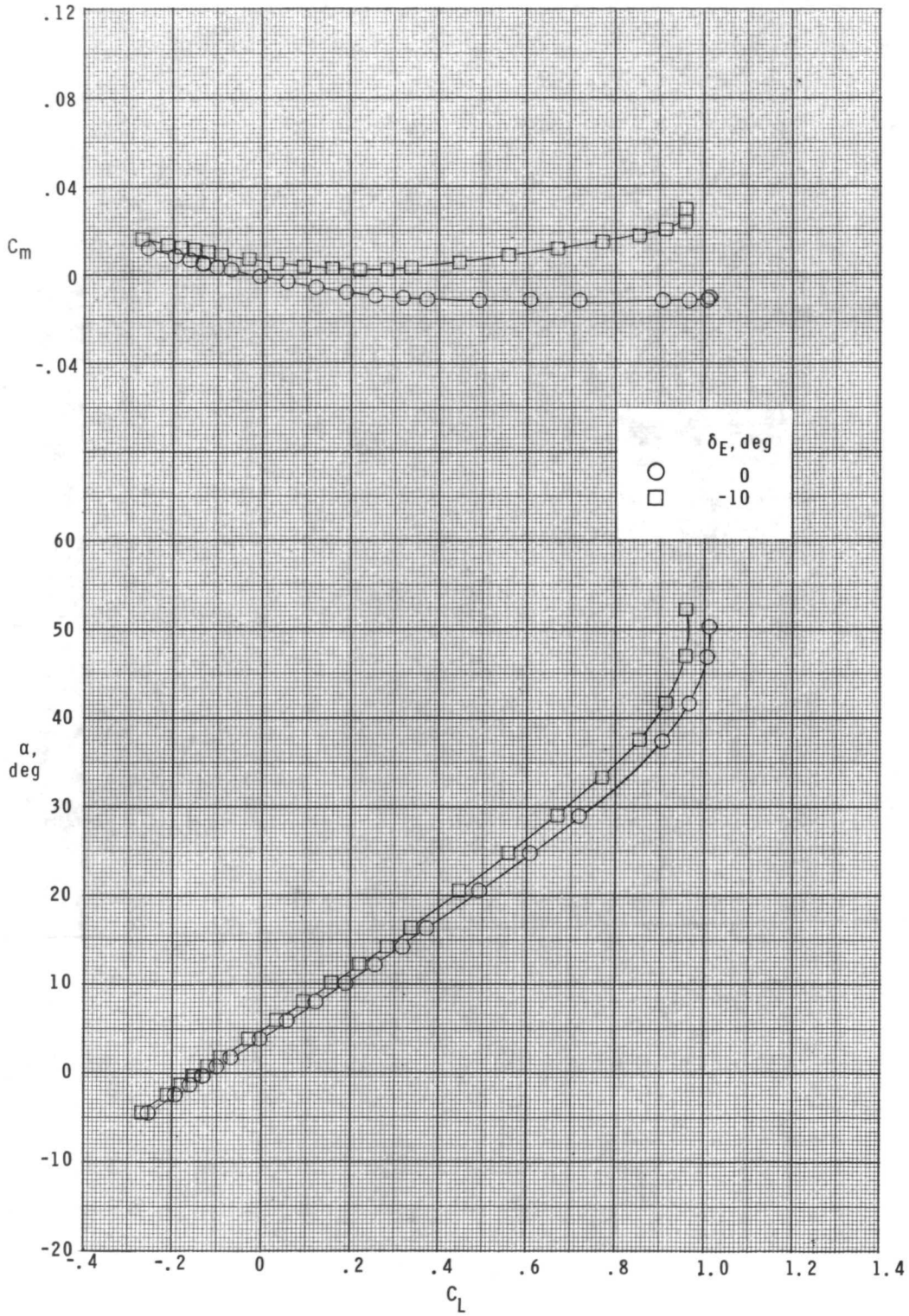

(b) M = 2.96.

Figure 7.- Continued.

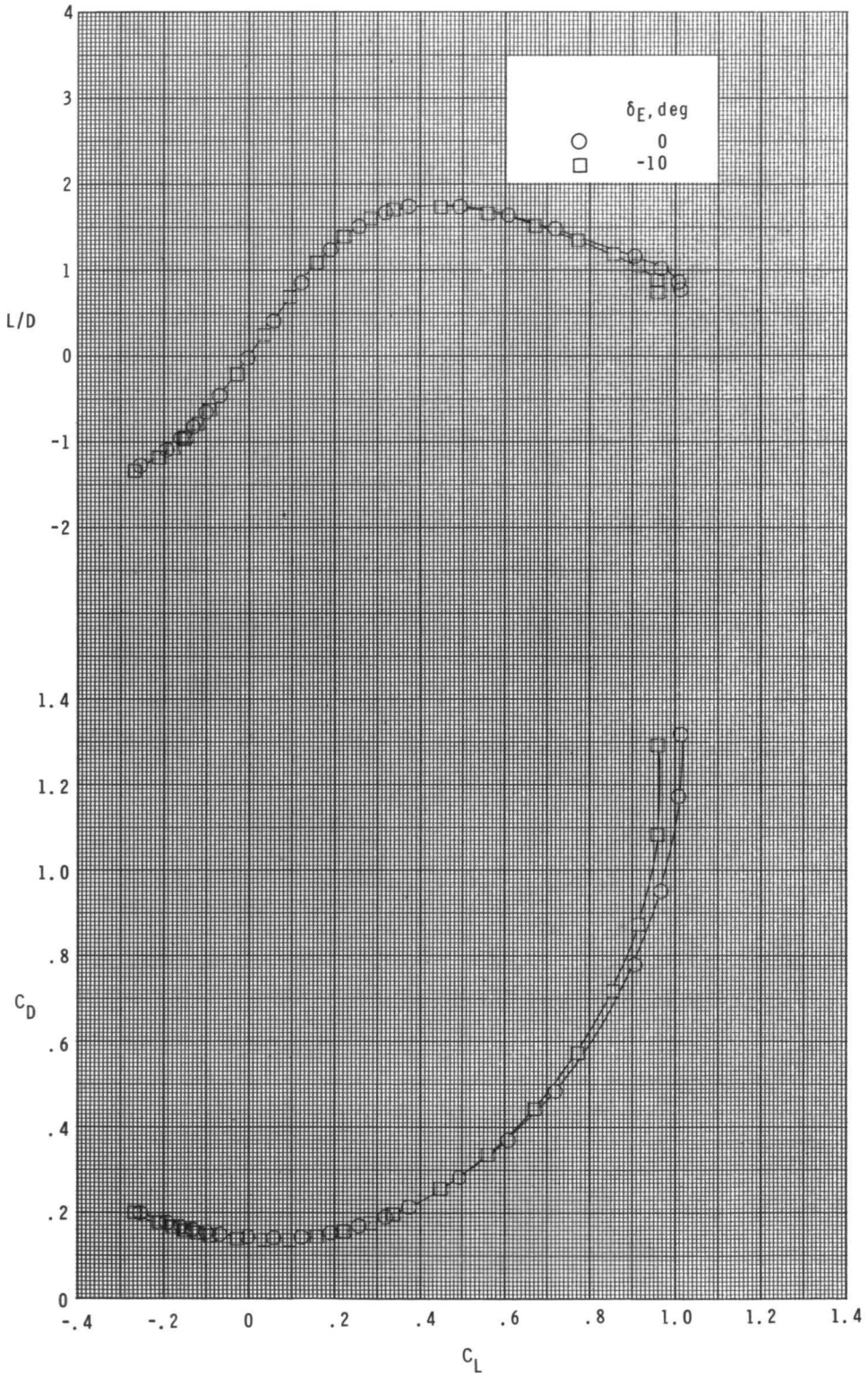

(b) Concluded.

Figure 7.- Continued.

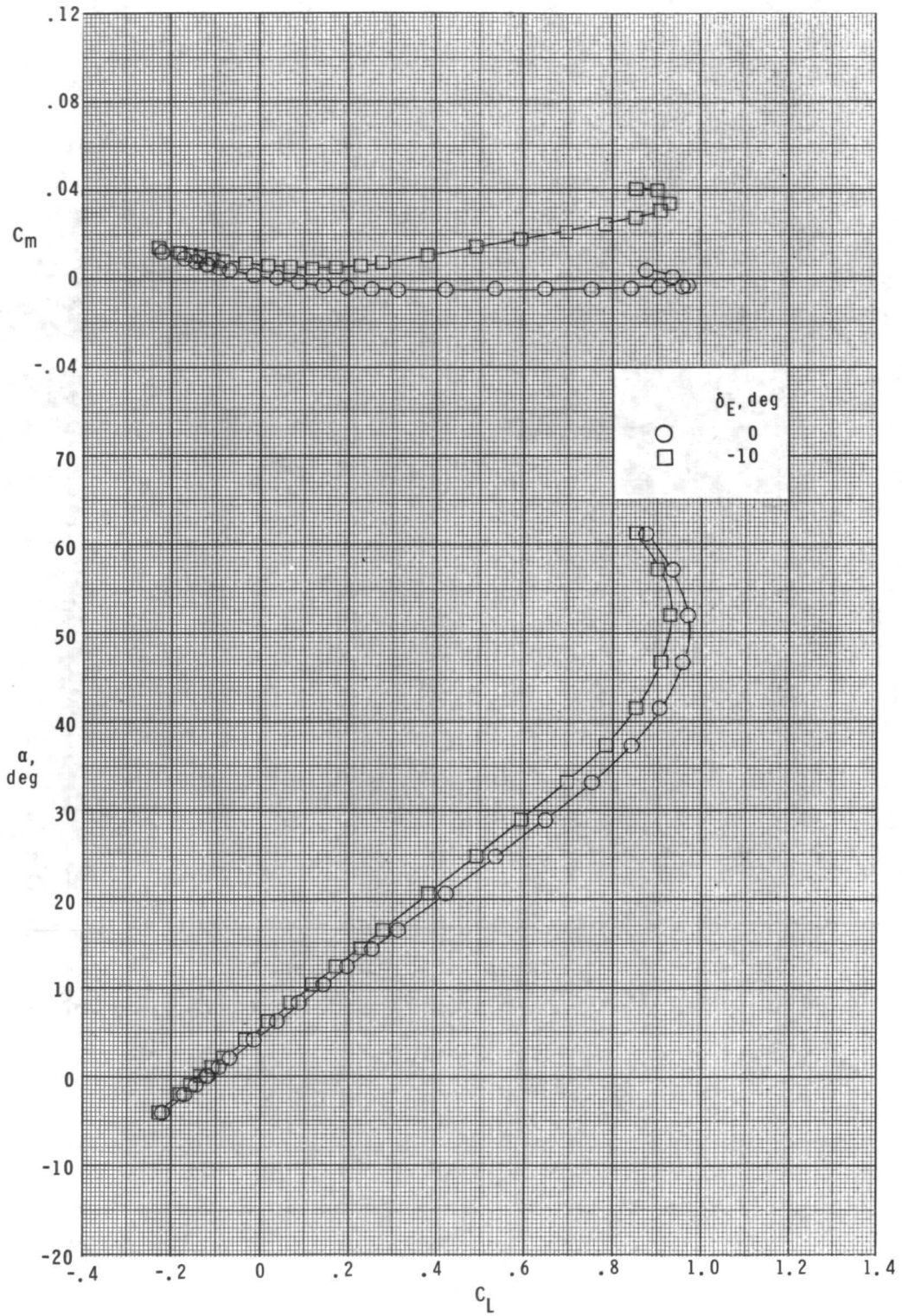

(c) M = 3.95.

Figure 7.- Continued.

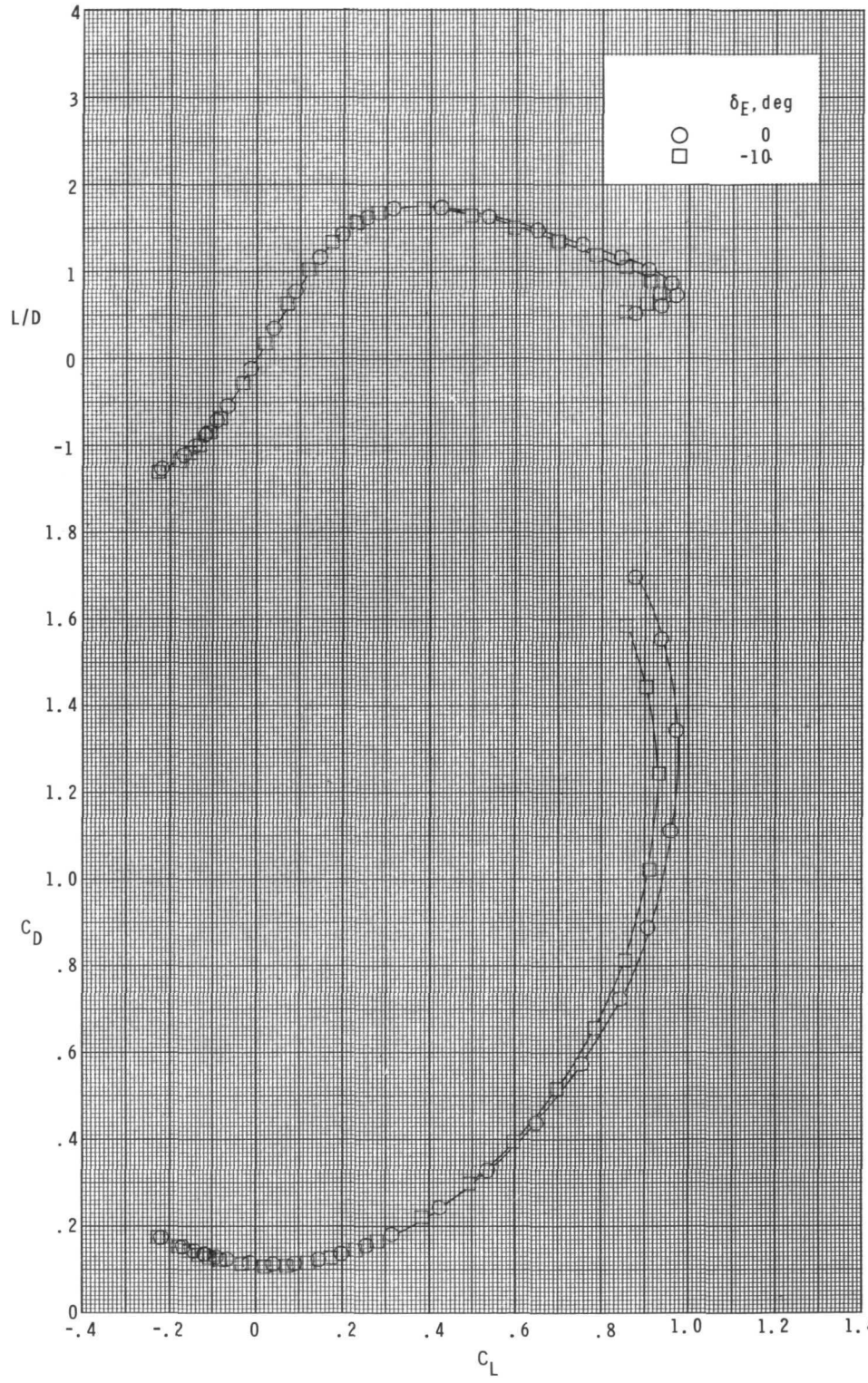

(c) Concluded.

Figure 7.- Continued.

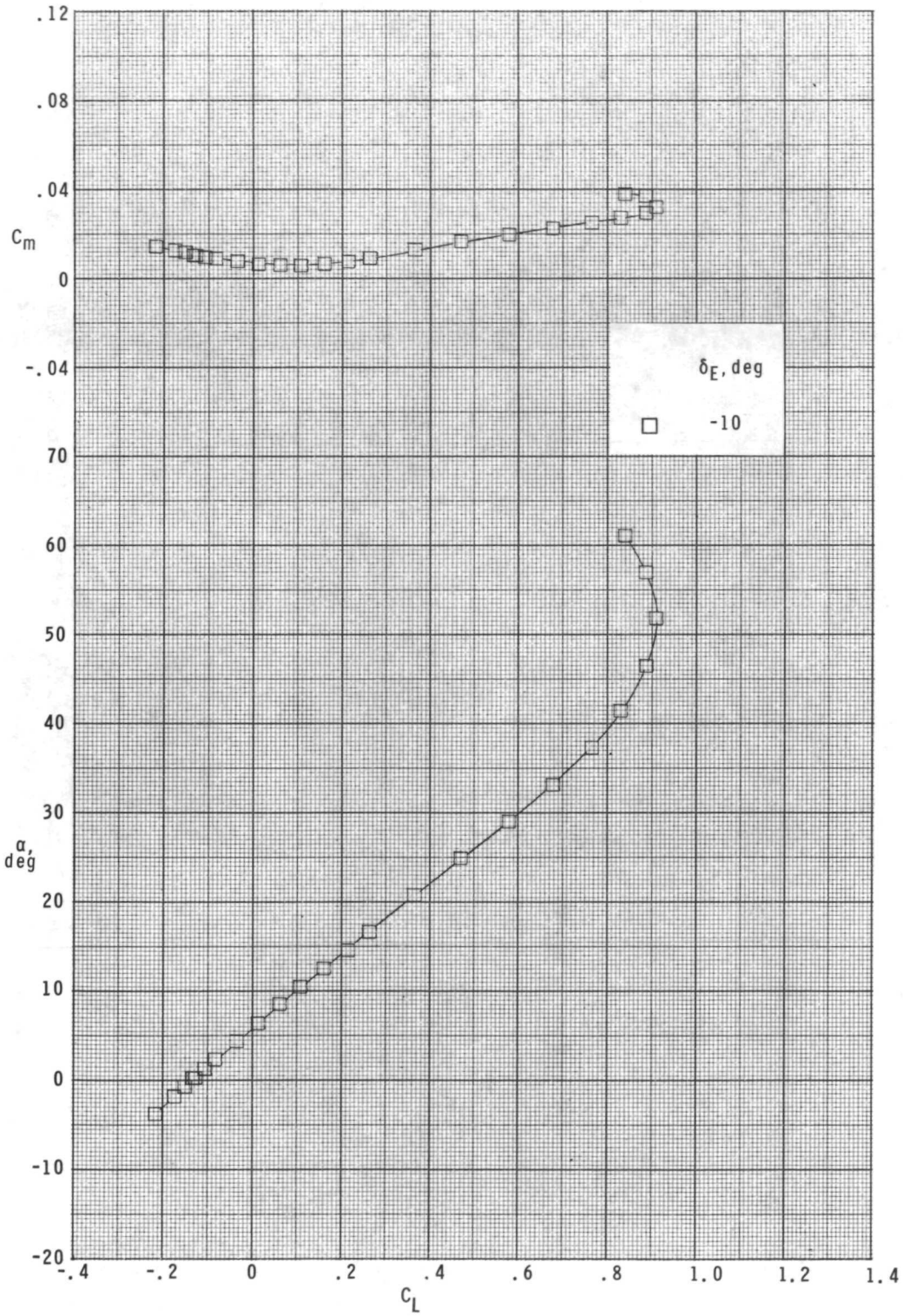

(d) M = 4.60.

Figure 7.- Continued.

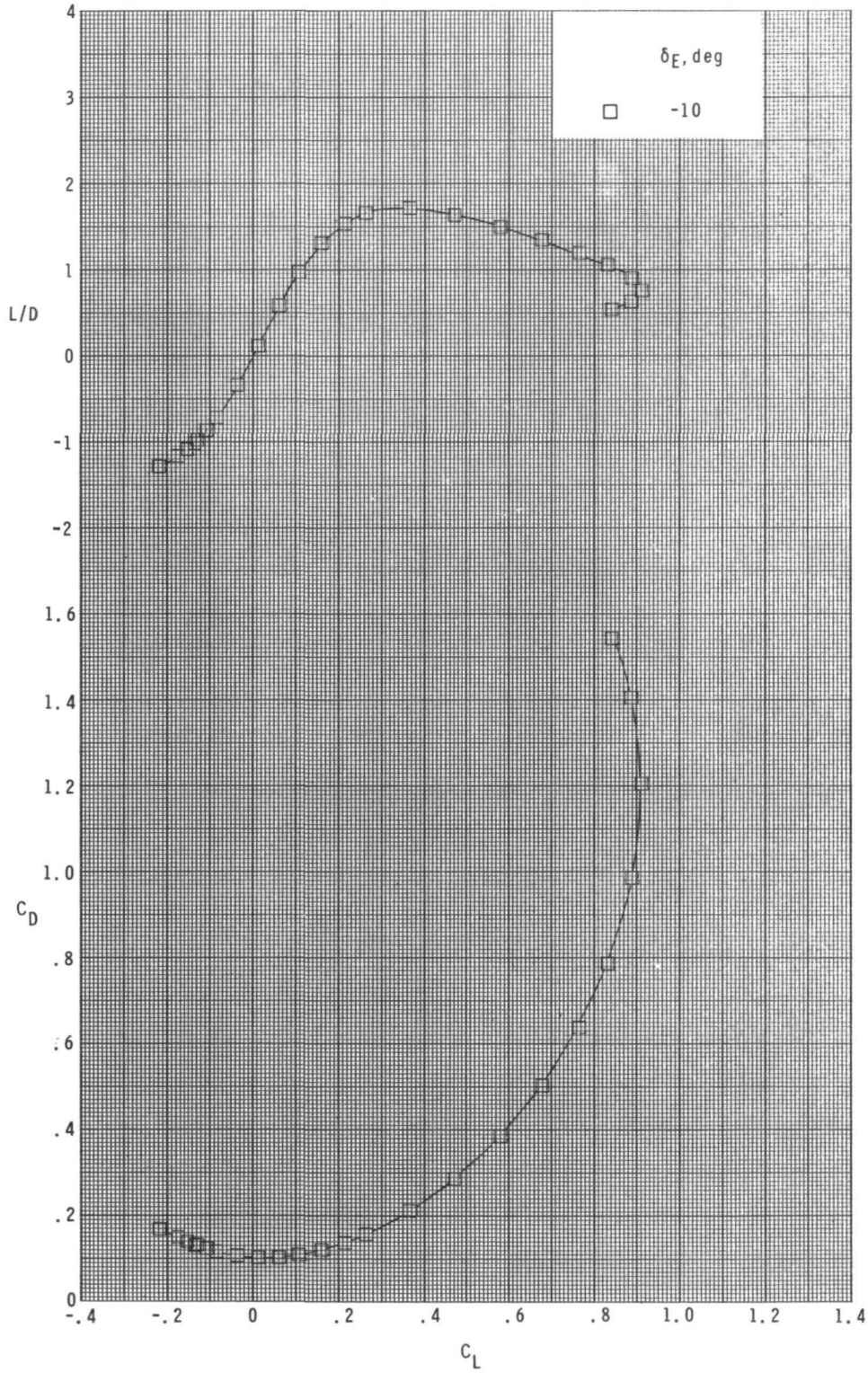

(d) Concluded.

Figure 7.- Concluded.

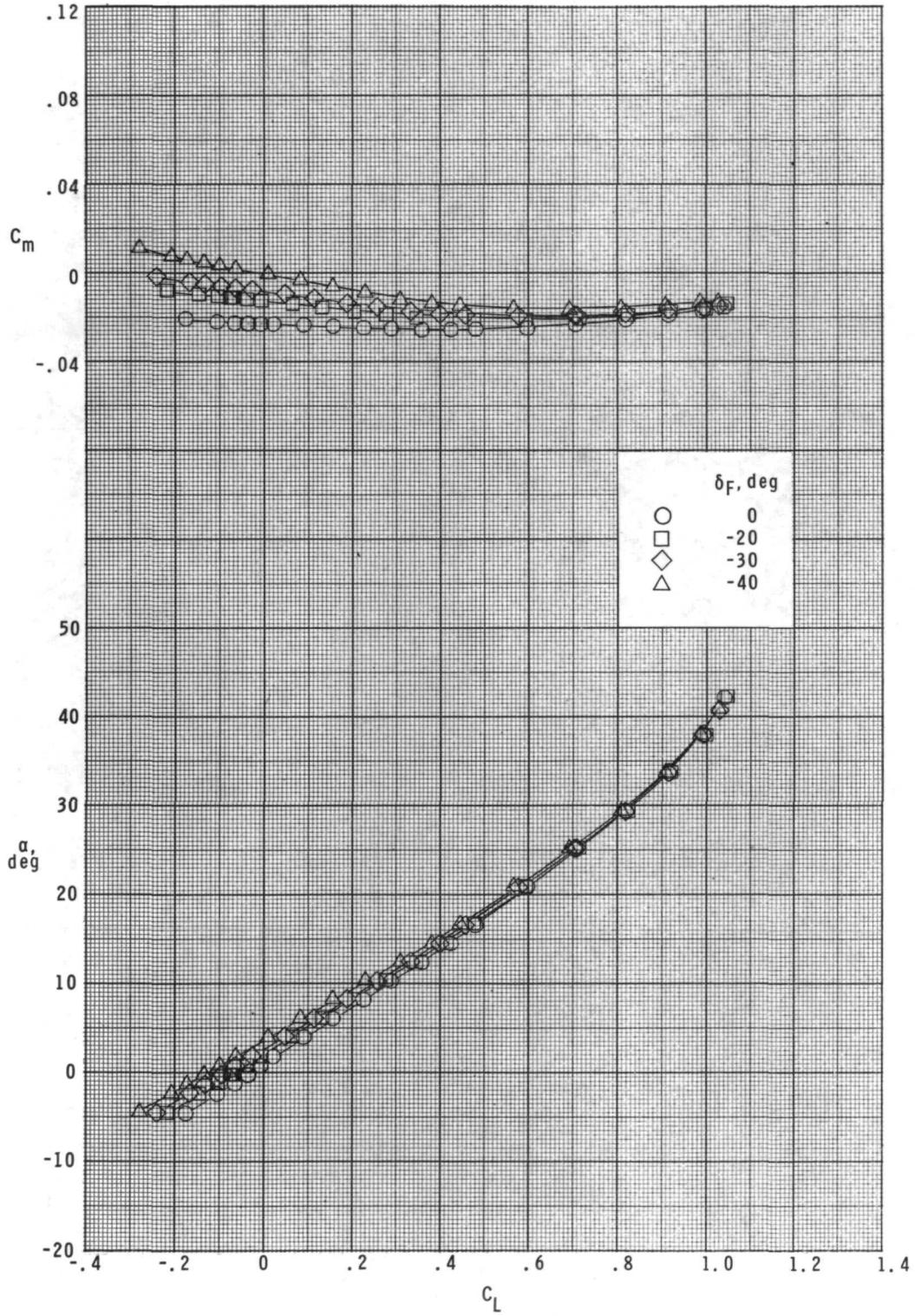

(a) M = 2.30.

Figure 8.- Effect of upper flap deflection on pitch characteristics. $\delta_E = 0^o$; $\delta_{R,L} = -20^o$; $\delta_{R,R} = +20^o$.

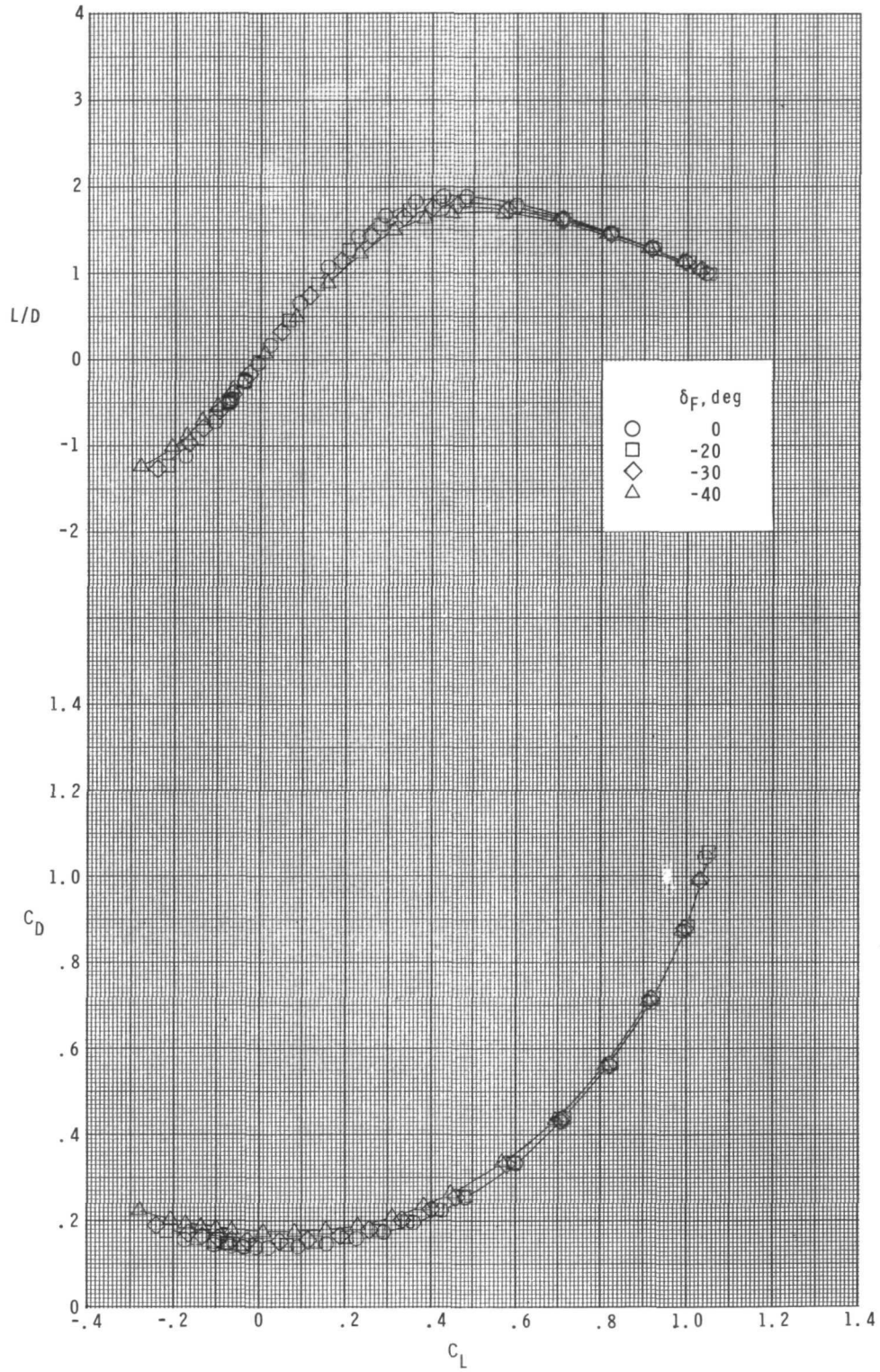

(a) Concluded.

Figure 8.- Continued.

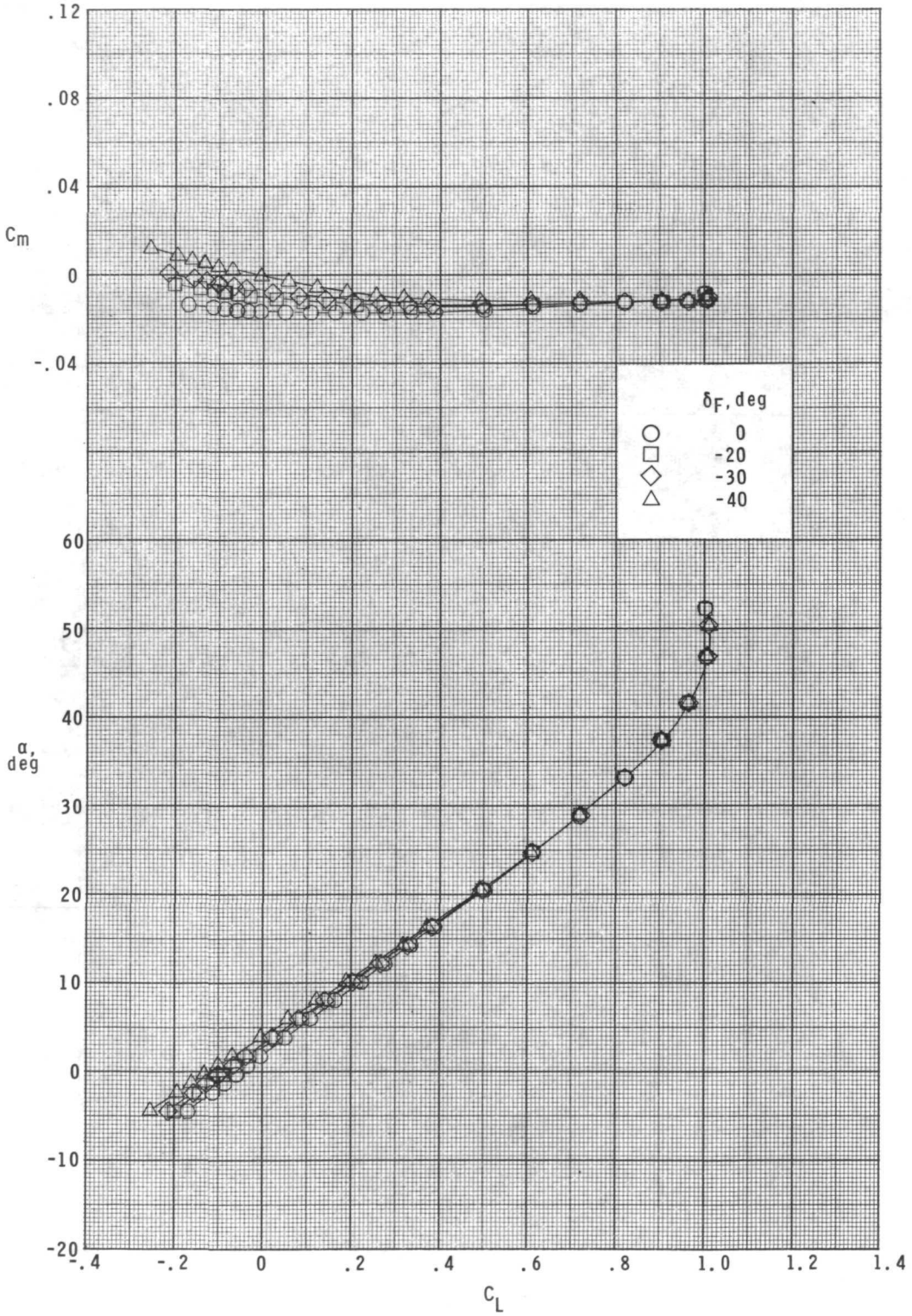

(b) M = 2.96.

Figure 8.- Continued.

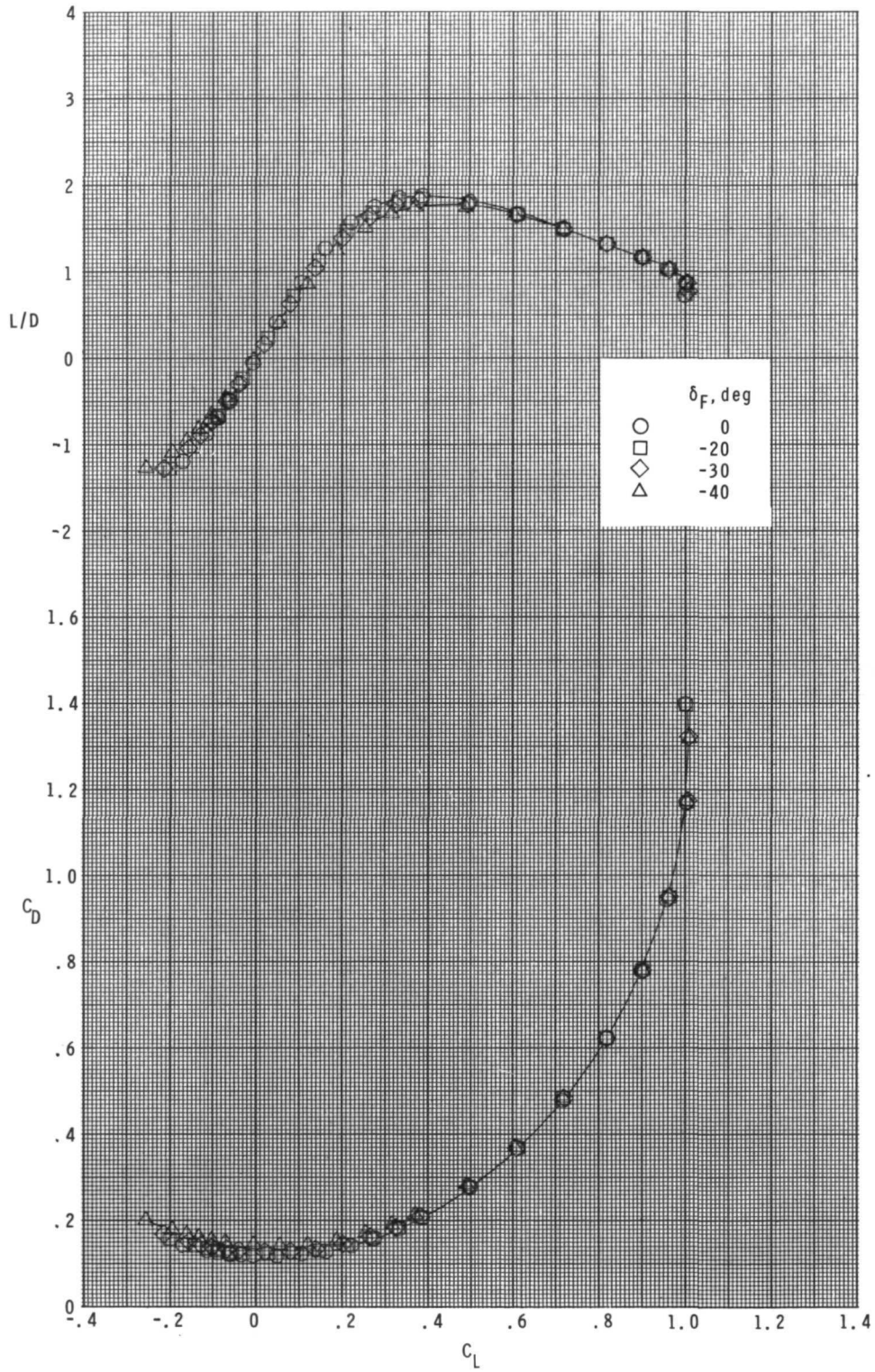

(b) Concluded.

Figure 8.- Continued.

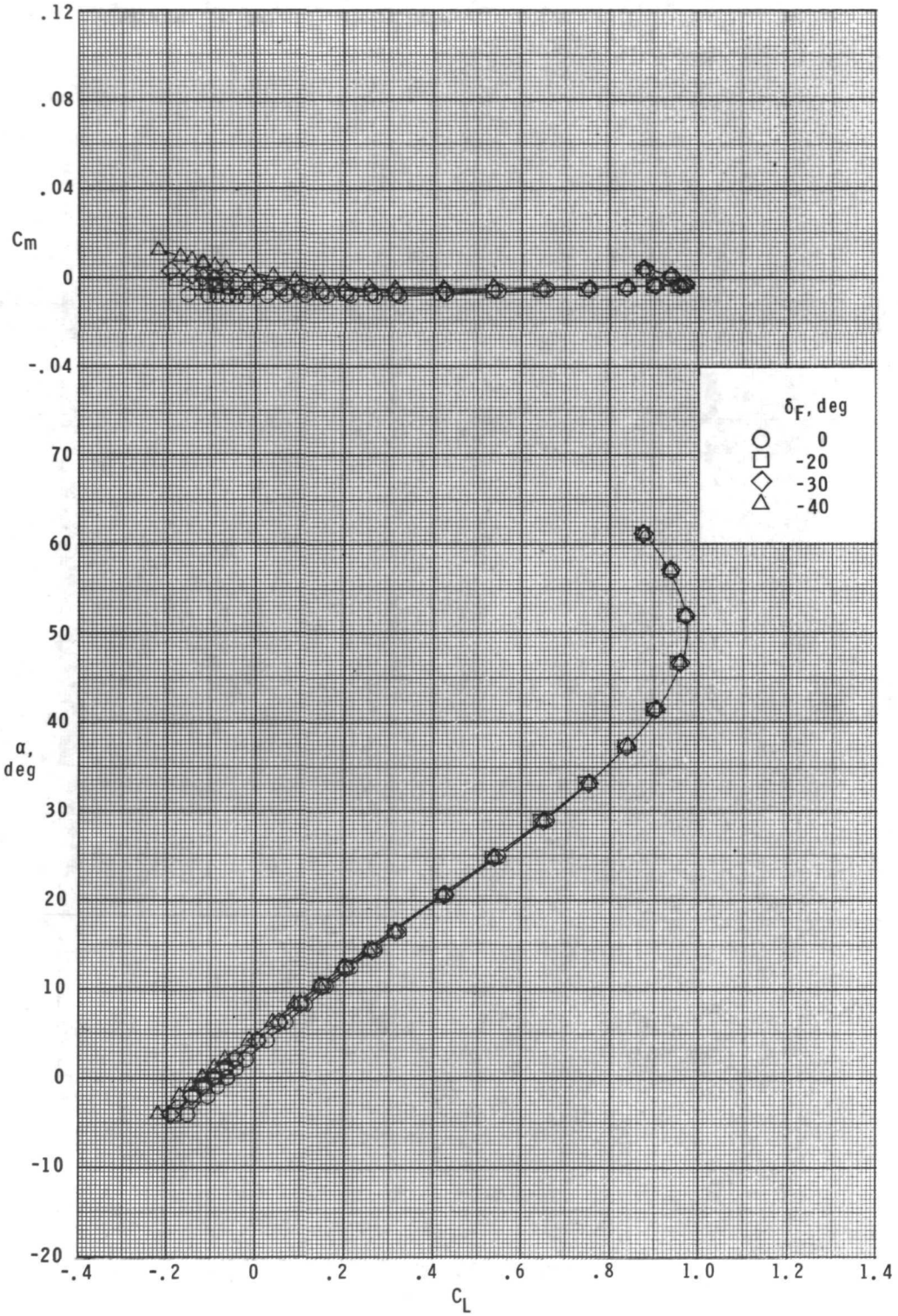

(c) M = 3.95.

Figure 8.- Continued.

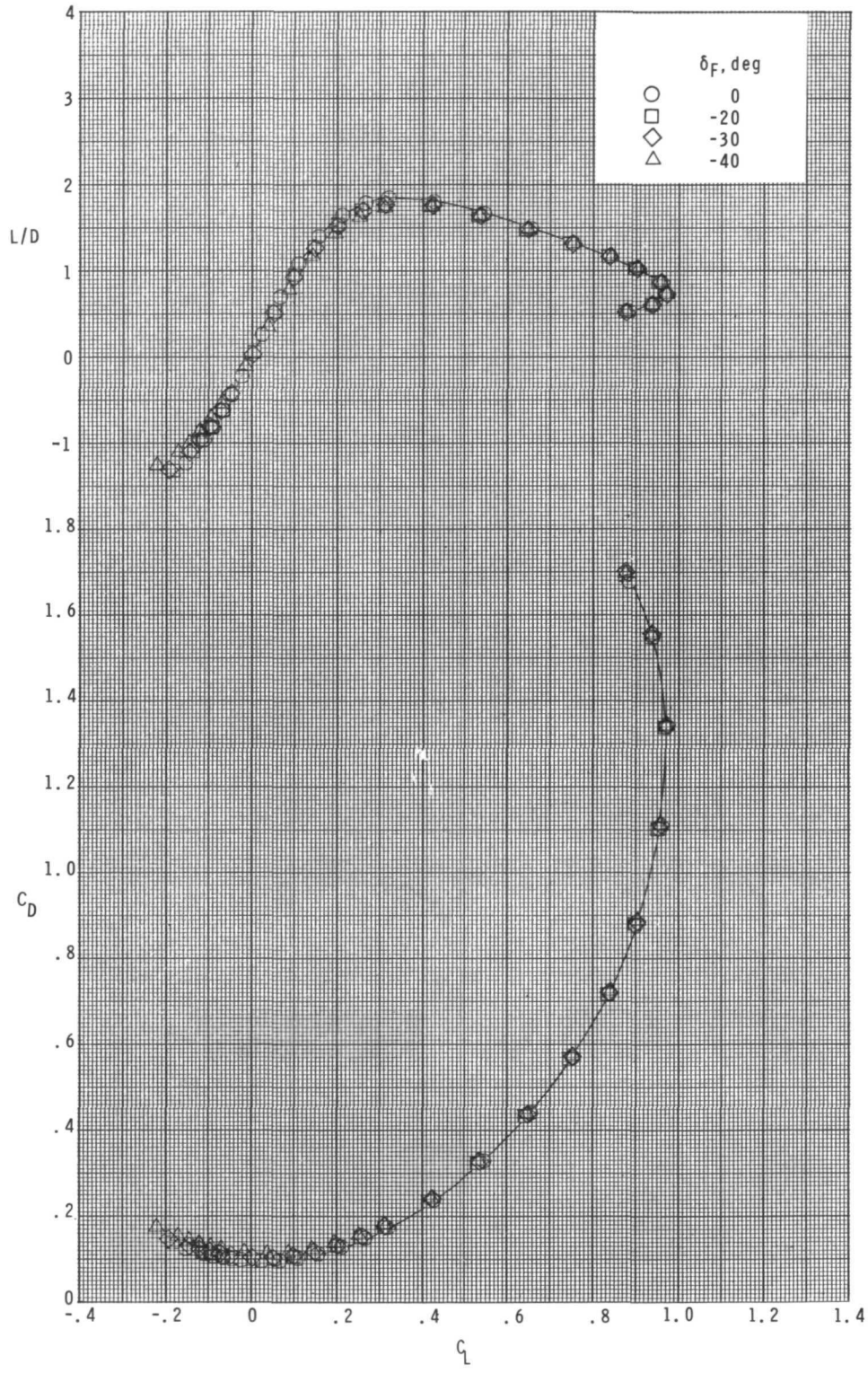

(c) Concluded.

Figure 8.- Continued.

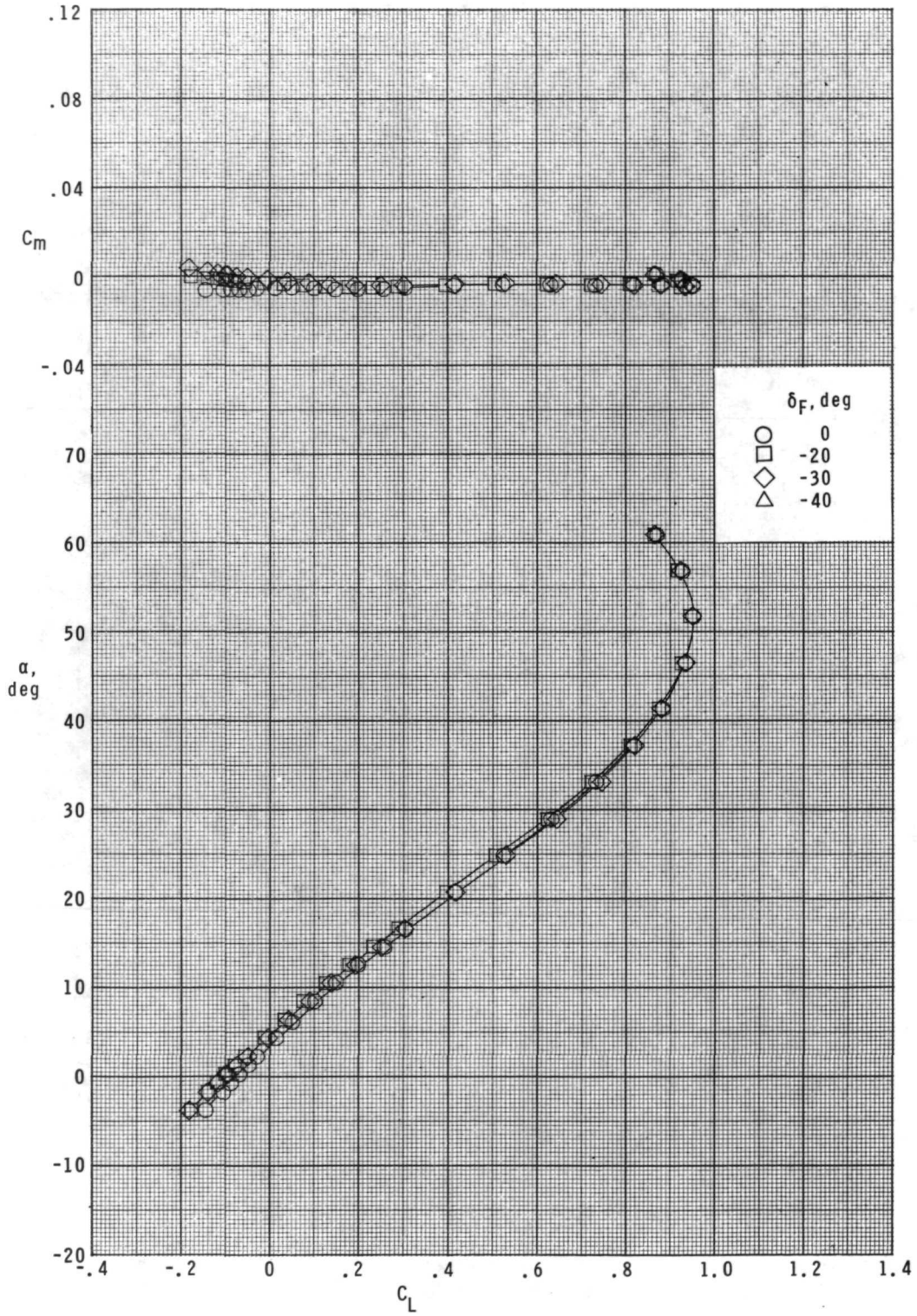

(d) M = 4.60.

Figure 8.- Continued.

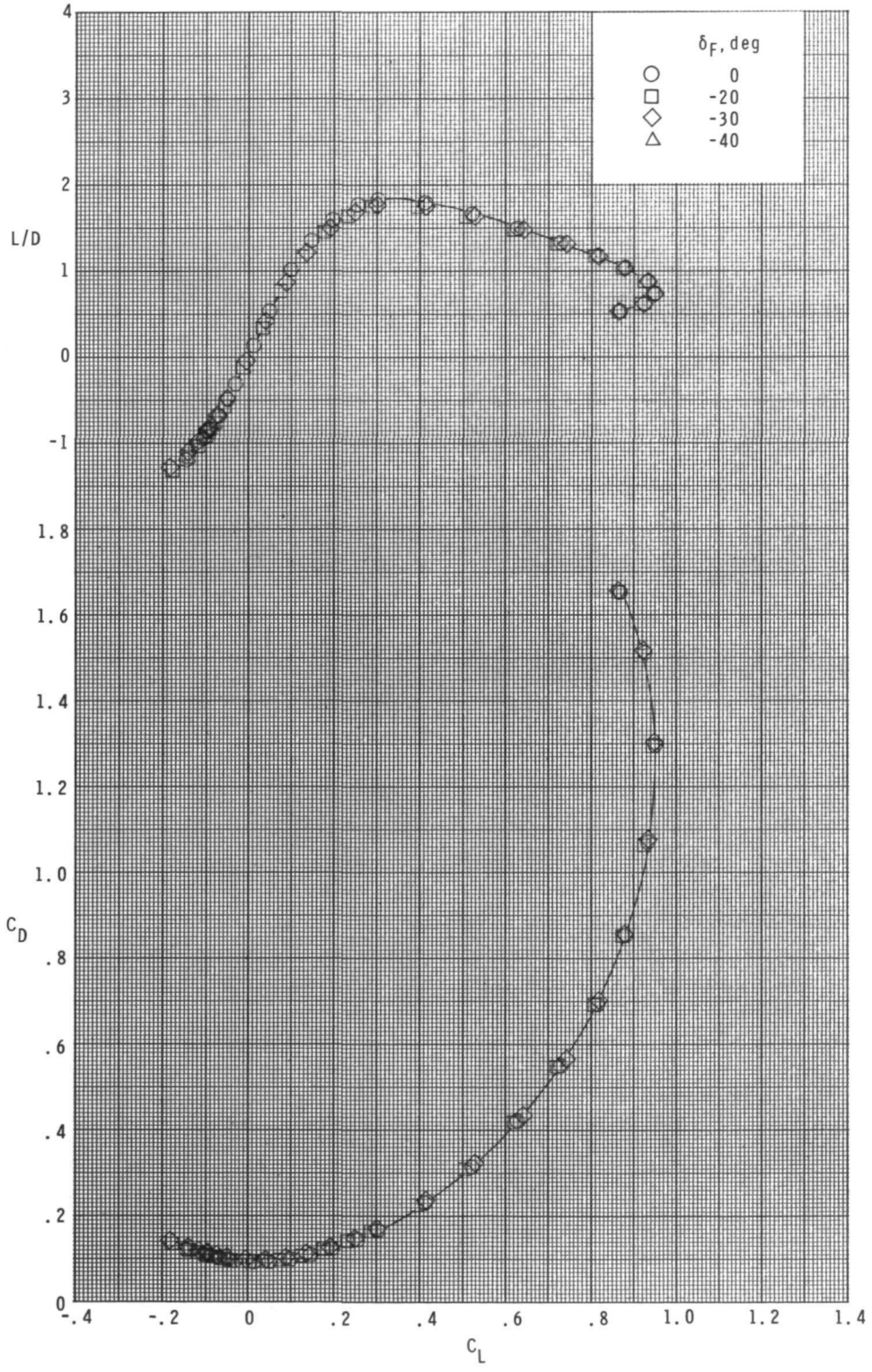

(d) Concluded.

Figure 8.- Concluded.

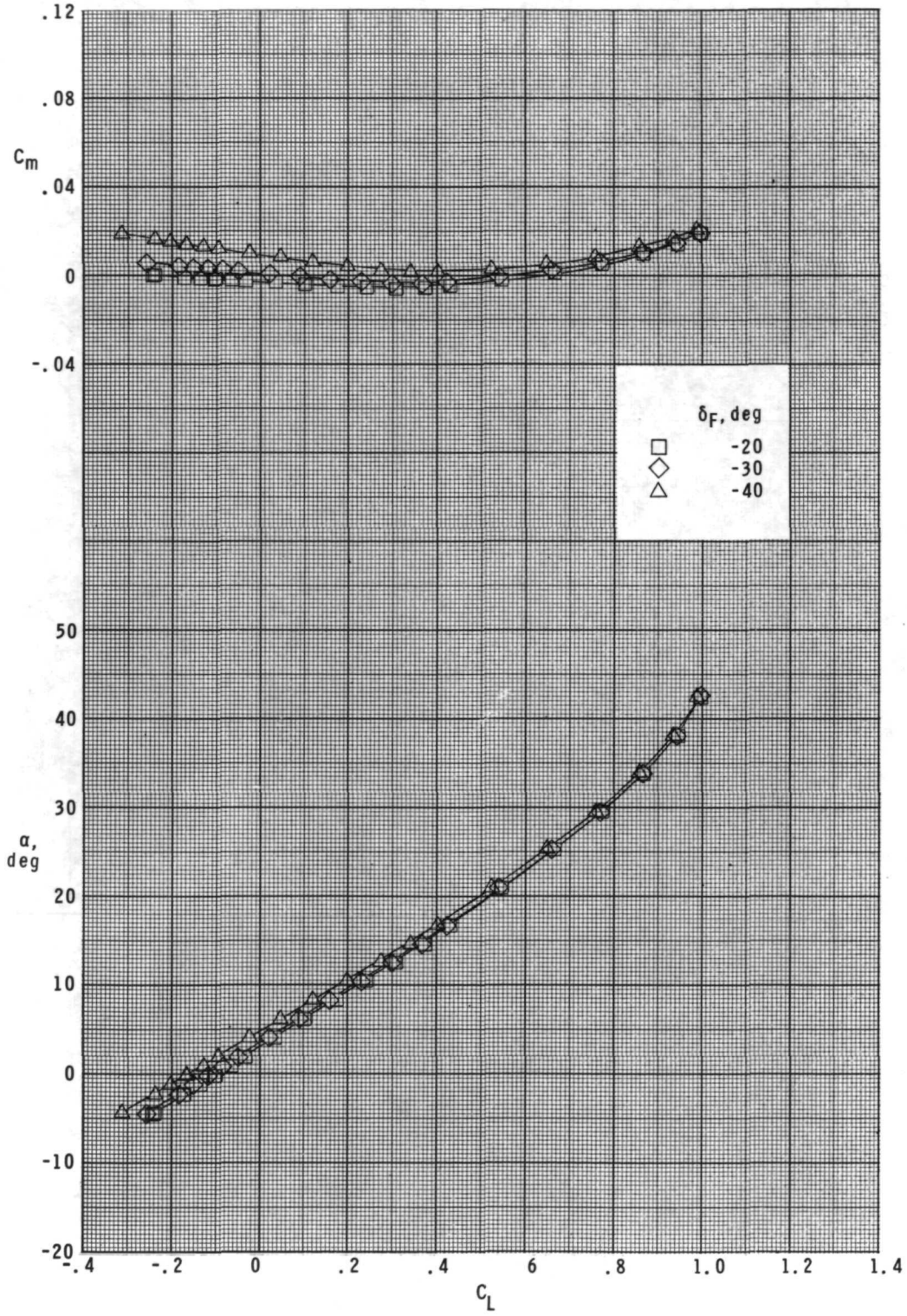

(a) M = 2.30.

Figure 9.- Effect of upper flap deflection on pitch characteristics. $\delta_E = -10^o$; $\delta_{R,L} = -20^o$; $\delta_{R,R} = +20^o$.

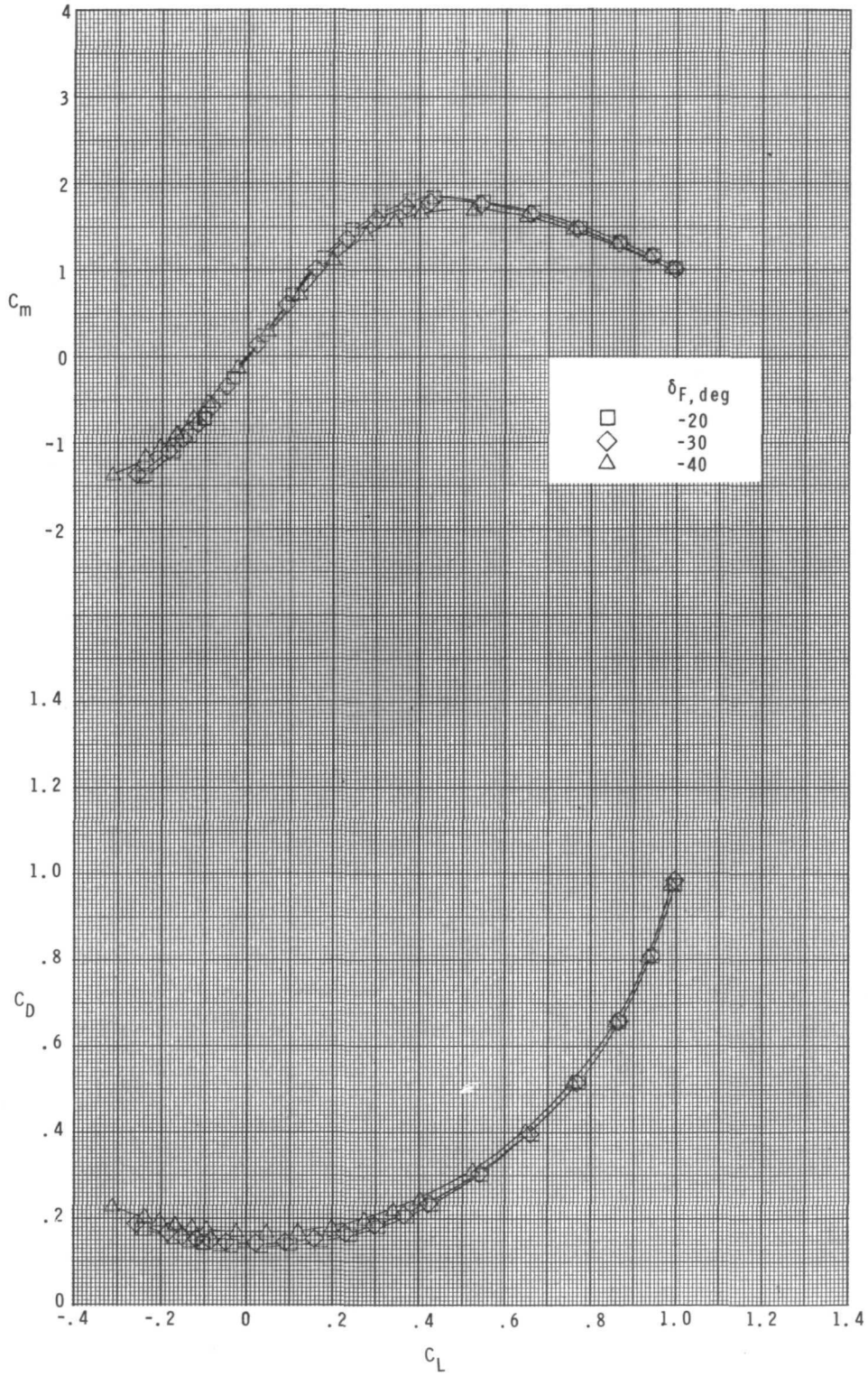

(a) Concluded.

Figure 9.- Continued.

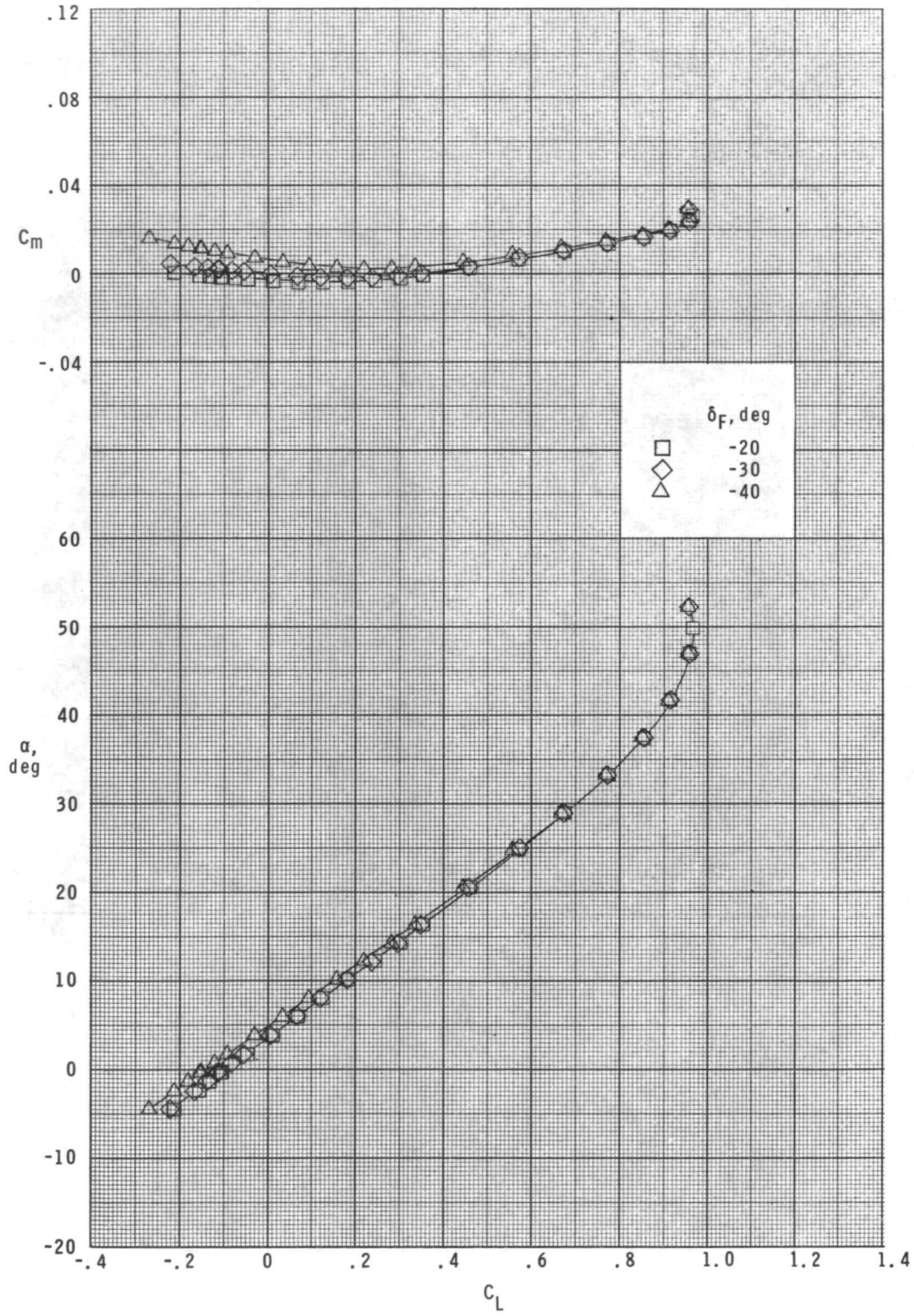

(b) M = 2.96.

Figure 9.- Continued.

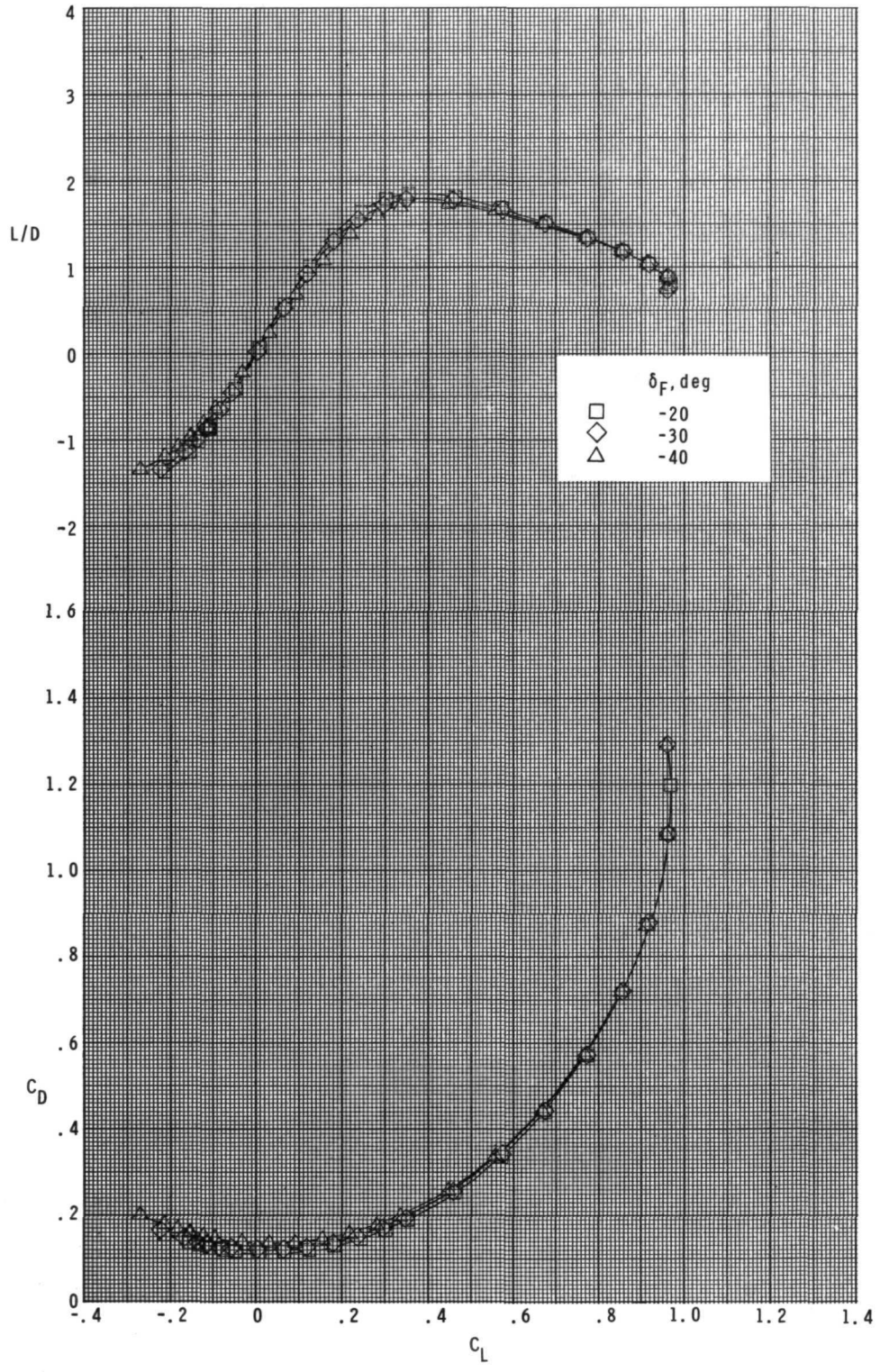

(b) Concluded.

Figure 9.- Continued.

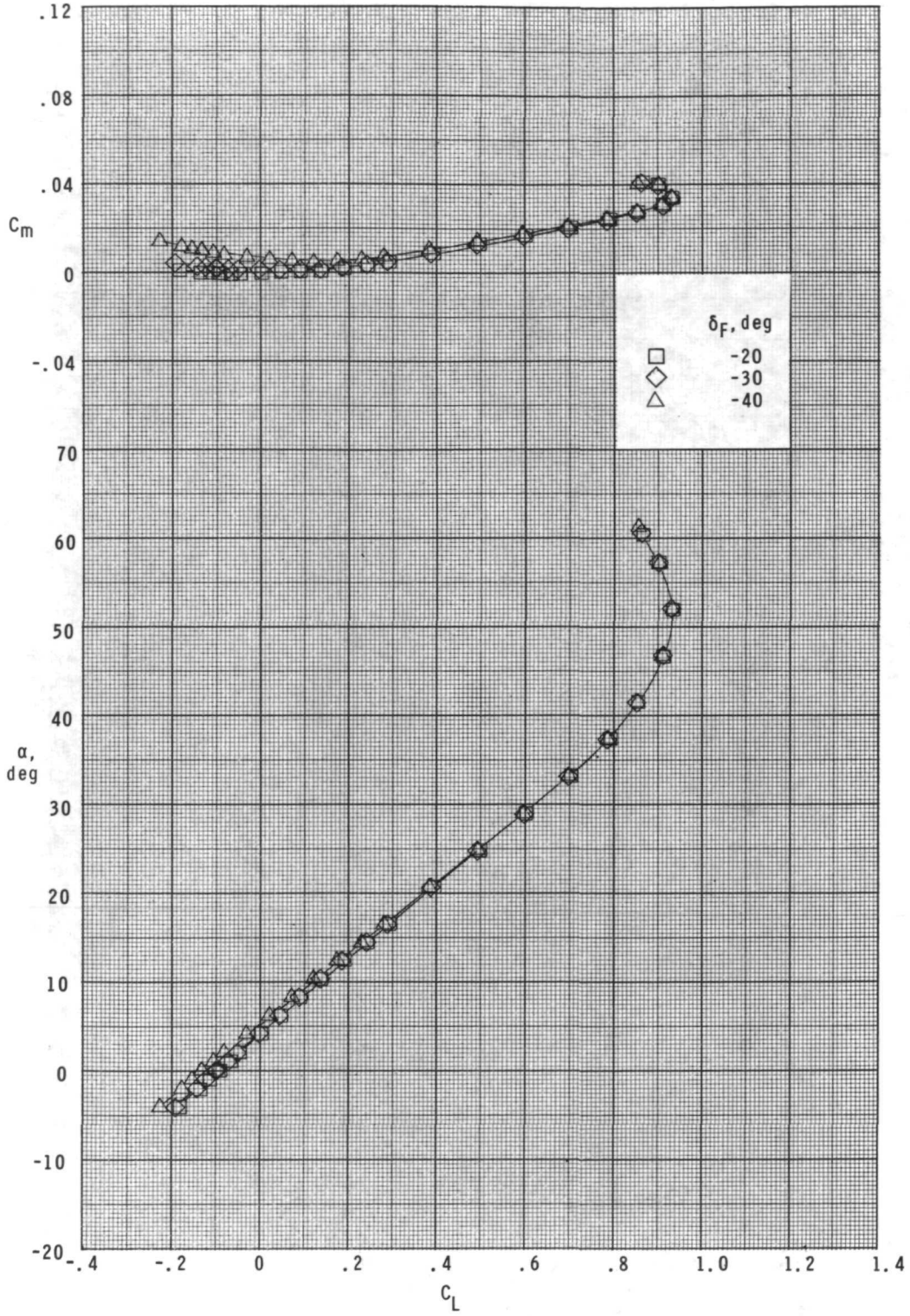

(c) M = 3.95.

Figure 9.- Continued.

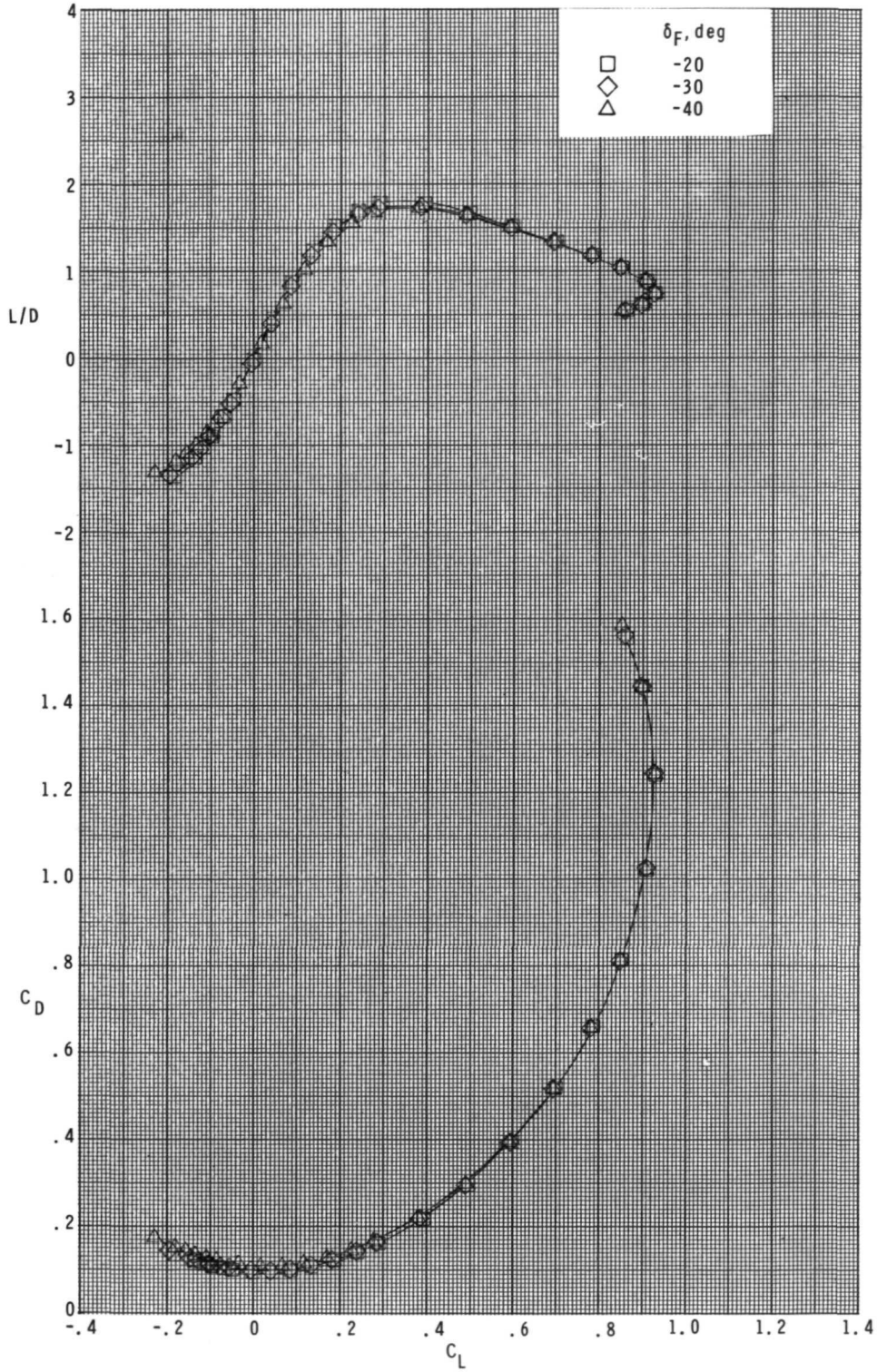

(c) Concluded.

Figure 9.- Continued.

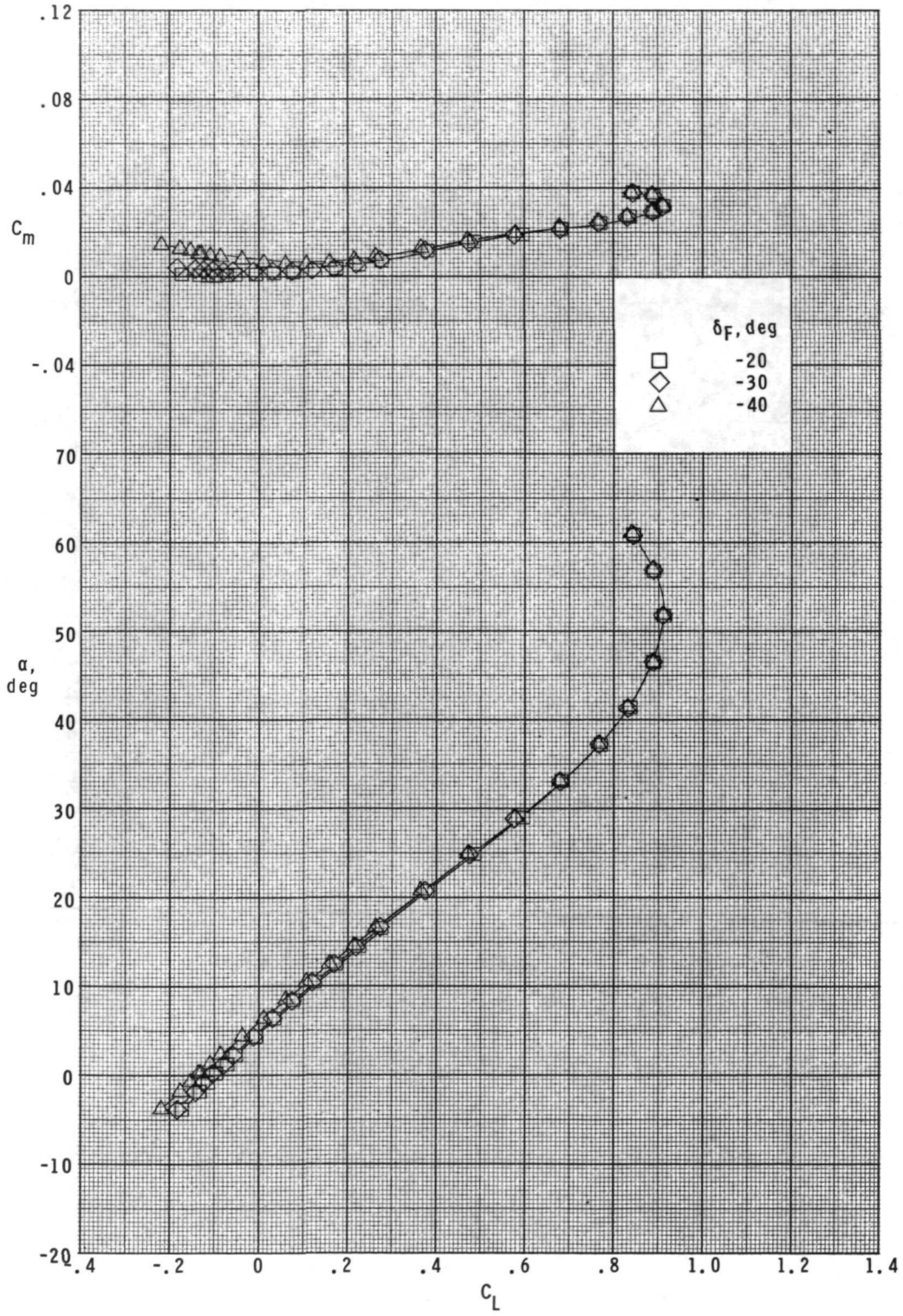

(d) M = 4.60.

Figure 9.- Continued.

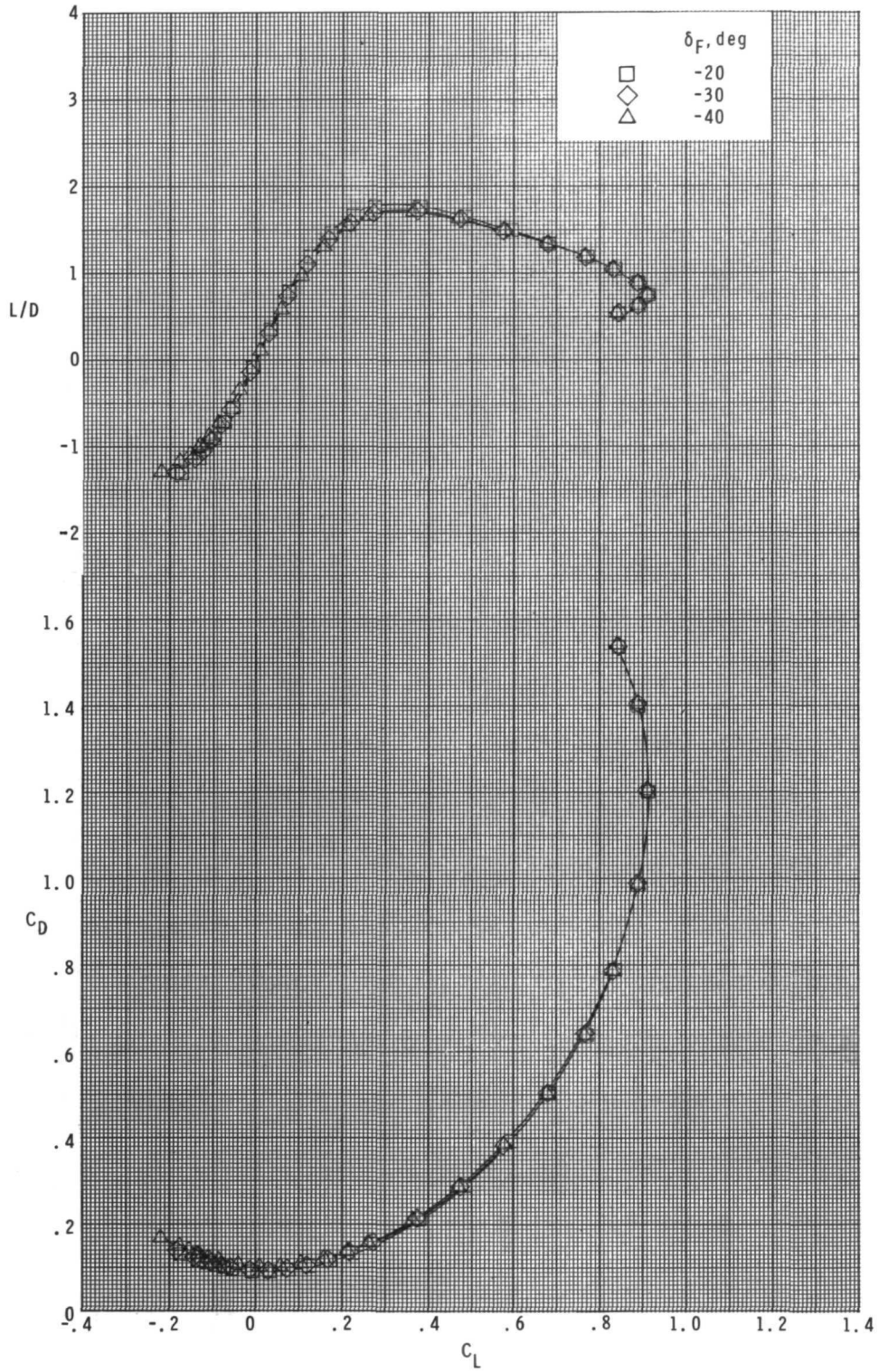

(d) Concluded.

Figure 9.- Concluded.

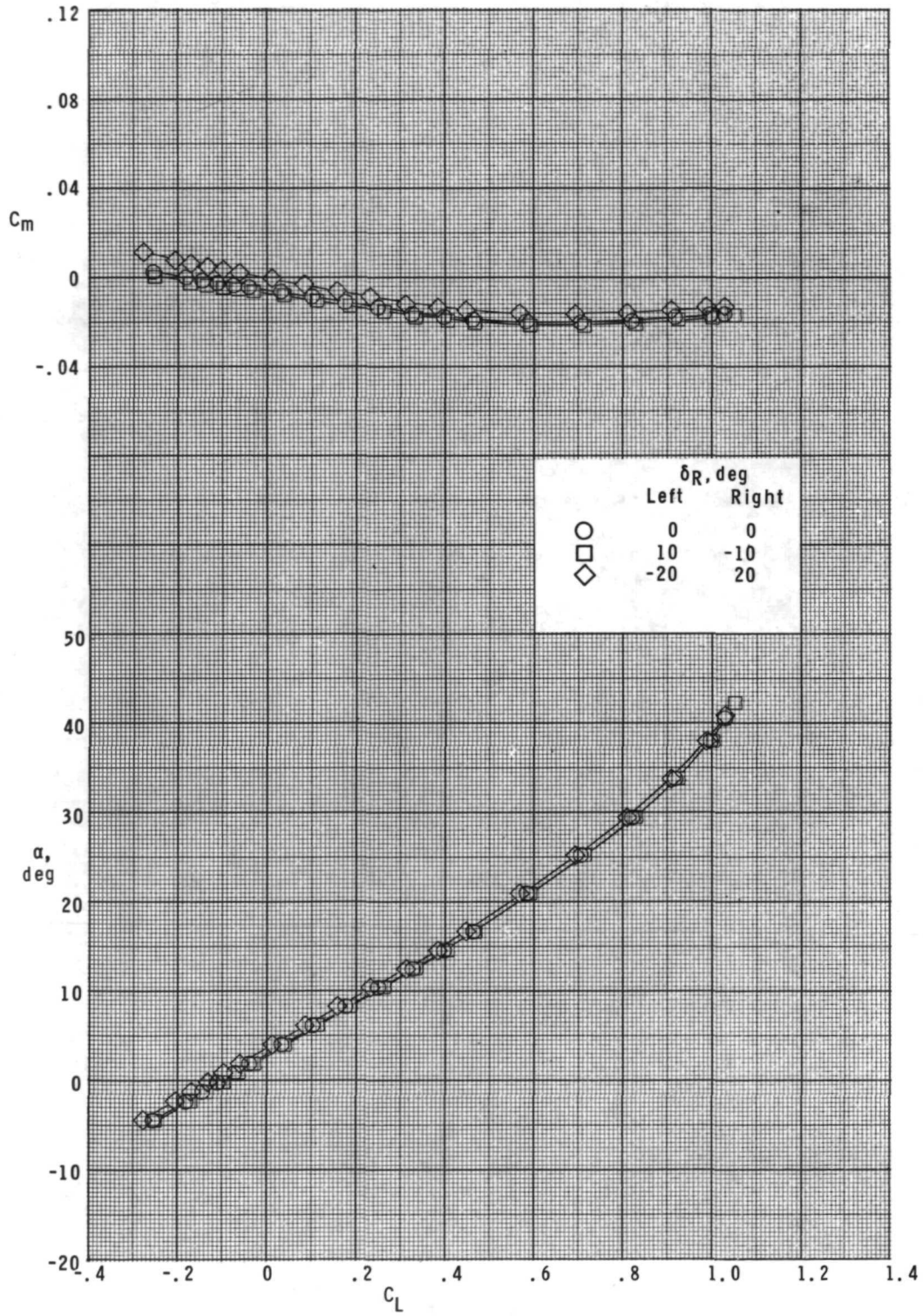

(a) M = 2.30.

Figure 10.- Effect of differential rudder deflections on pitch characteristics. $\delta_E = 0^o$; $\delta_F = -40^o$.

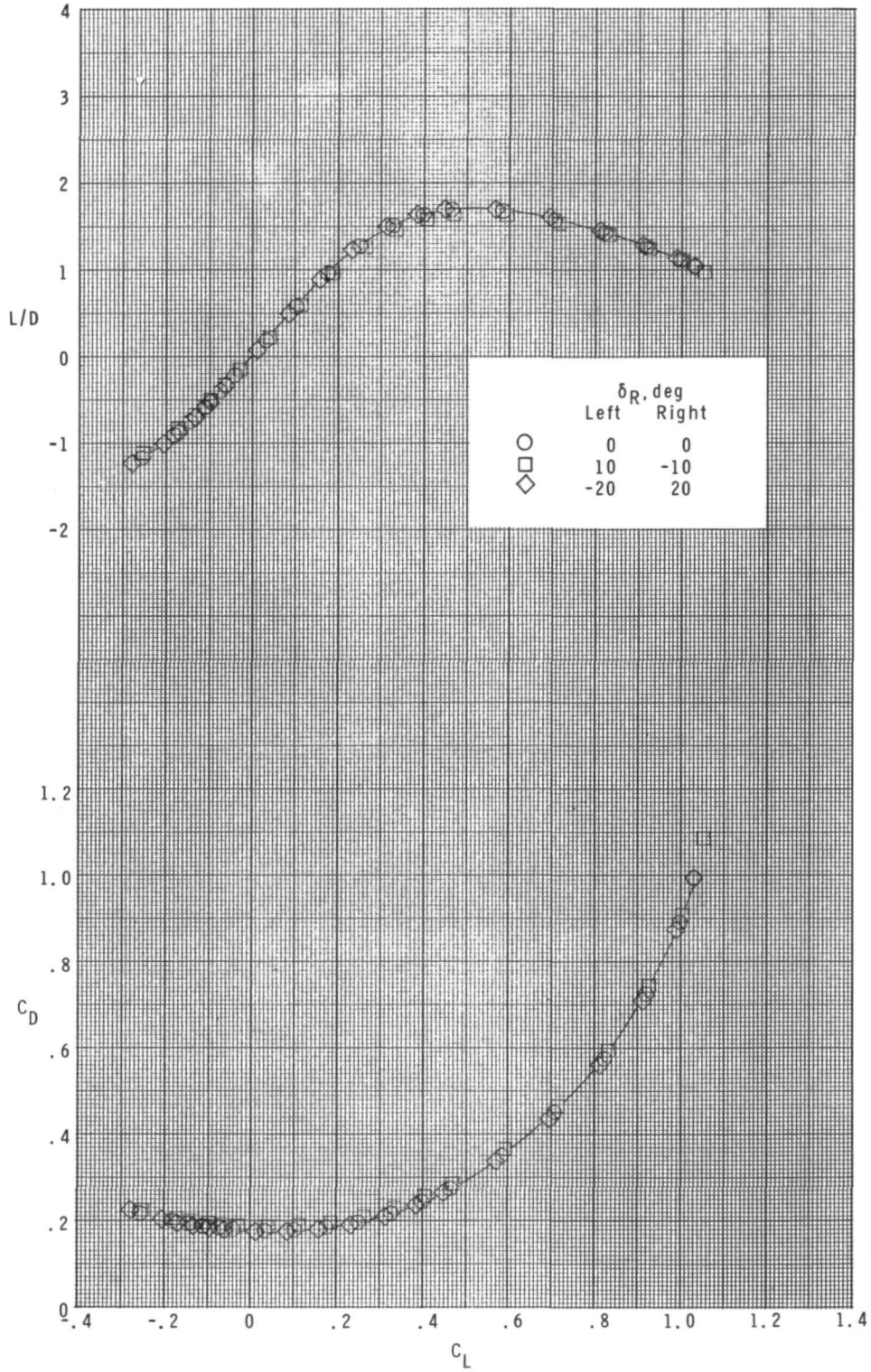

(a) Concluded.

Figure 10.- Continued.

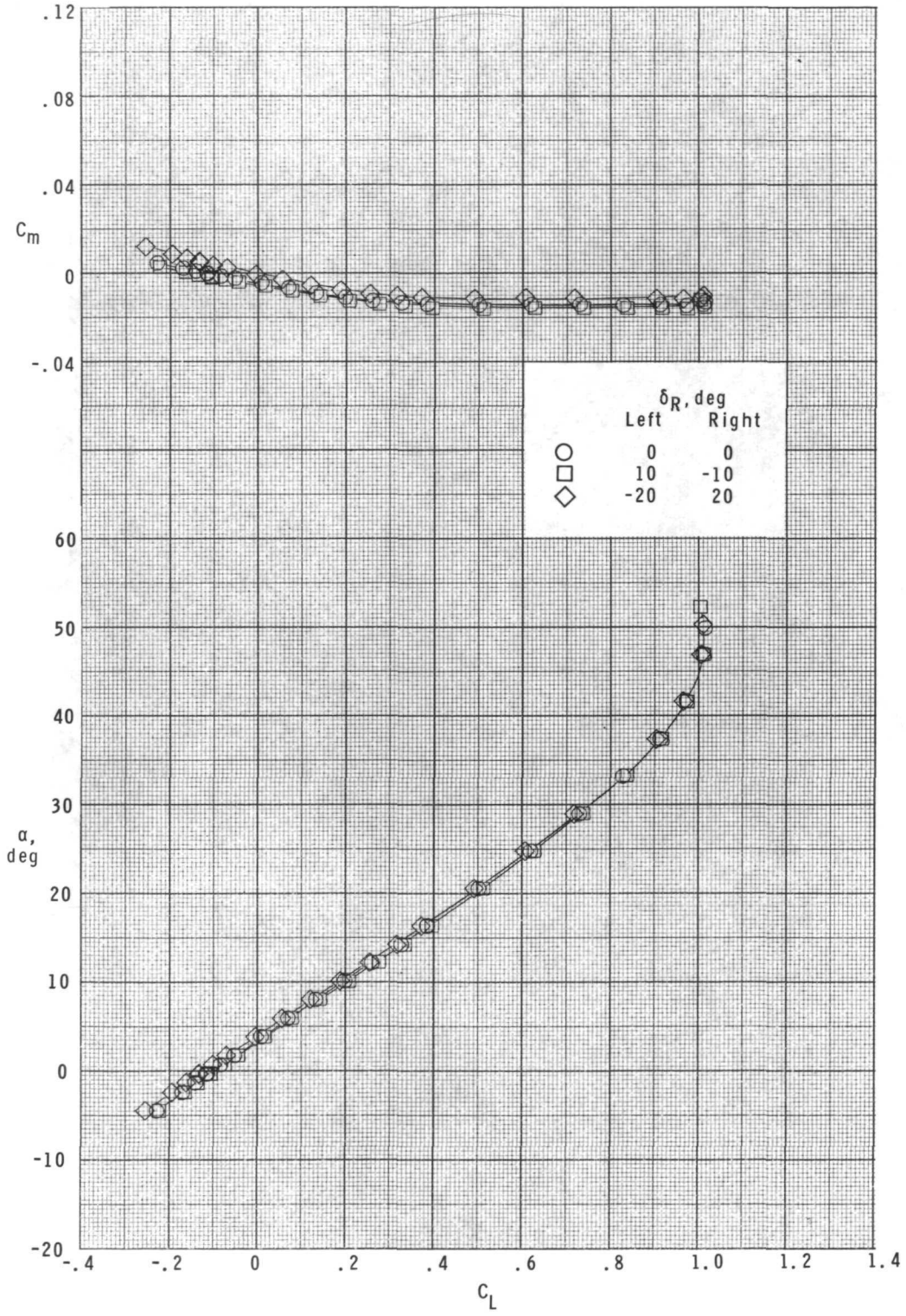

(b) M = 2.96.

Figure 10.- Continued.

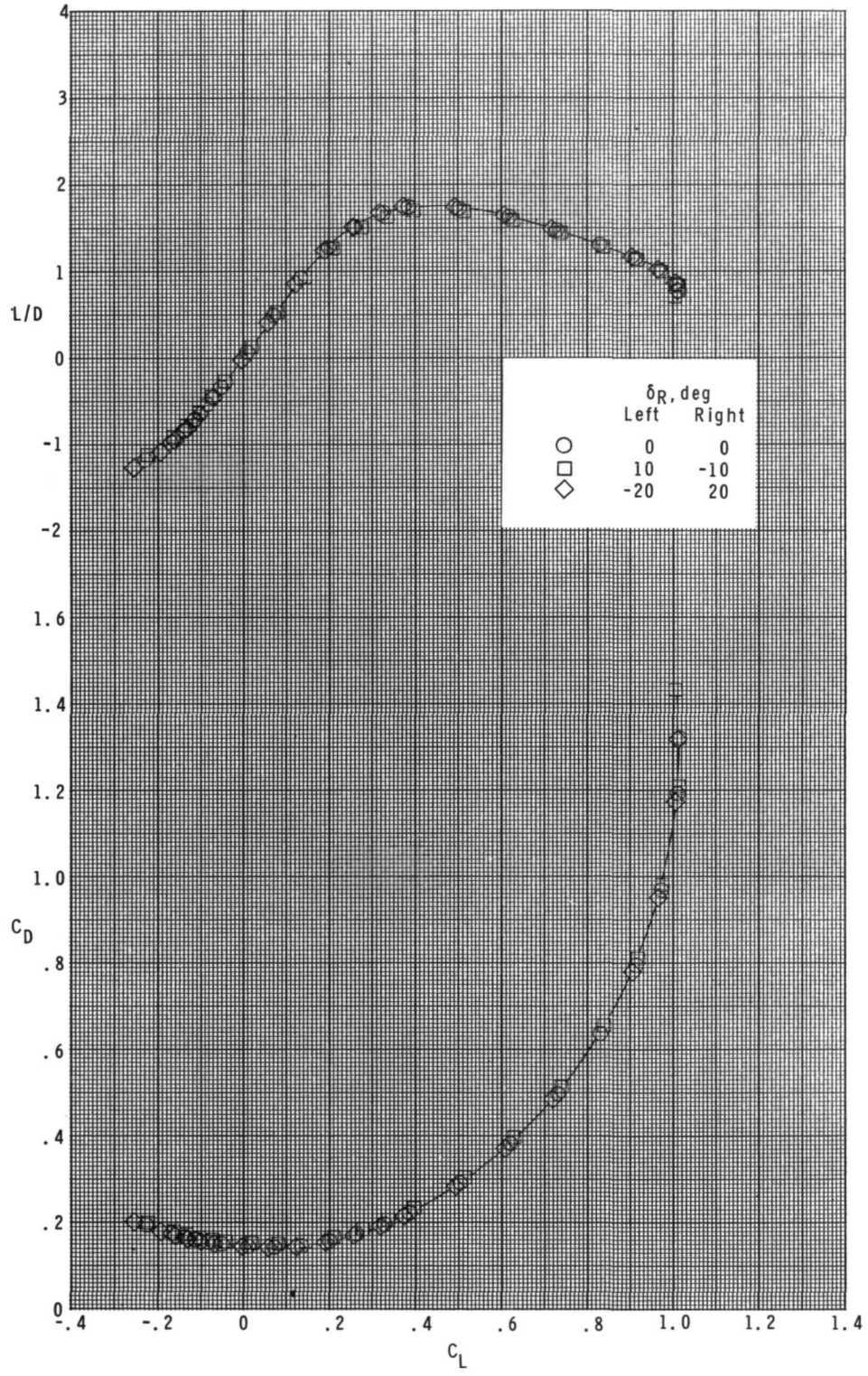

(b) Concluded.

Figure 10.- Continued.

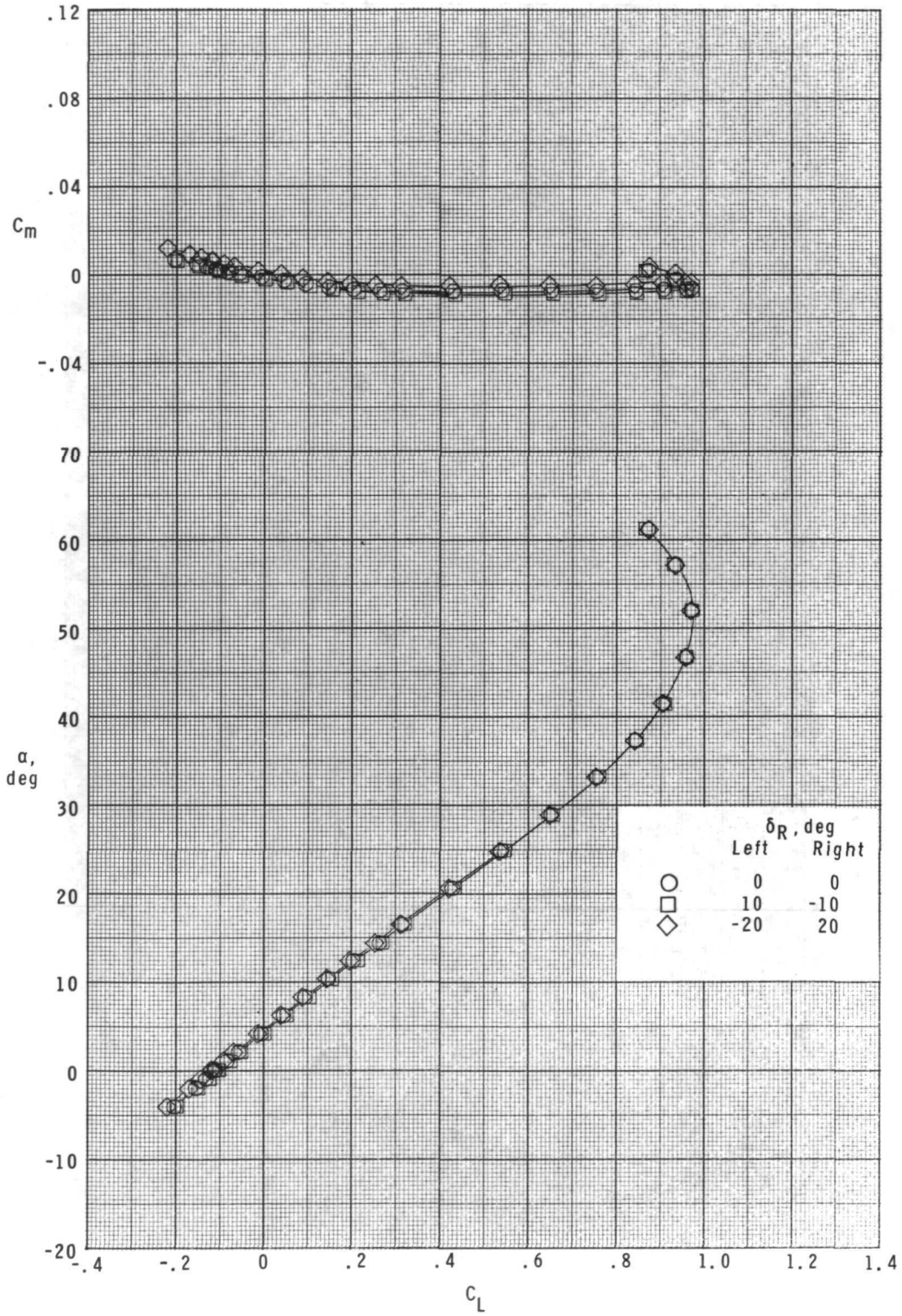

(c) M = 3.95.

Figure 10.- Continued.

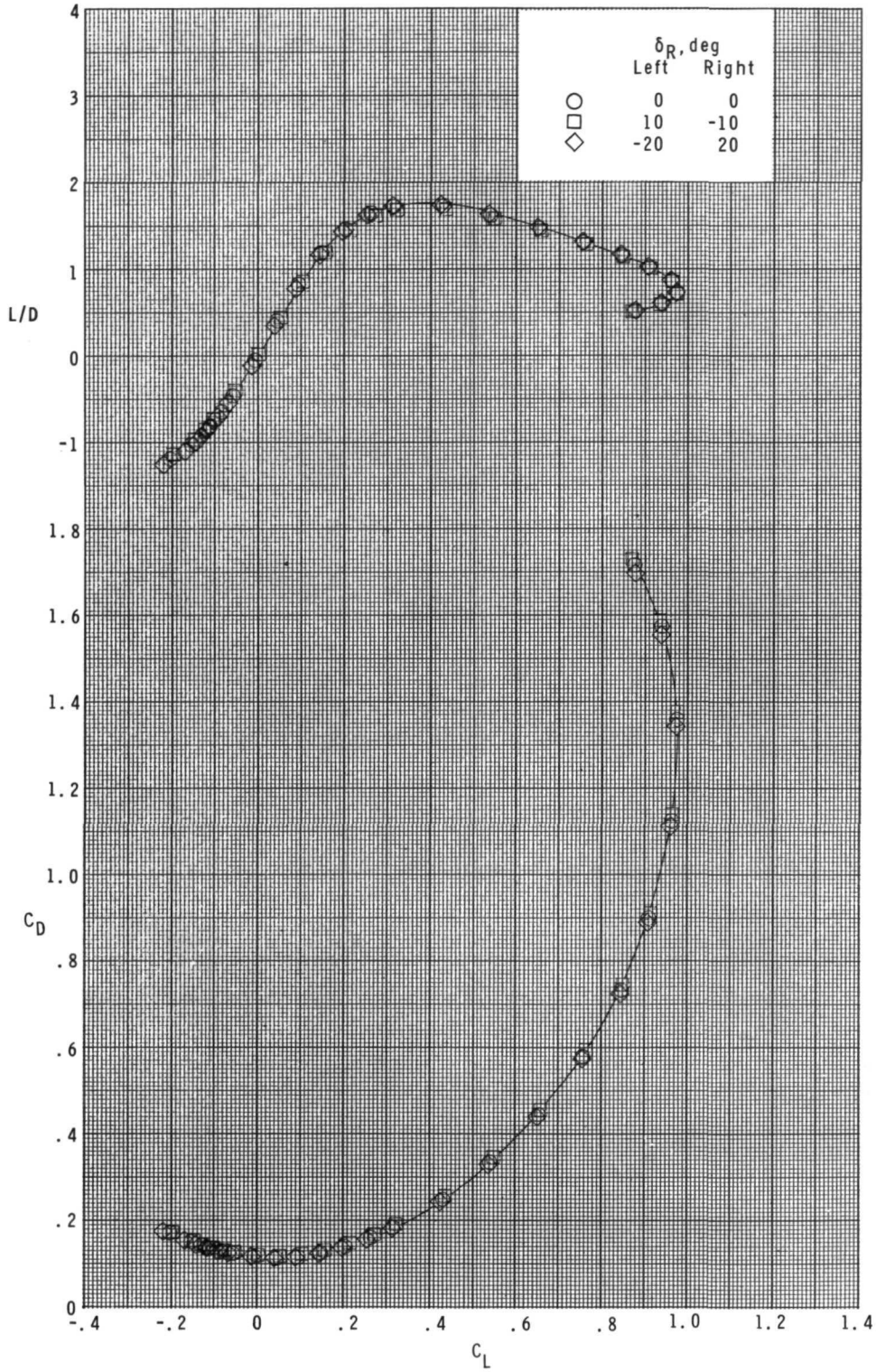

(c) Concluded.

Figure 10.- Continued.

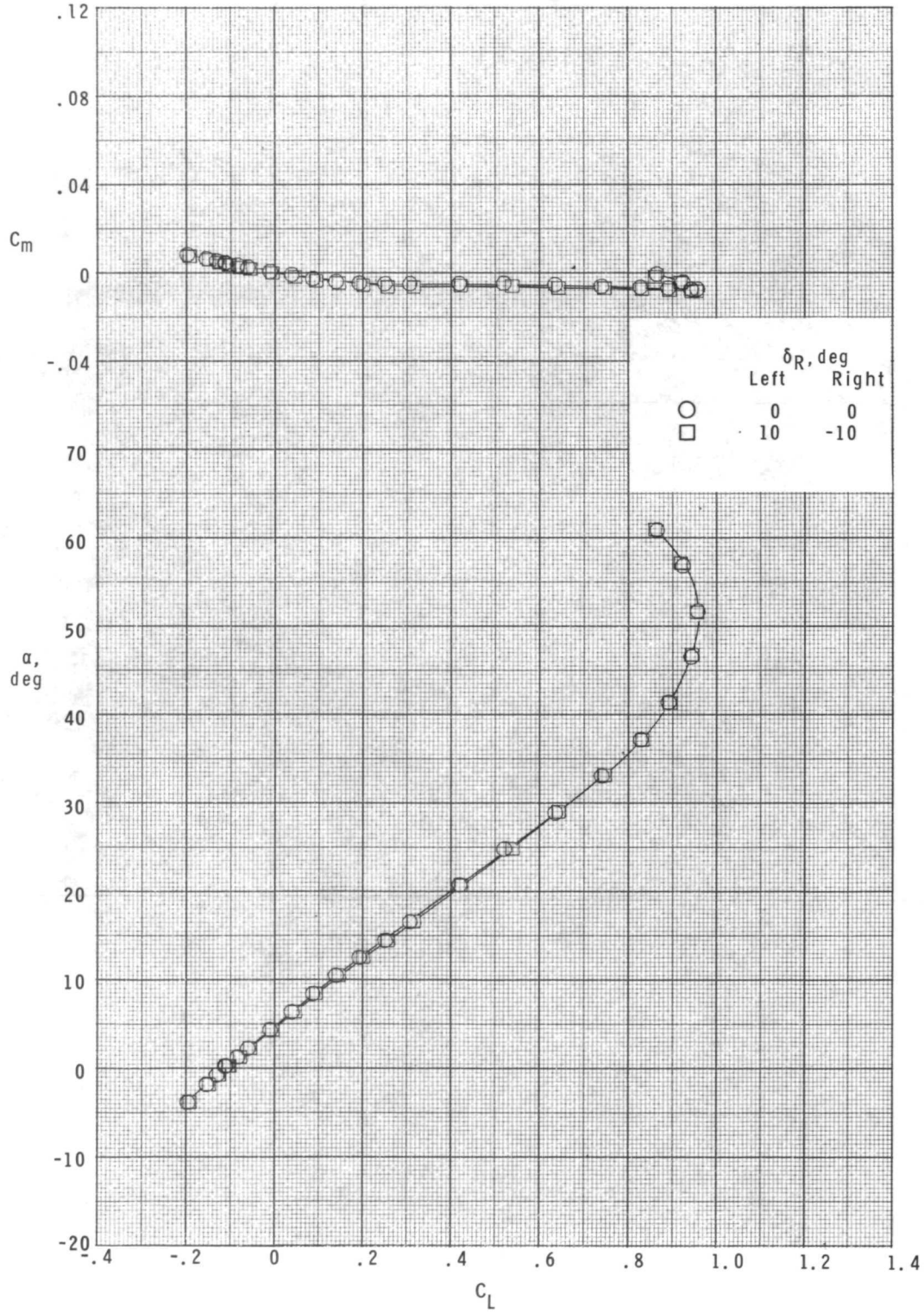

(d) M = 4.60.

Figure 10.- Continued.

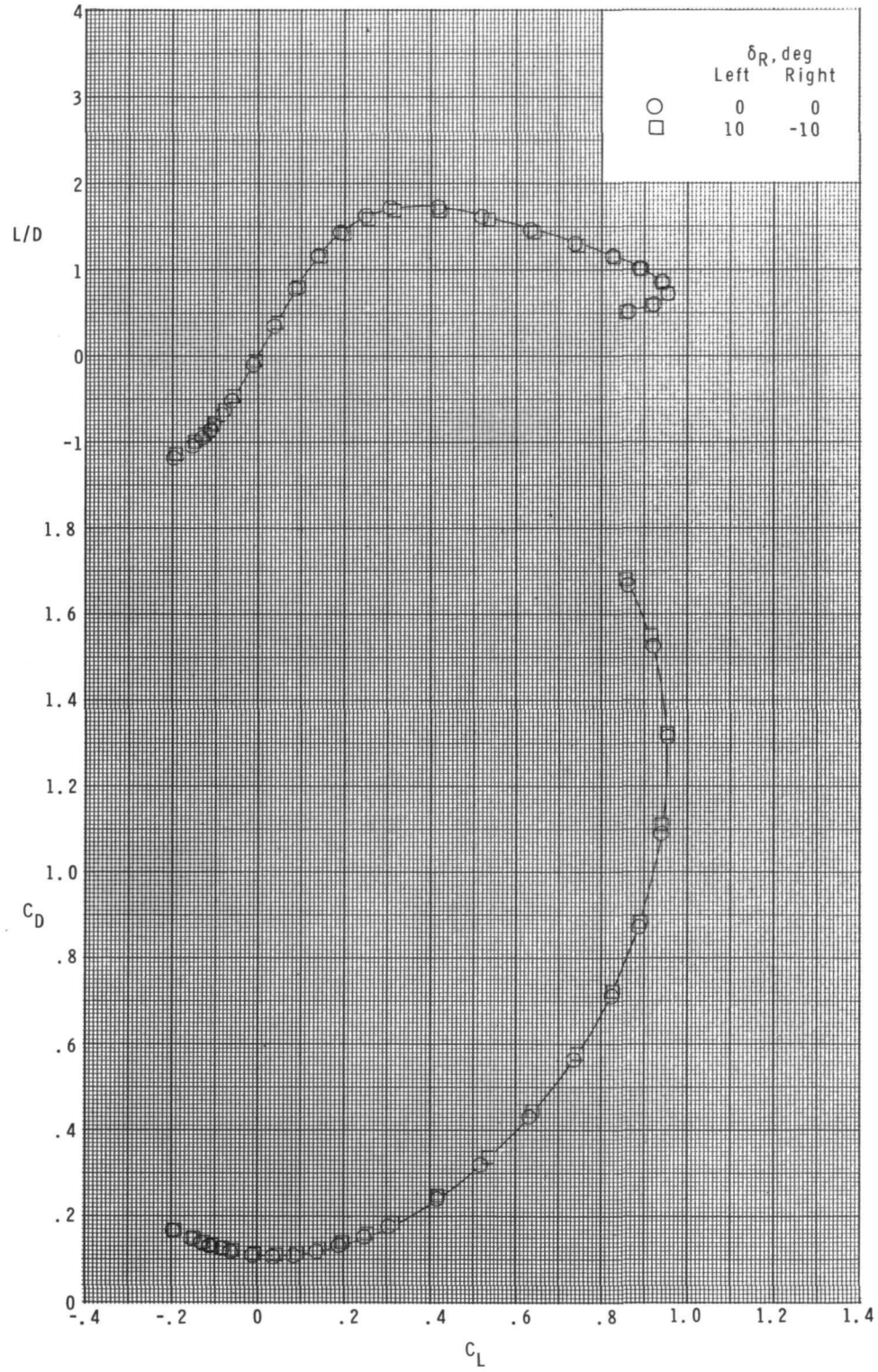

(d) Concluded.

Figure 10.- Concluded.

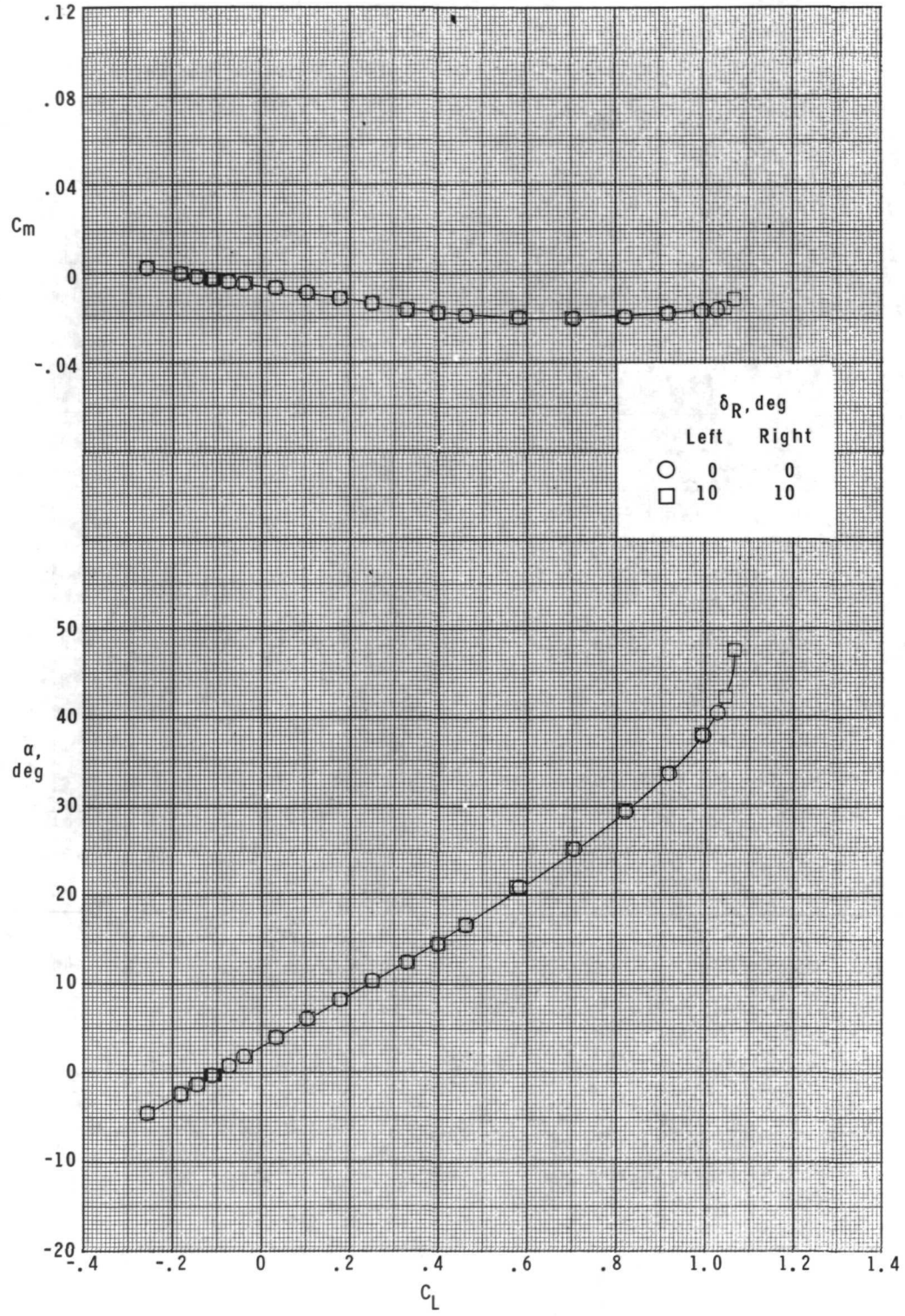

(a) M = 2.30.

Figure 11.- Effect of rudder deflection on pitch characteristics. $\delta_E = 0^o$; $\delta_F = -40^o$.

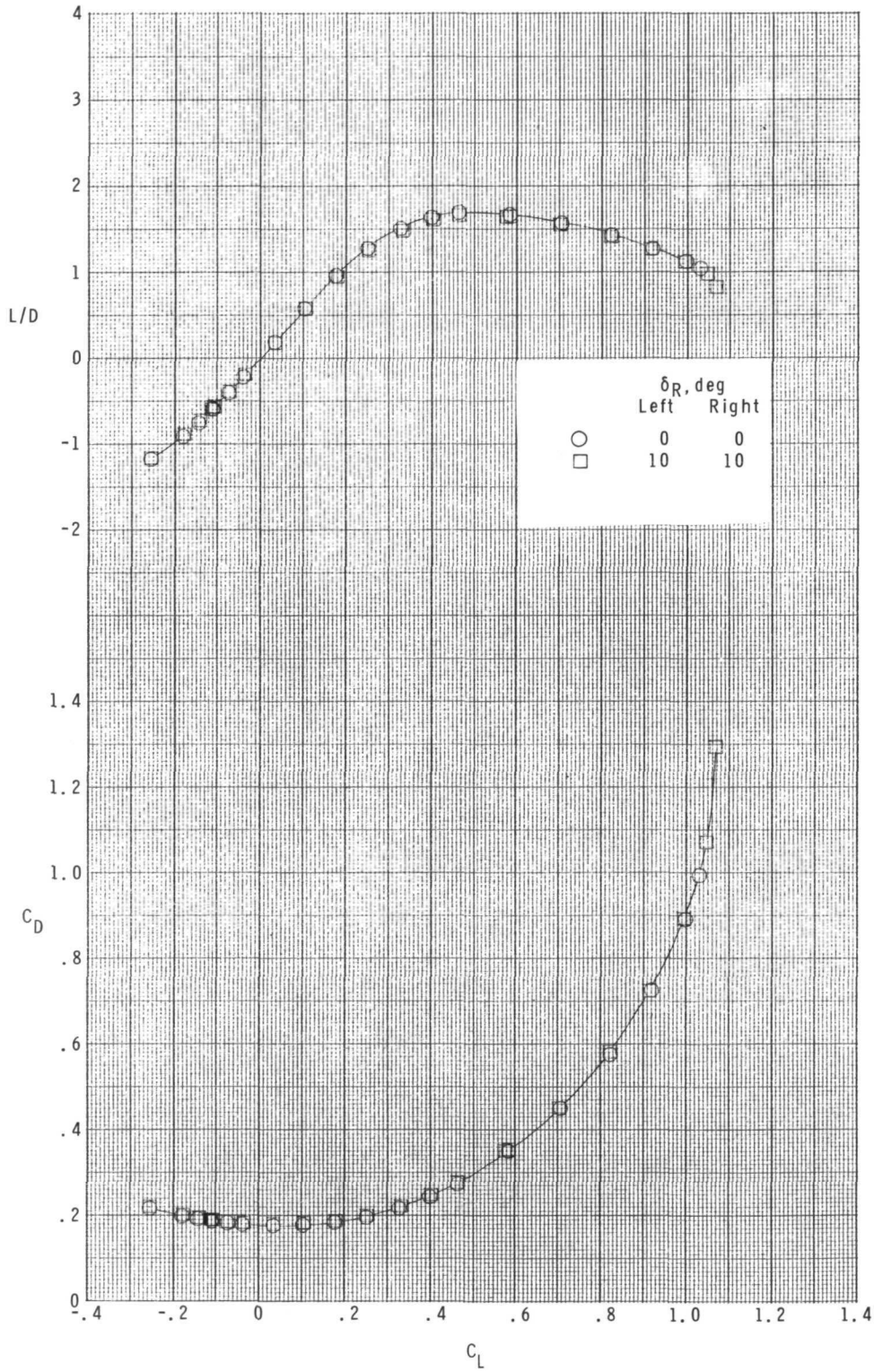

(a) Concluded.

Figure 11.- Continued.

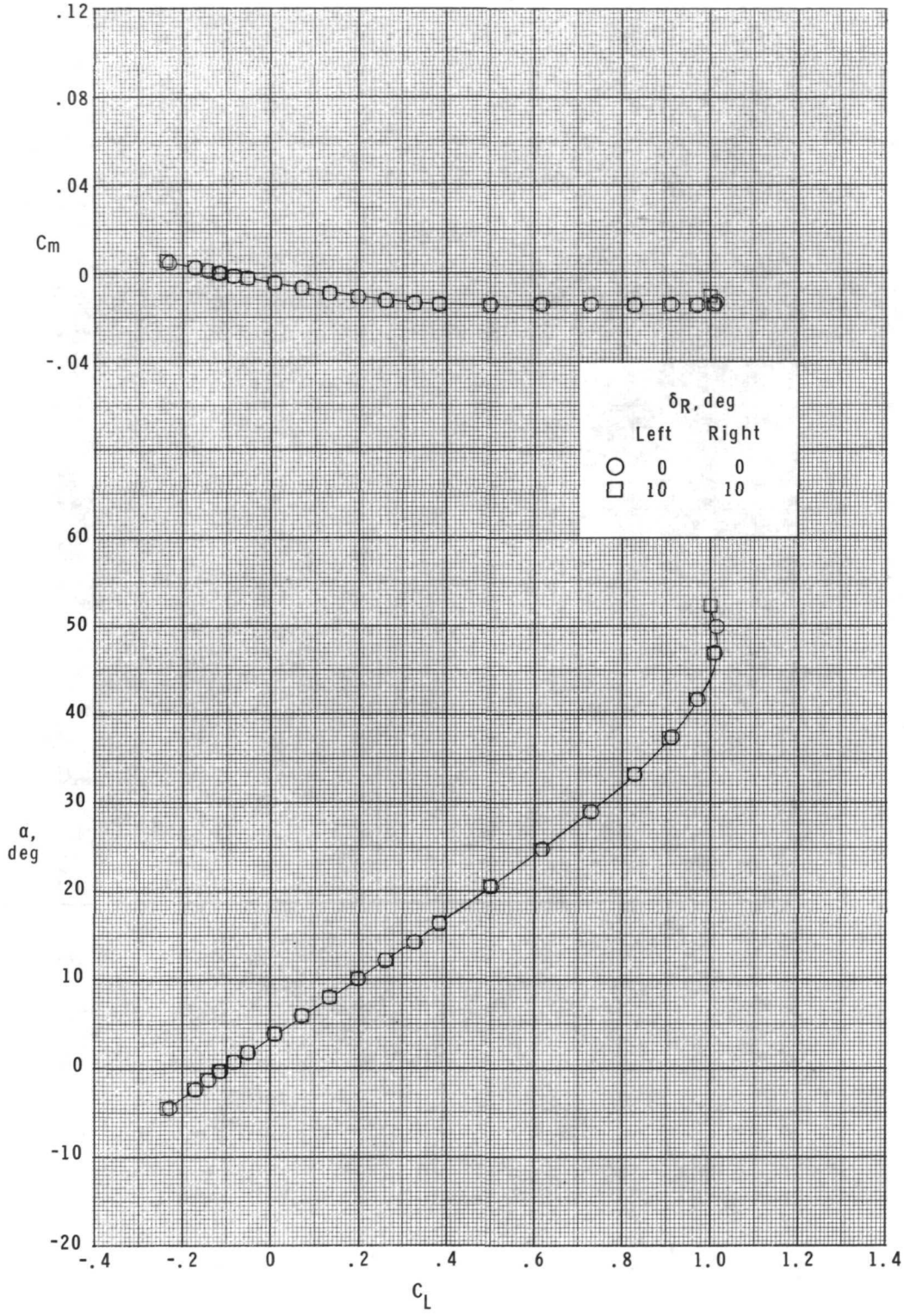

(b) M = 2.96.

Figure 11.- Continued.

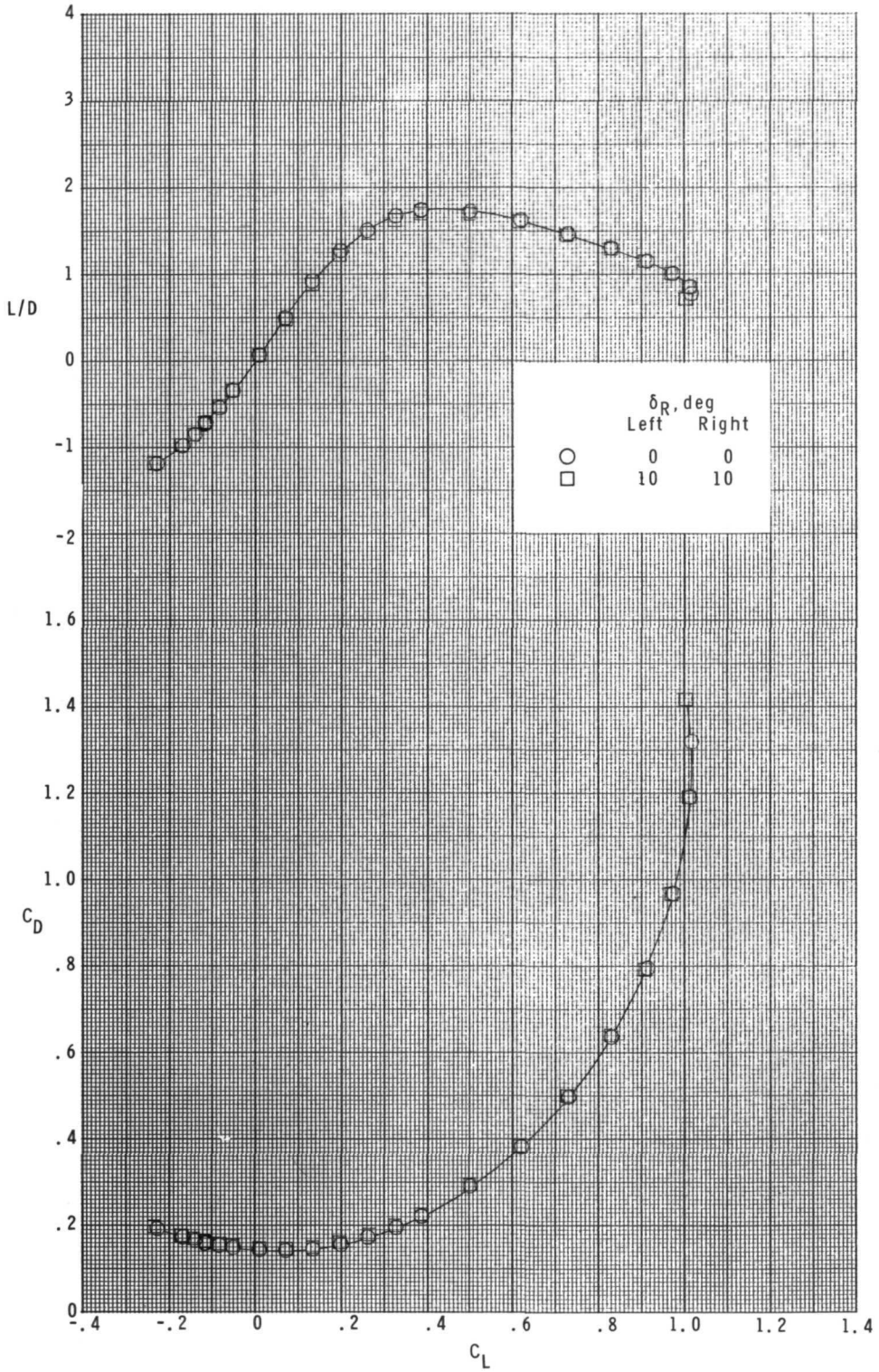

(b) Concluded.

Figure 11.- Continued.

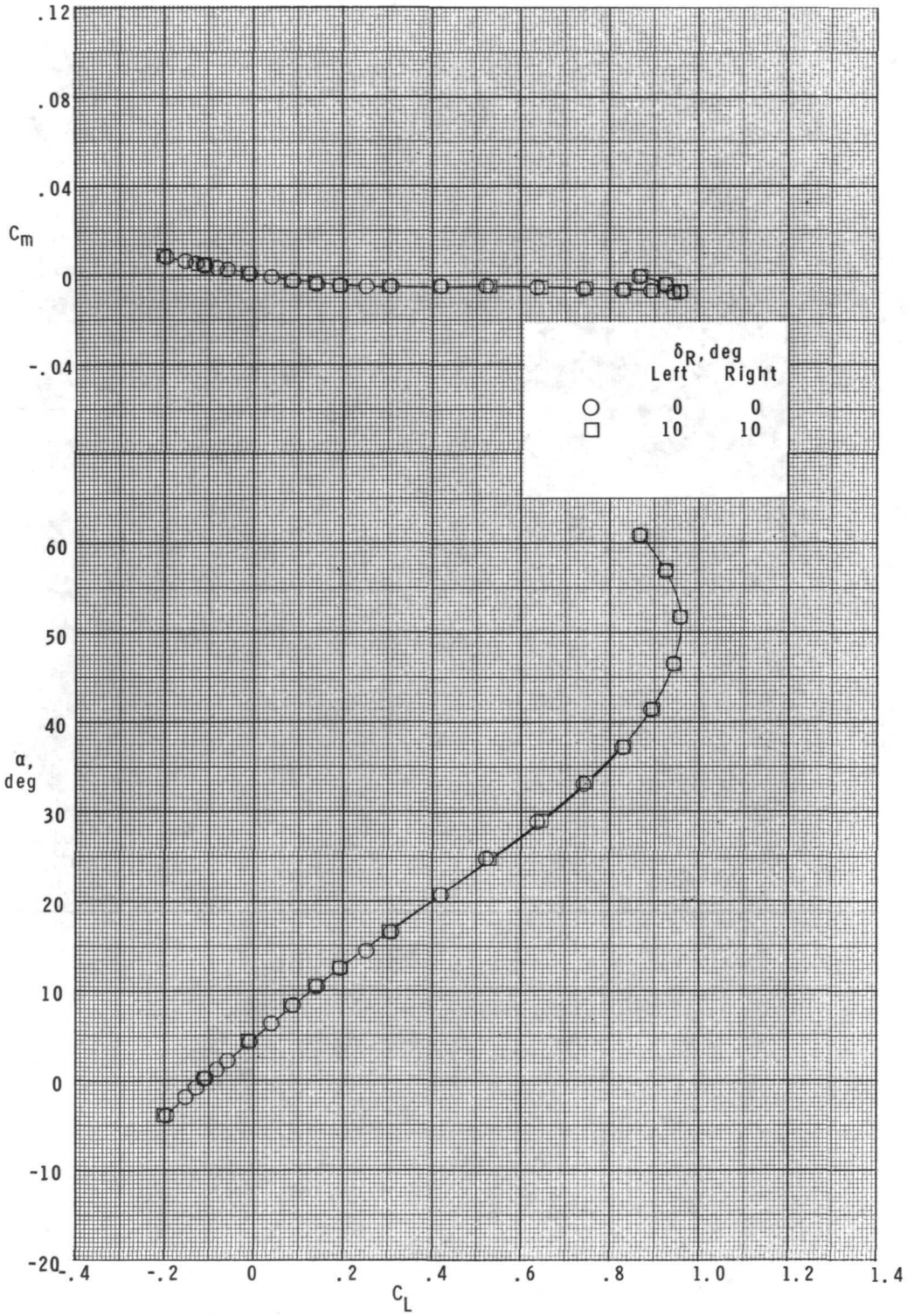

(c) M = 4.60.

Figure 11.- Continued.

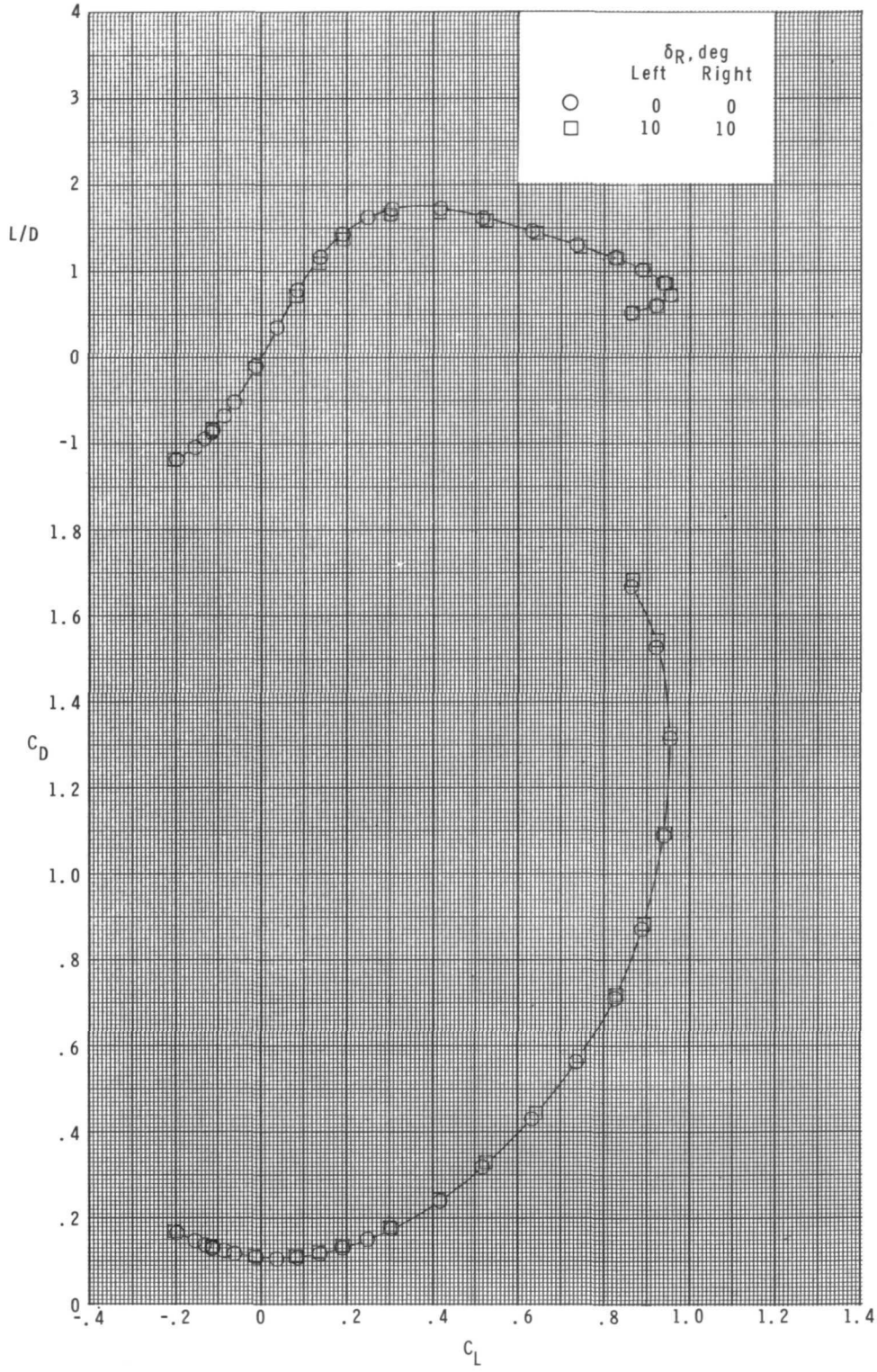

(c) Concluded.

Figure 11.- Concluded.

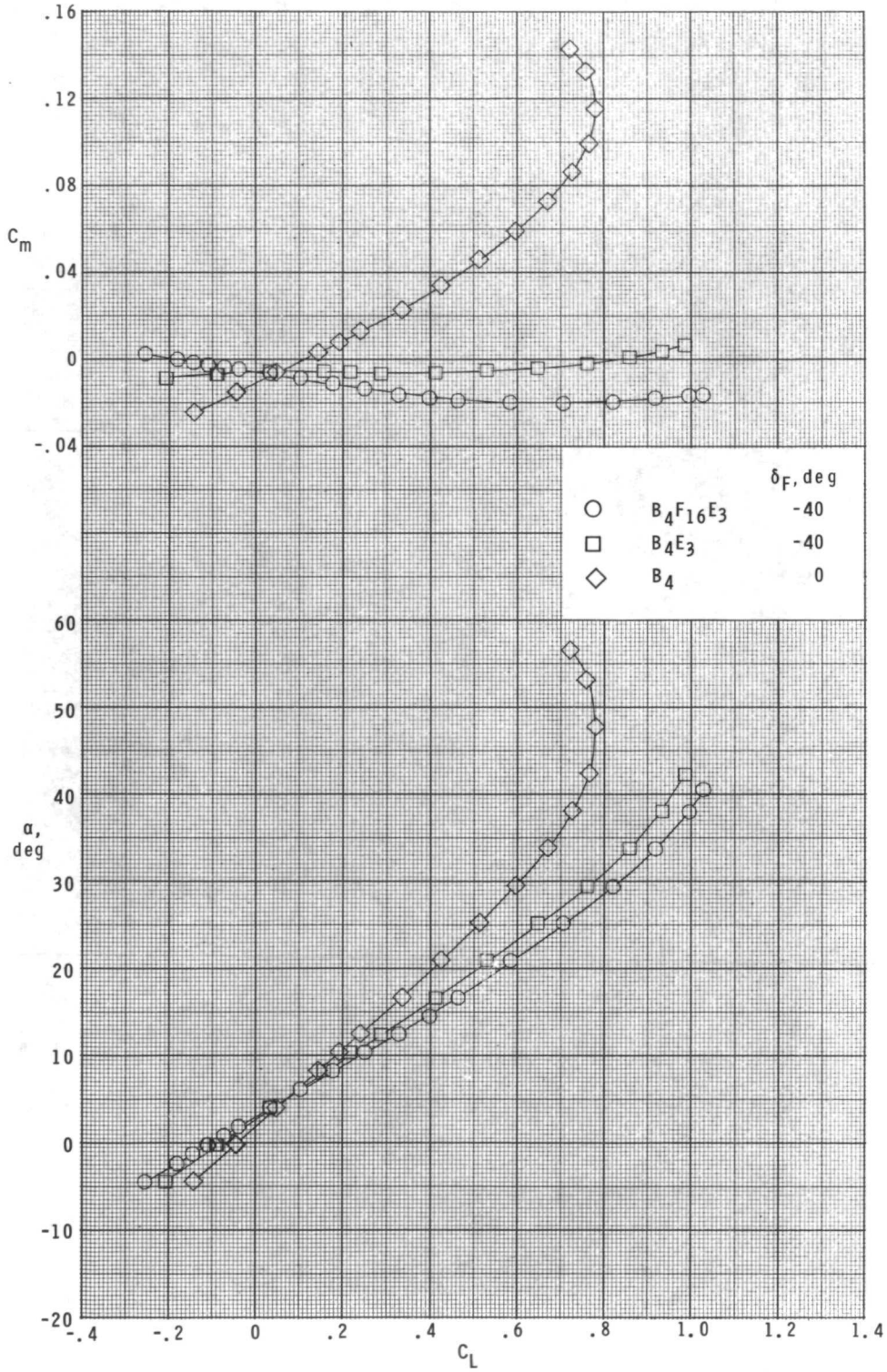

(a) M = 2.30.

Figure 12.- Effect of fins and lower flap on pitch characteristics. $\delta_E = 0^o$; $\delta_{R,L} = 0^o$; $\delta_{R,R} = 0^o$.

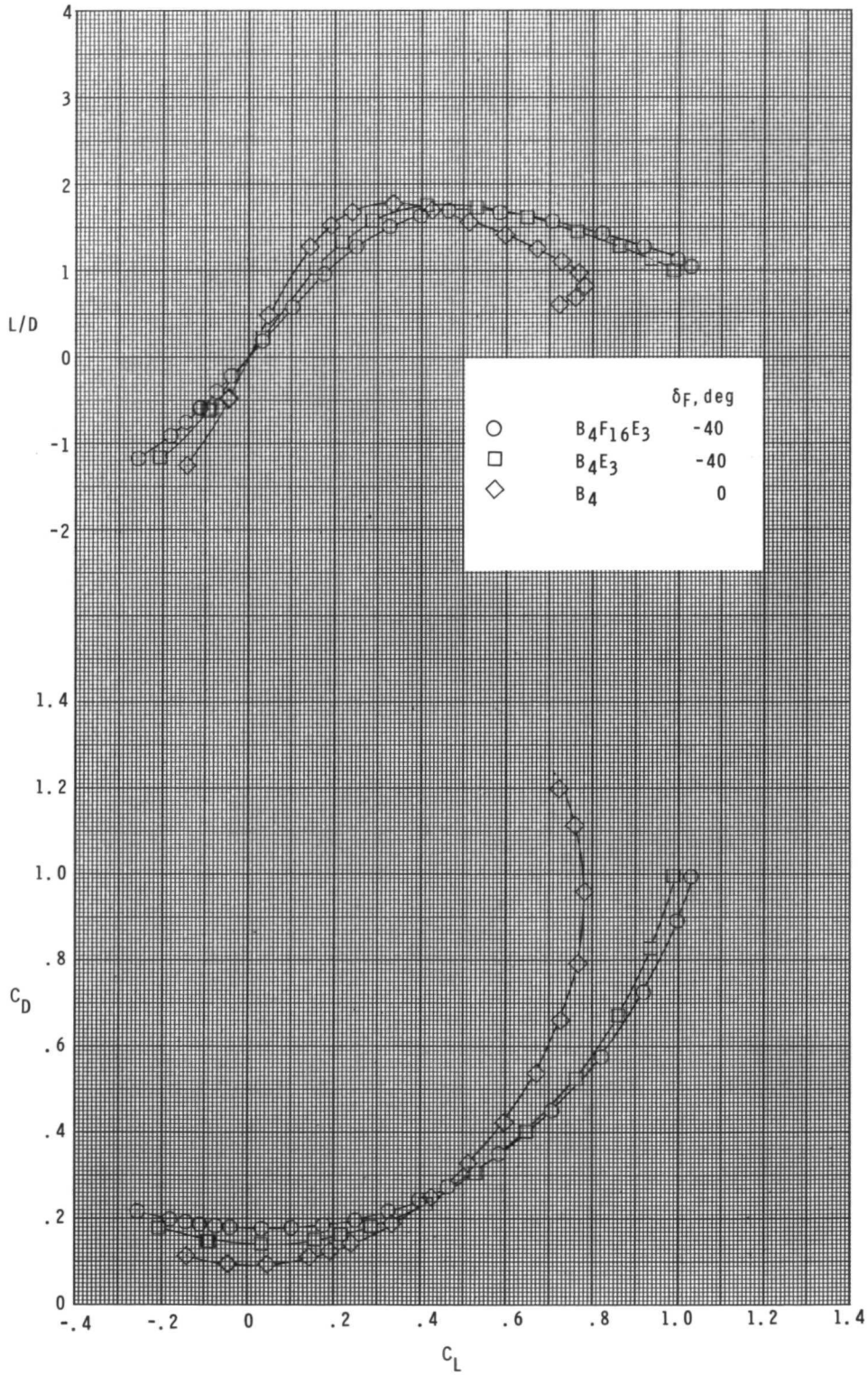

(a) Concluded.

Figure 12.- Continued.

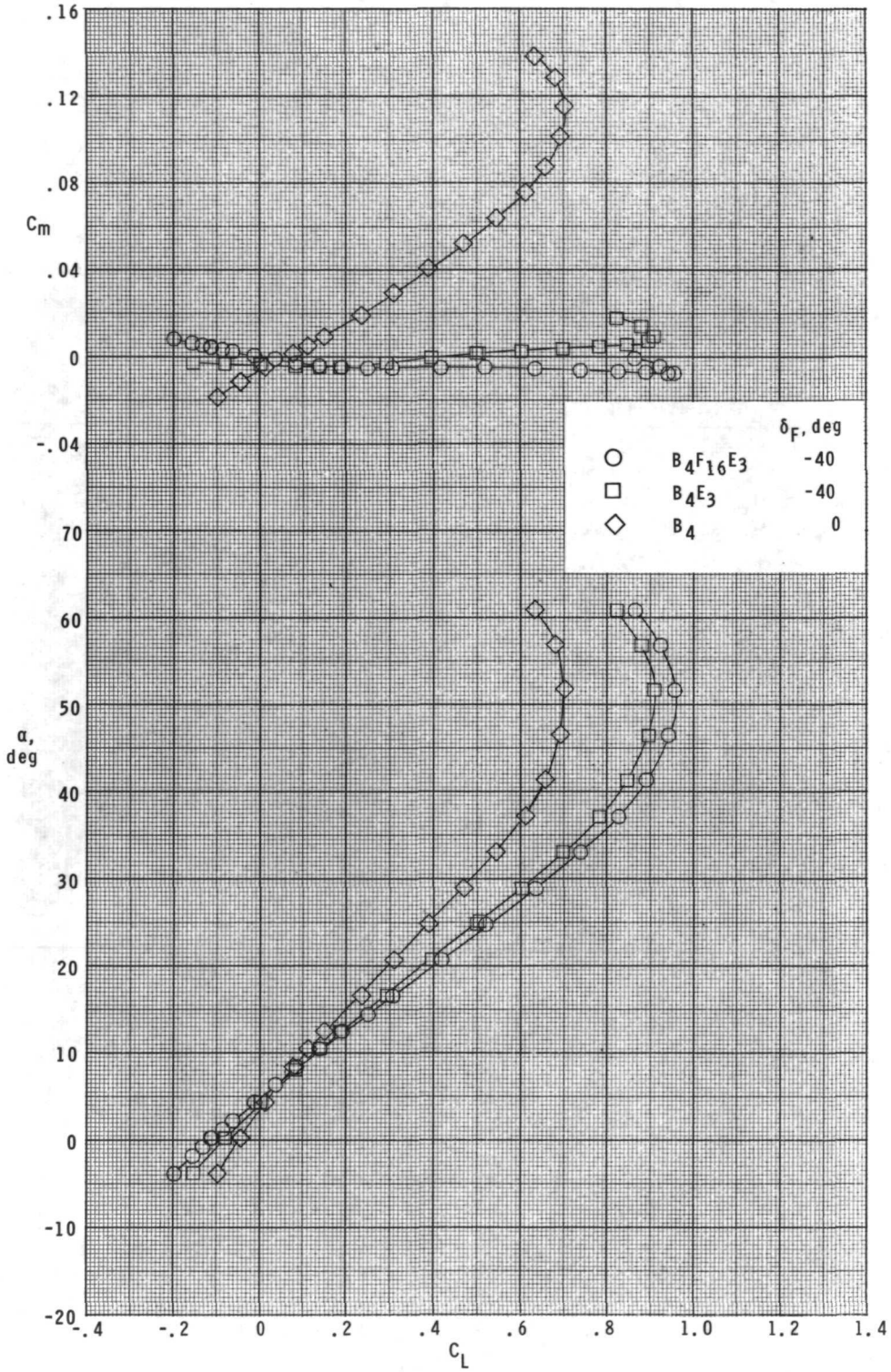

(b) M = 4.60.

Figure 12.- Continued.

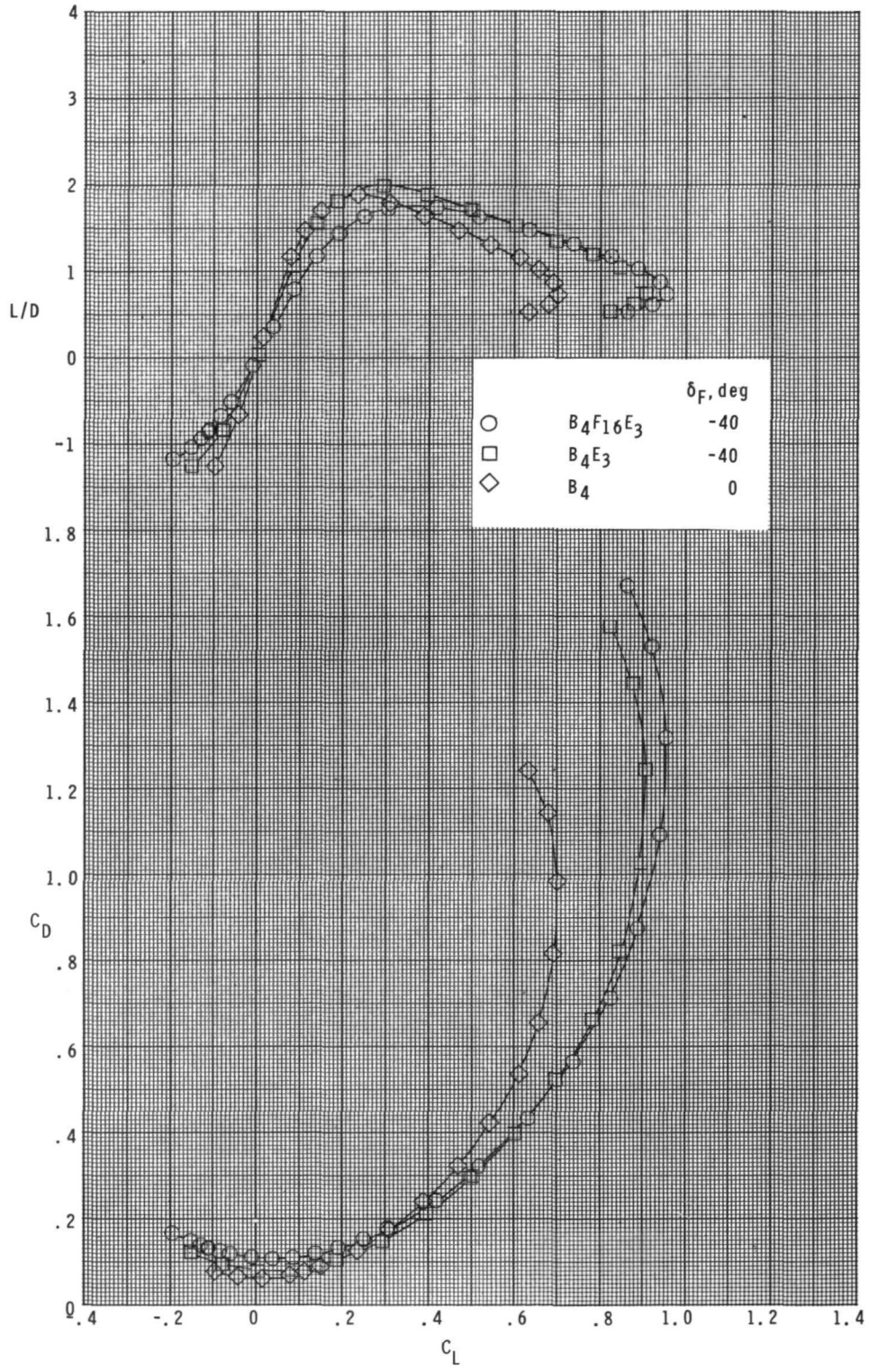

(b) Concluded.

Figure 12.- Concluded.

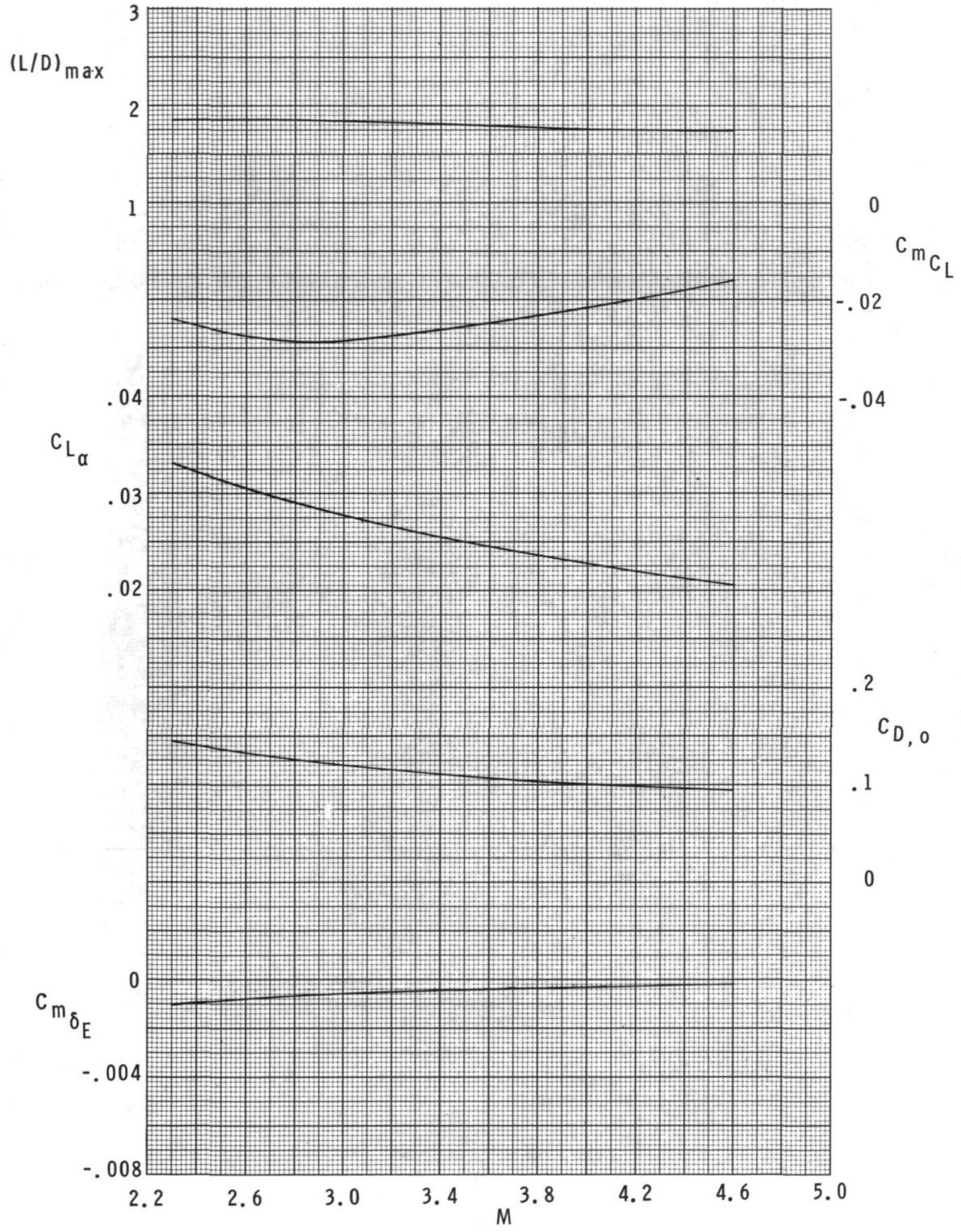

Figure 13.- Summary of longitudinal aerodynamic characteristics. $\delta_E = 0^o$; $\delta_F = -20^o$; $\delta_{R,L} = -20^o$; $\delta_{R,R} = +20^o$.

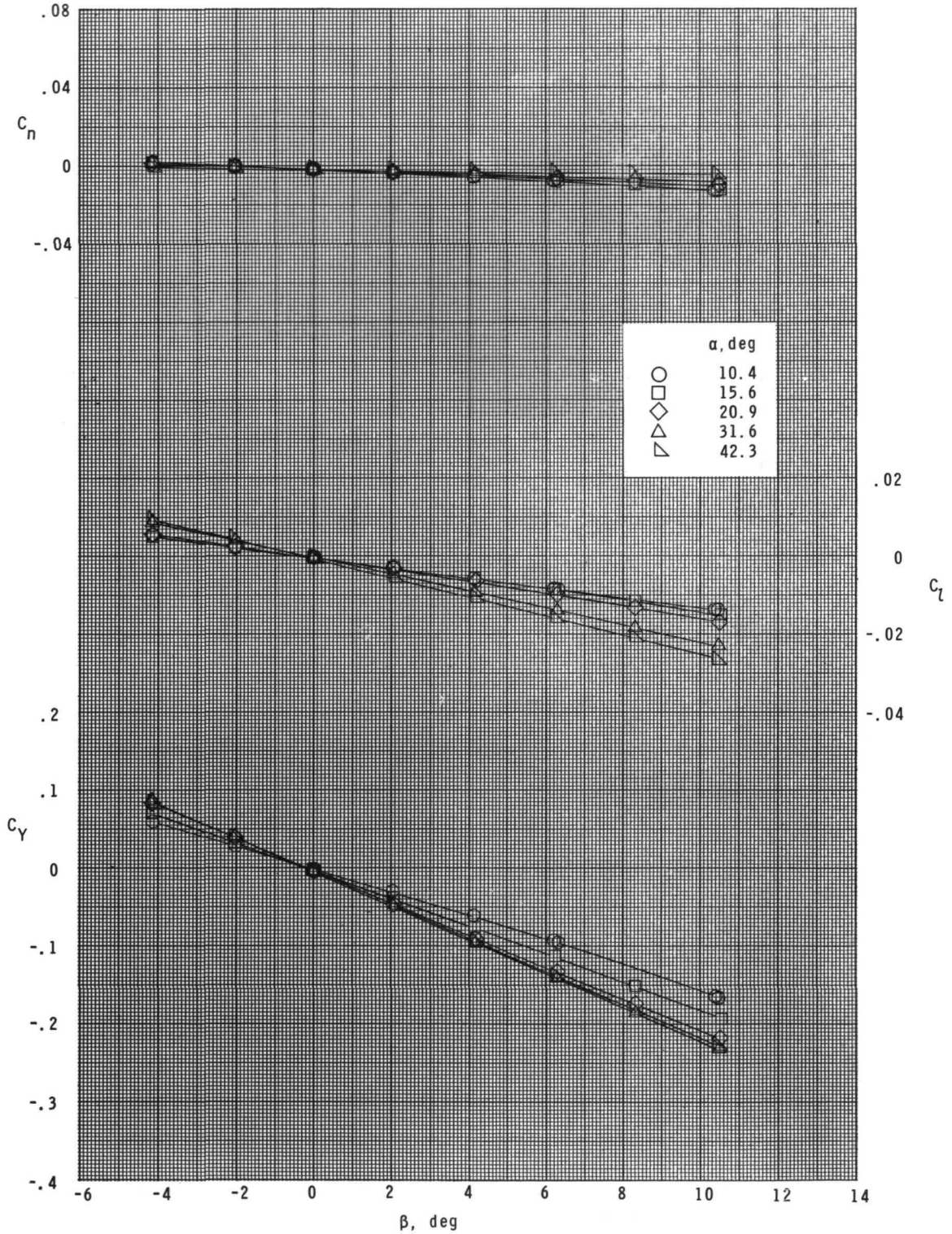

(a) M = 2.30.

Figure 14.- Lateral characteristics in sideslip. $\delta_E = 0^o$; $\delta_F = -20^o$; $\delta_{R,L} = -20^o$; $\delta_{R,R} = +20^o$.

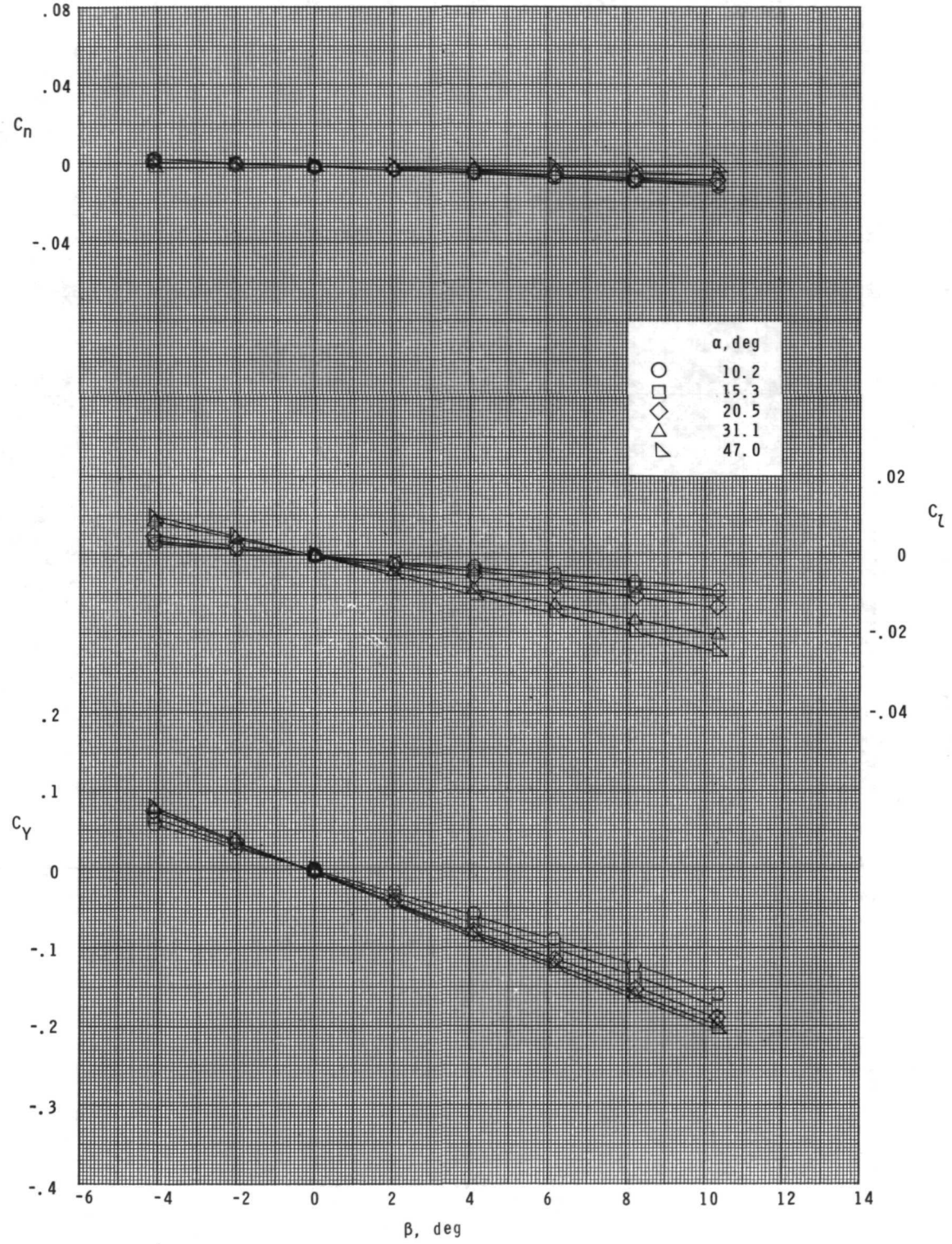

(b) M = 2.96.

Figure 14.- Continued.

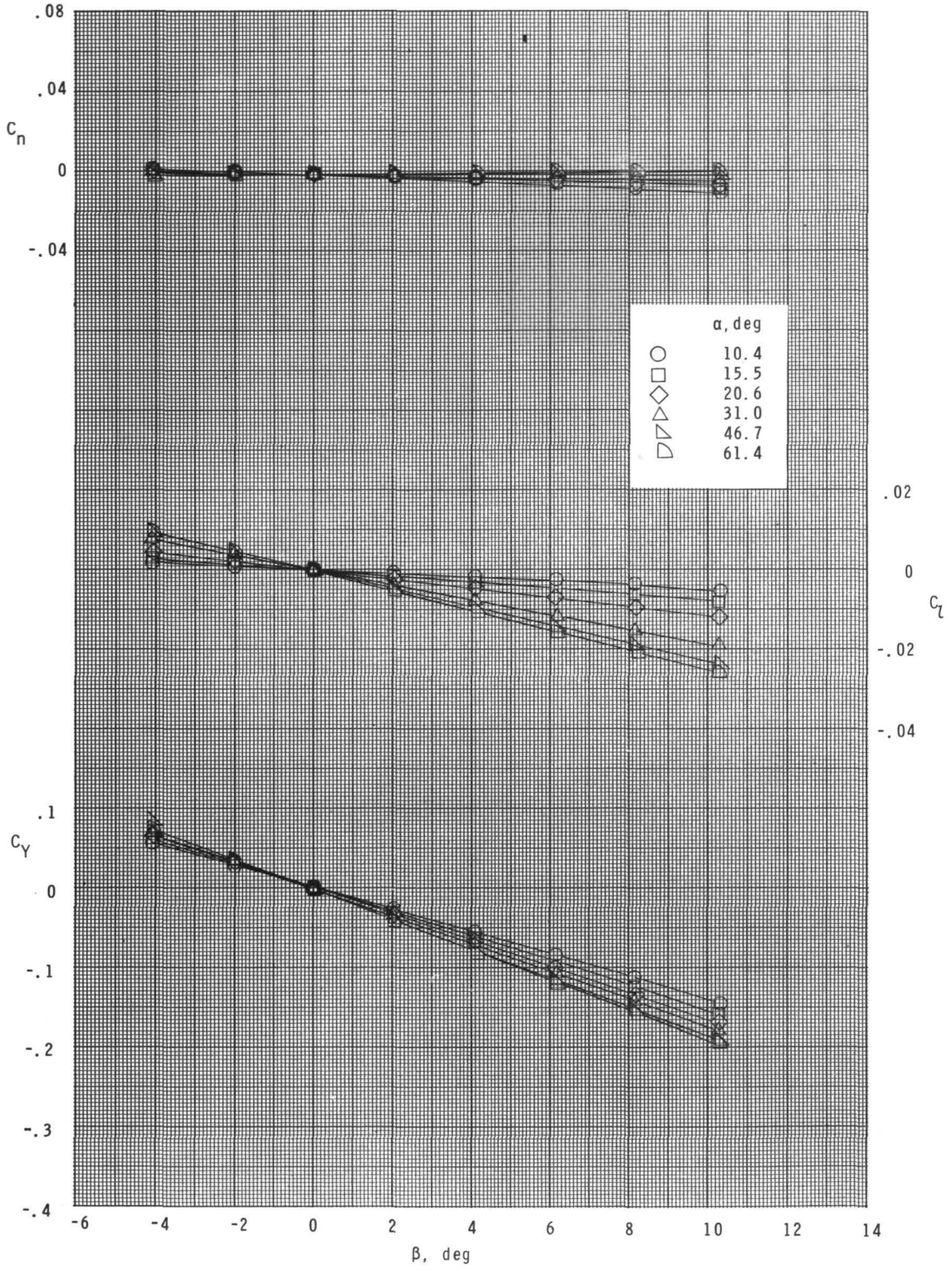

(c) M = 3.95.

Figure 14.- Continued.

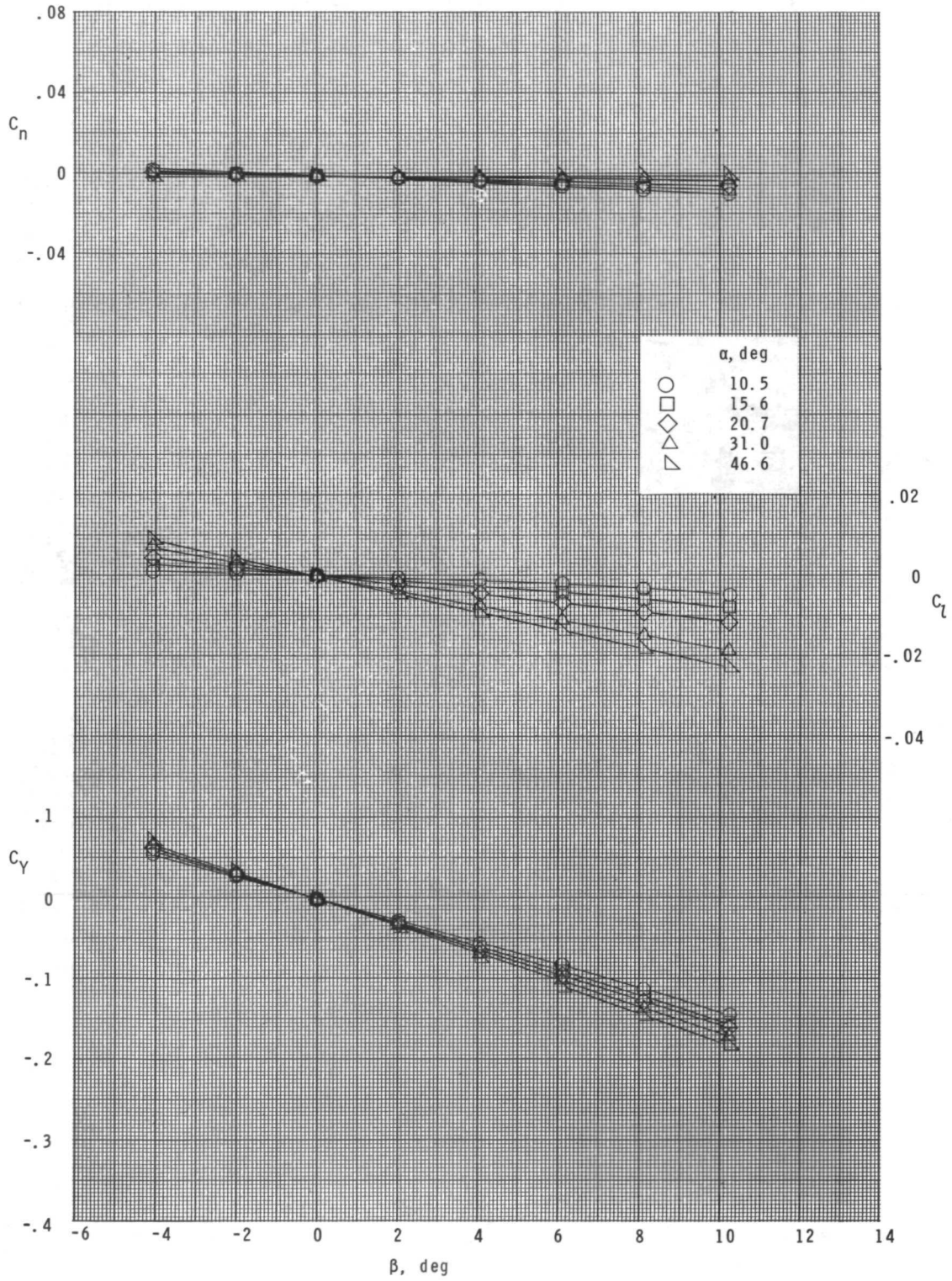

(d) M = 4.60.

Figure 14.- Concluded.

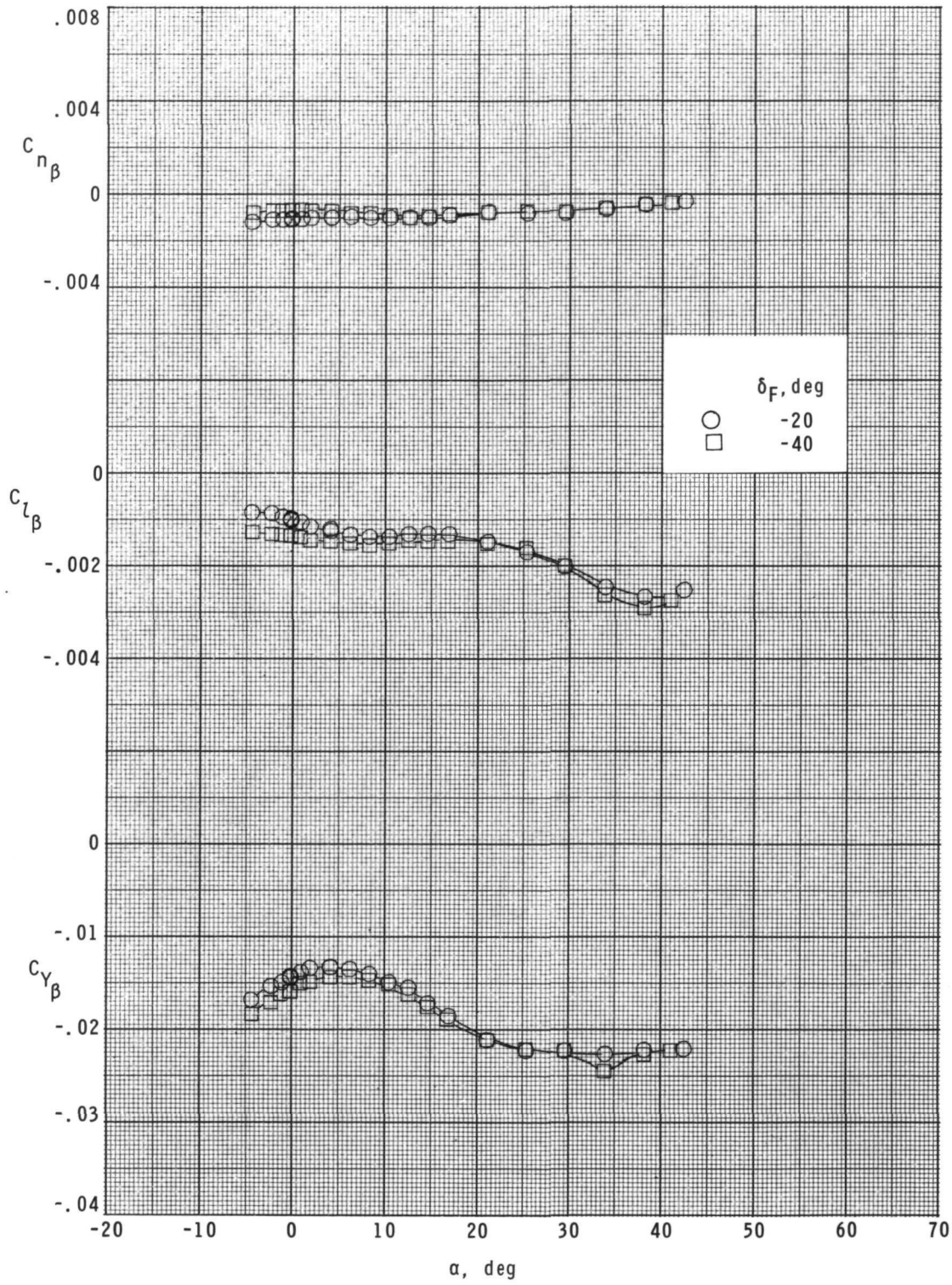

(a) M = 2.30.

Figure 15.- Effect of upper flap deflection on lateral parameters. $\delta_E = 0^o$; $\delta_{R,L} = -20^o$; $\delta_{R,R} = +20^o$.

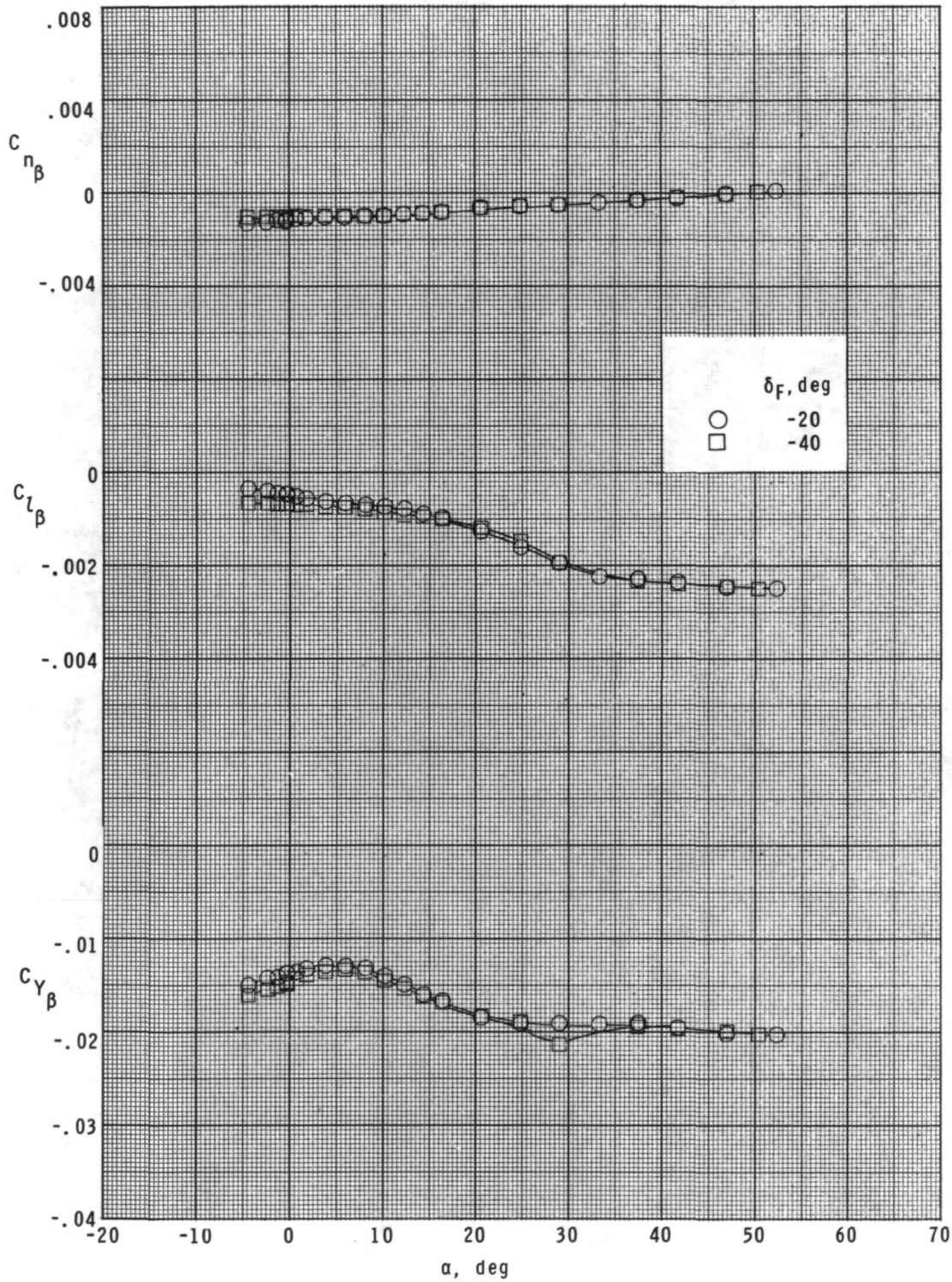

(b) M = 2.96.

Figure 15.- Continued.

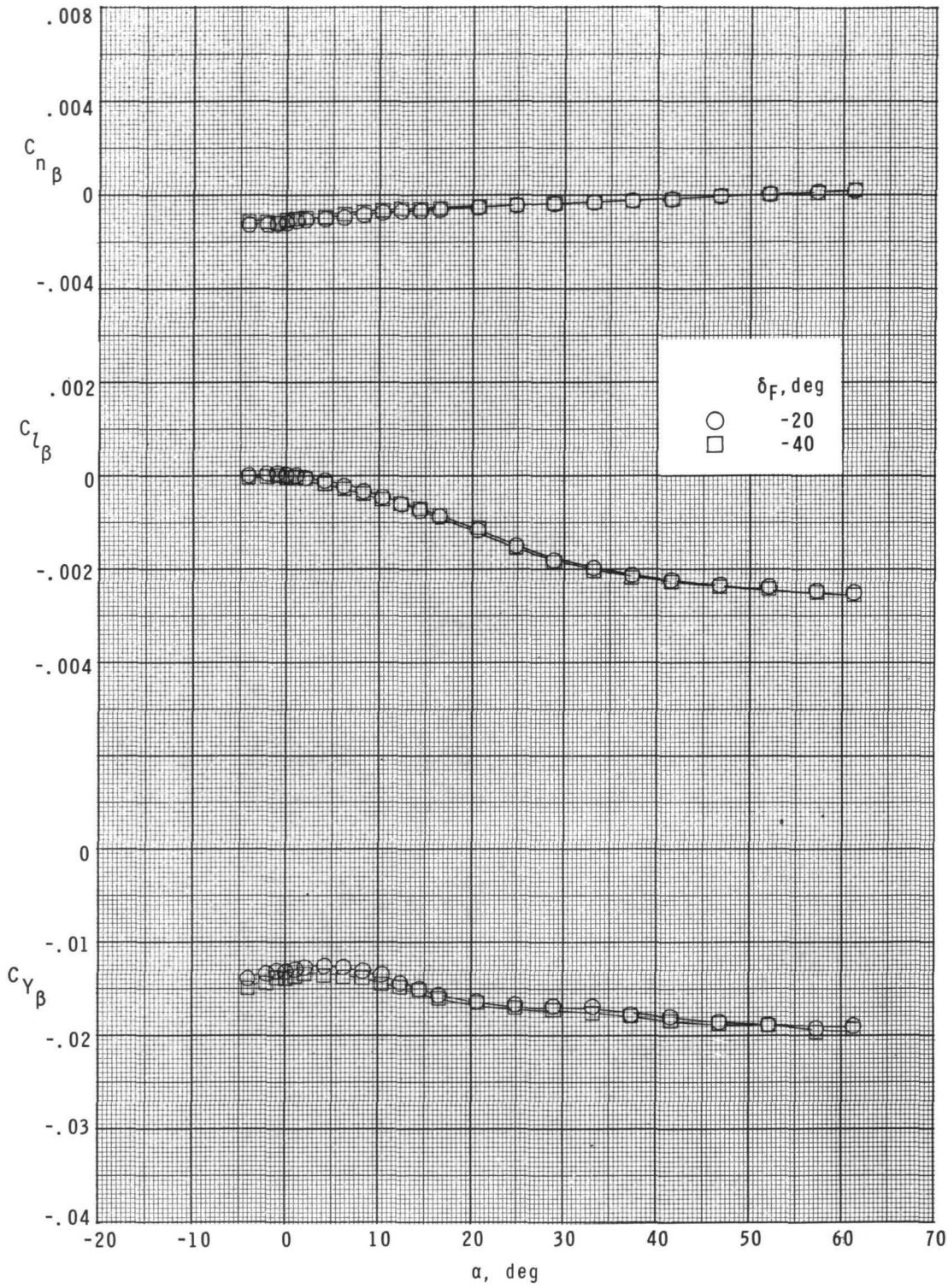

(c) M = 3.95.

Figure 15.- Continued.

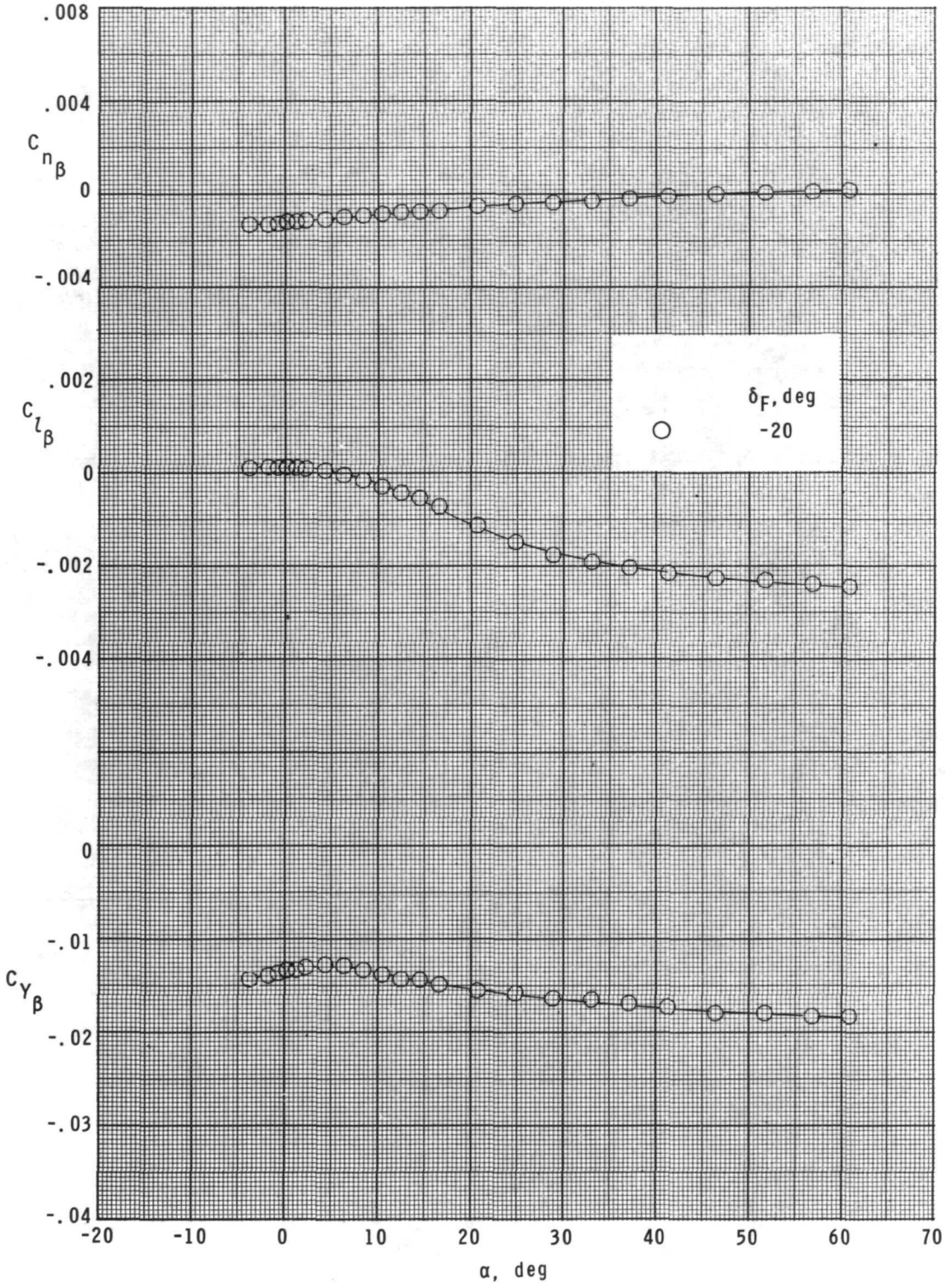

(d) M = 4.60.

Figure 15.- Concluded.

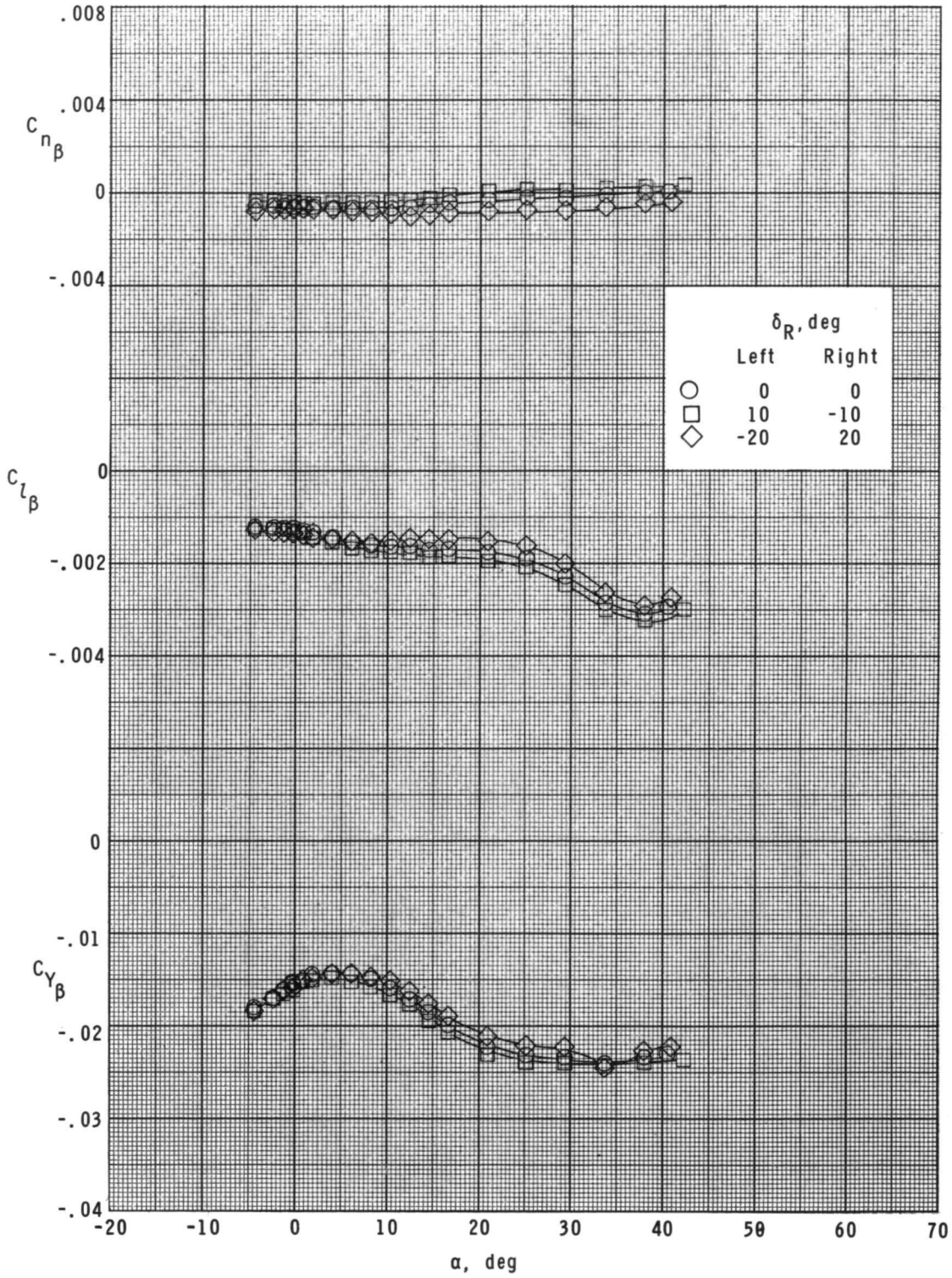

(a) M = 2.30.

Figure 16.- Effect of differential rudder deflections on lateral parameters. $\delta_E = 0^o$; $\delta_F = -40^o$.

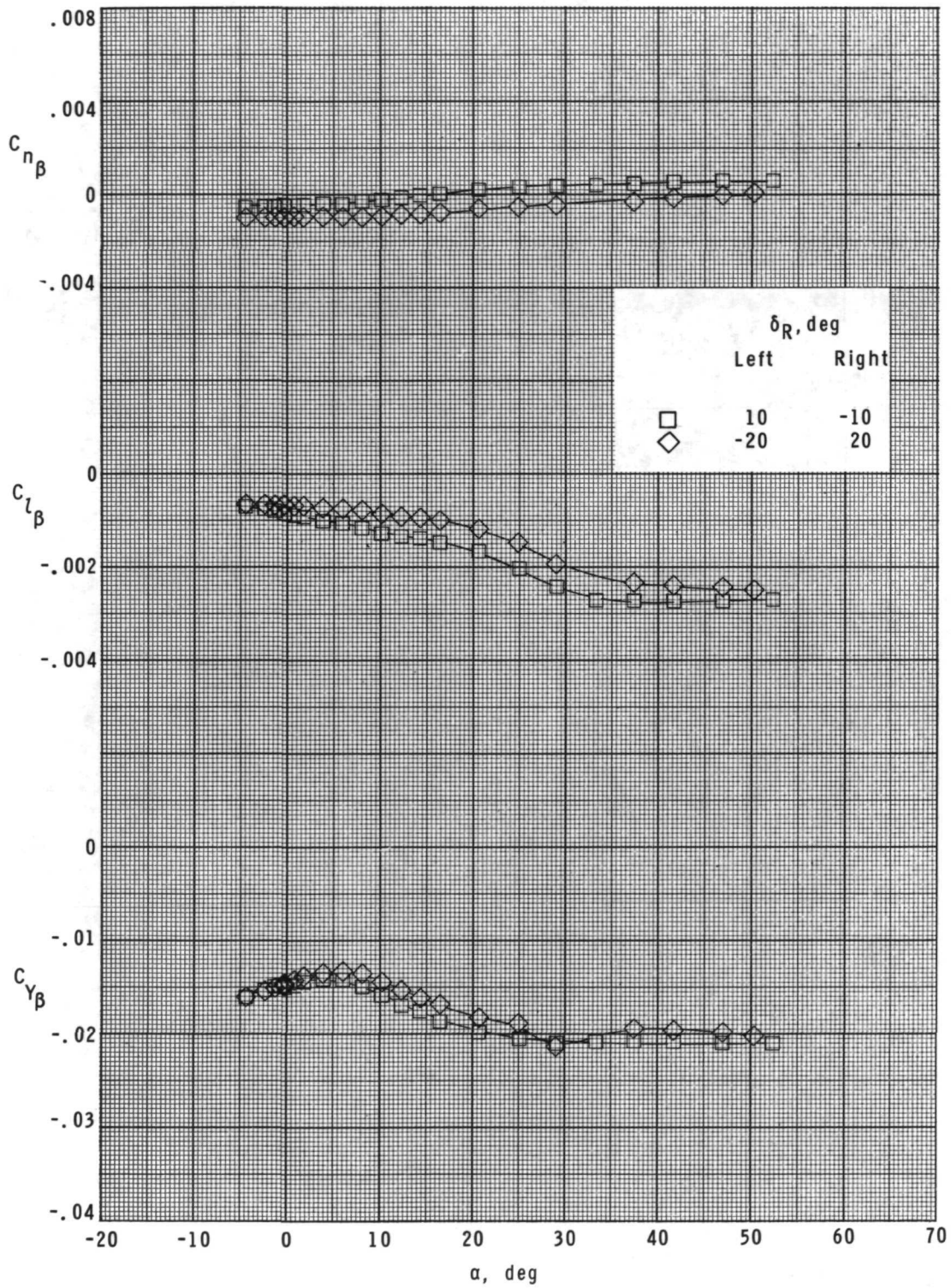

(b) M = 2.96.

Figure 16.- Continued.

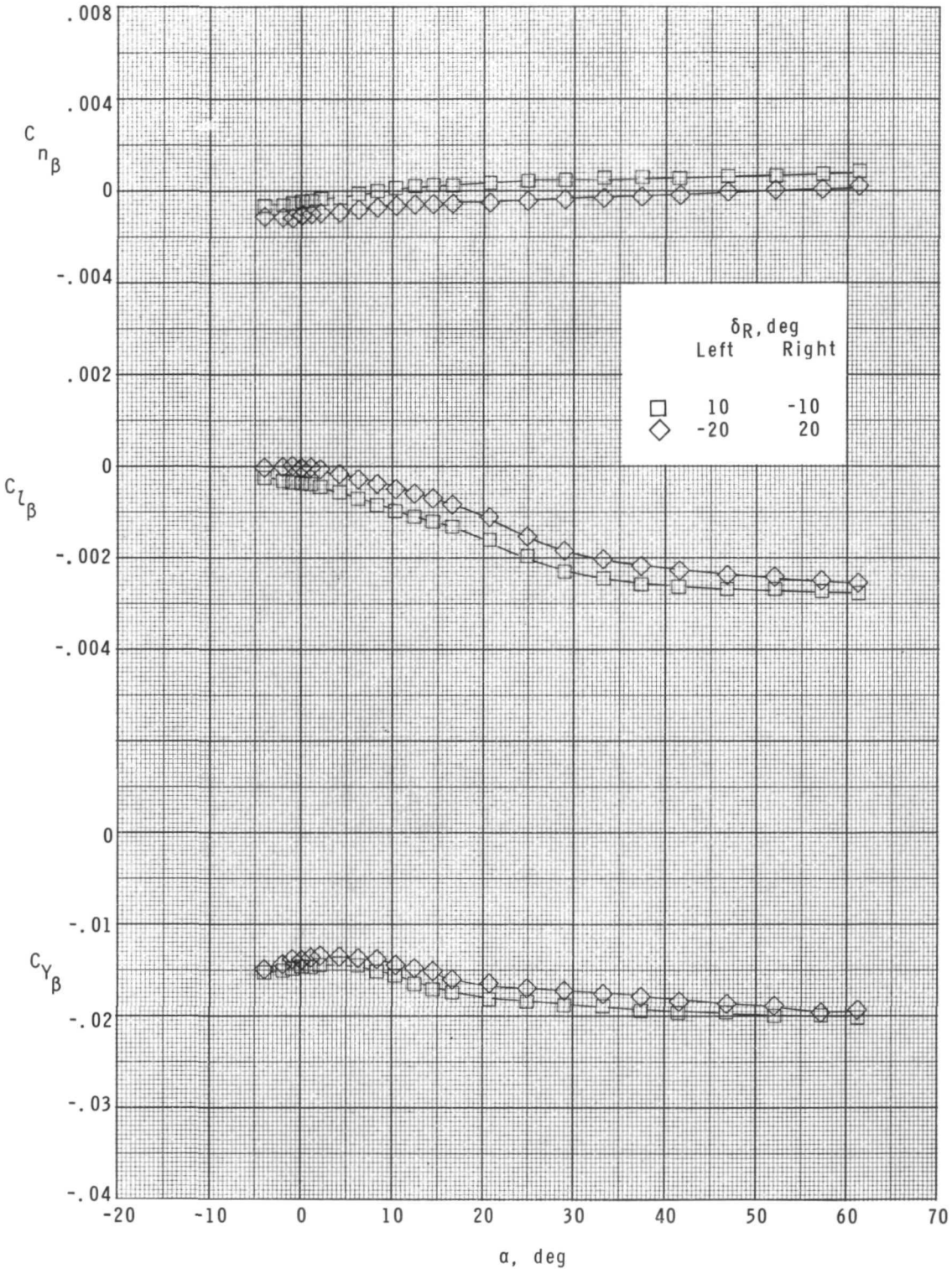

(c) M = 3.95.

Figure 16.- Continued.

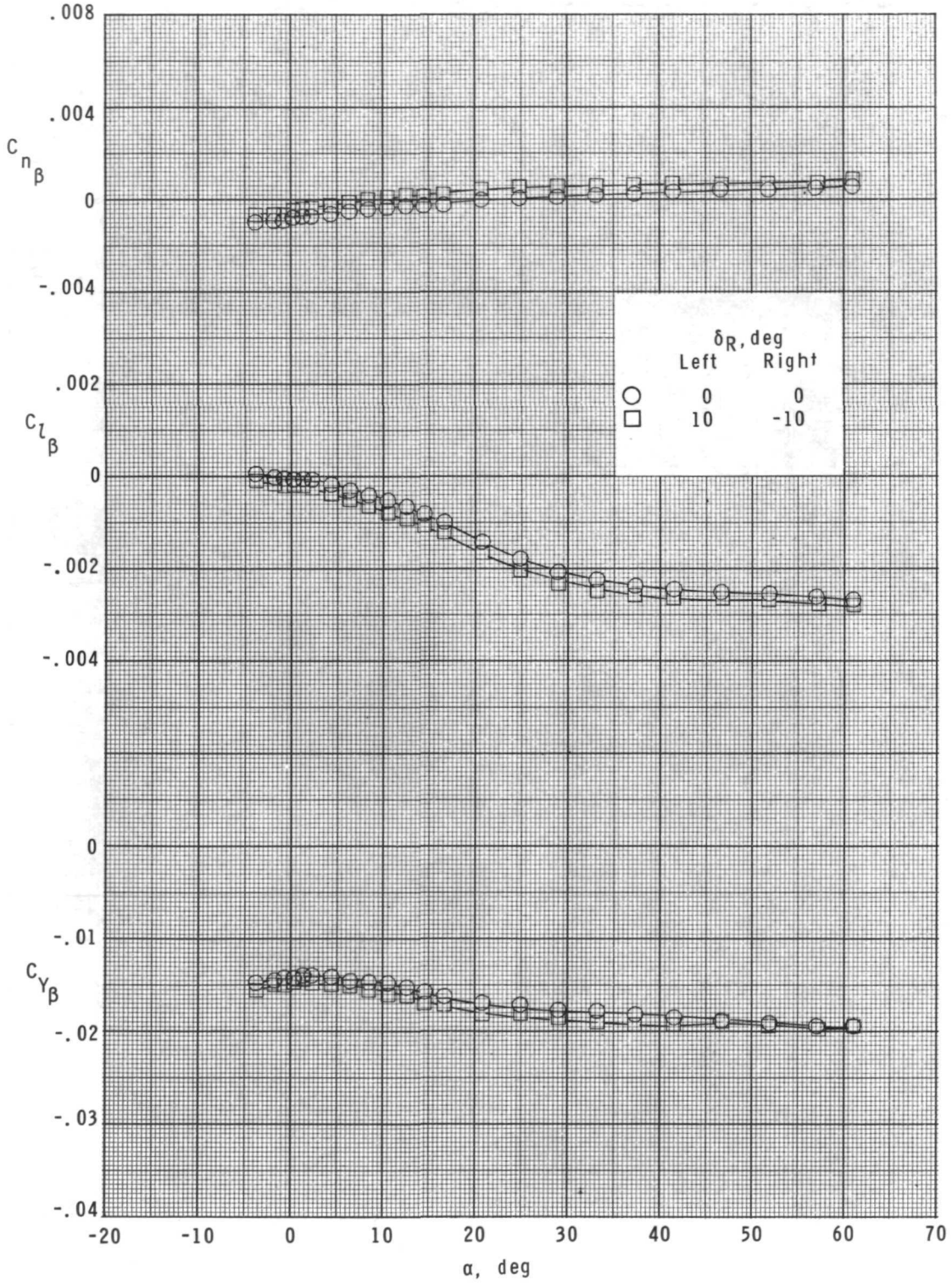

(d) M = 4.60.

Figure 16.- Concluded.

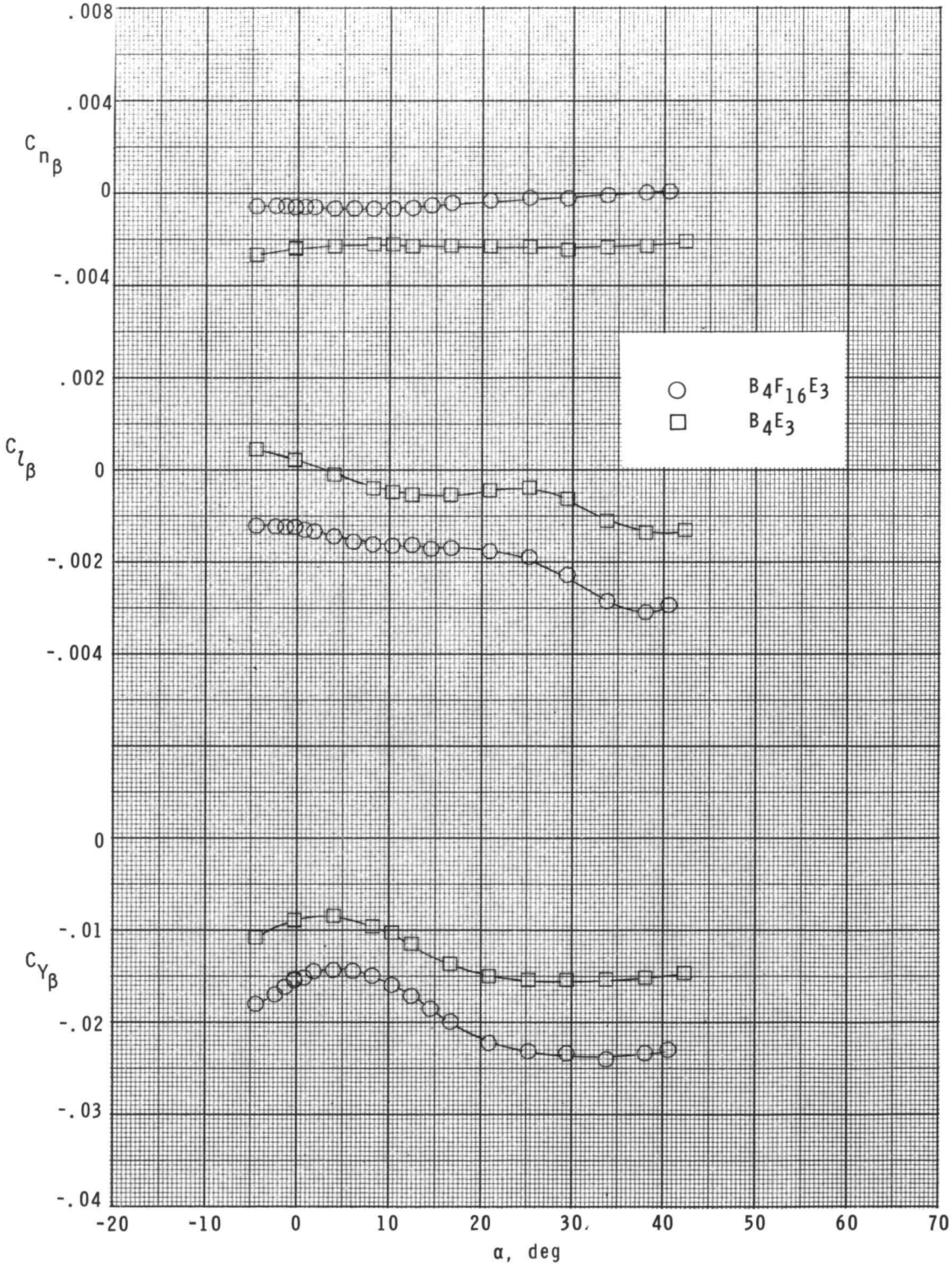

(a) M = 2.30.

Figure 17.- Effect of fins on lateral parameters. $\delta_E = 0^o$; $\delta_F = -40^o$; $\delta_{R,L} = 0^o$; $\delta_{R,R} = 0^o$.

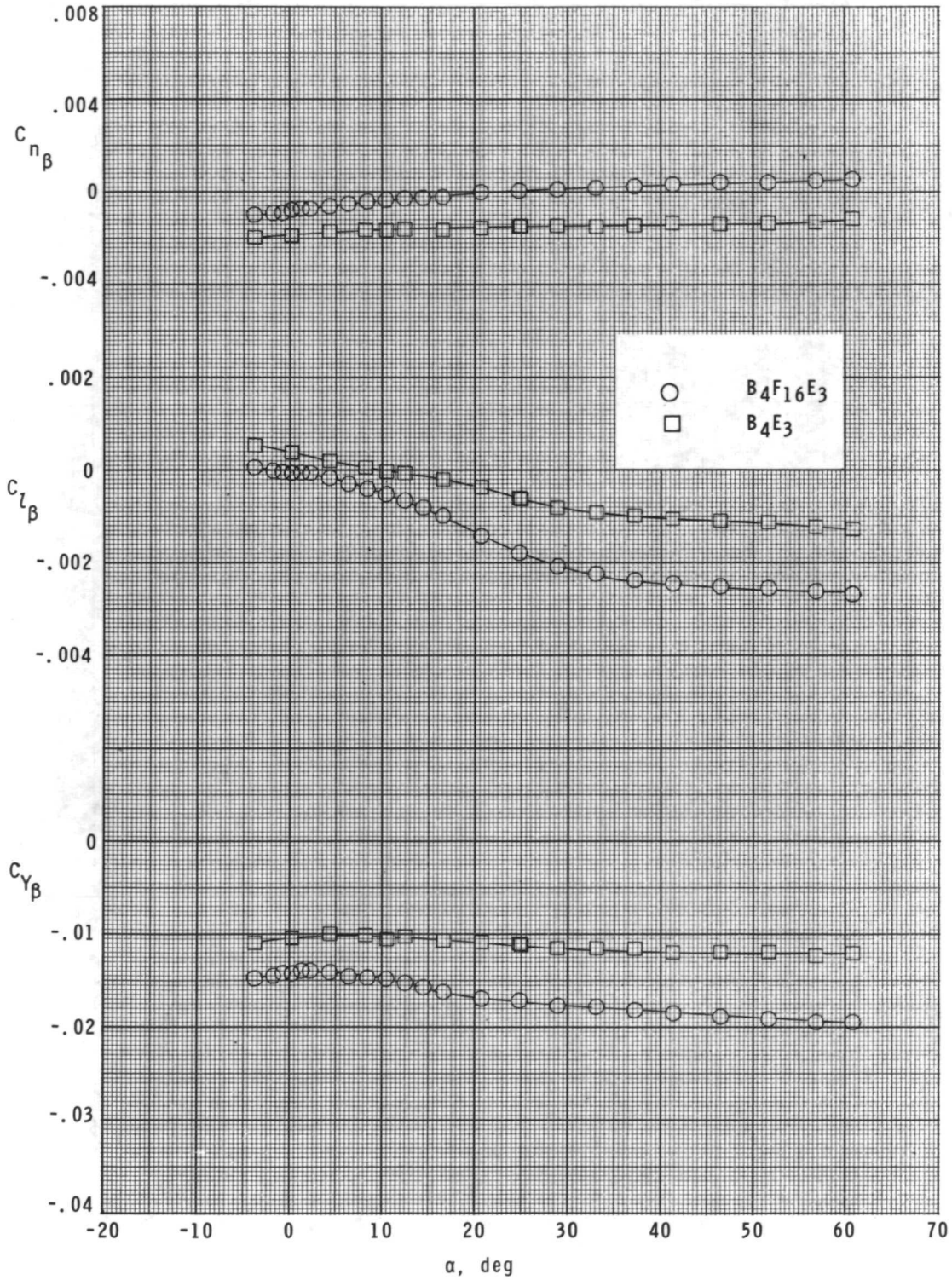

(b) M = 4.60.

Figure 17.- Concluded.

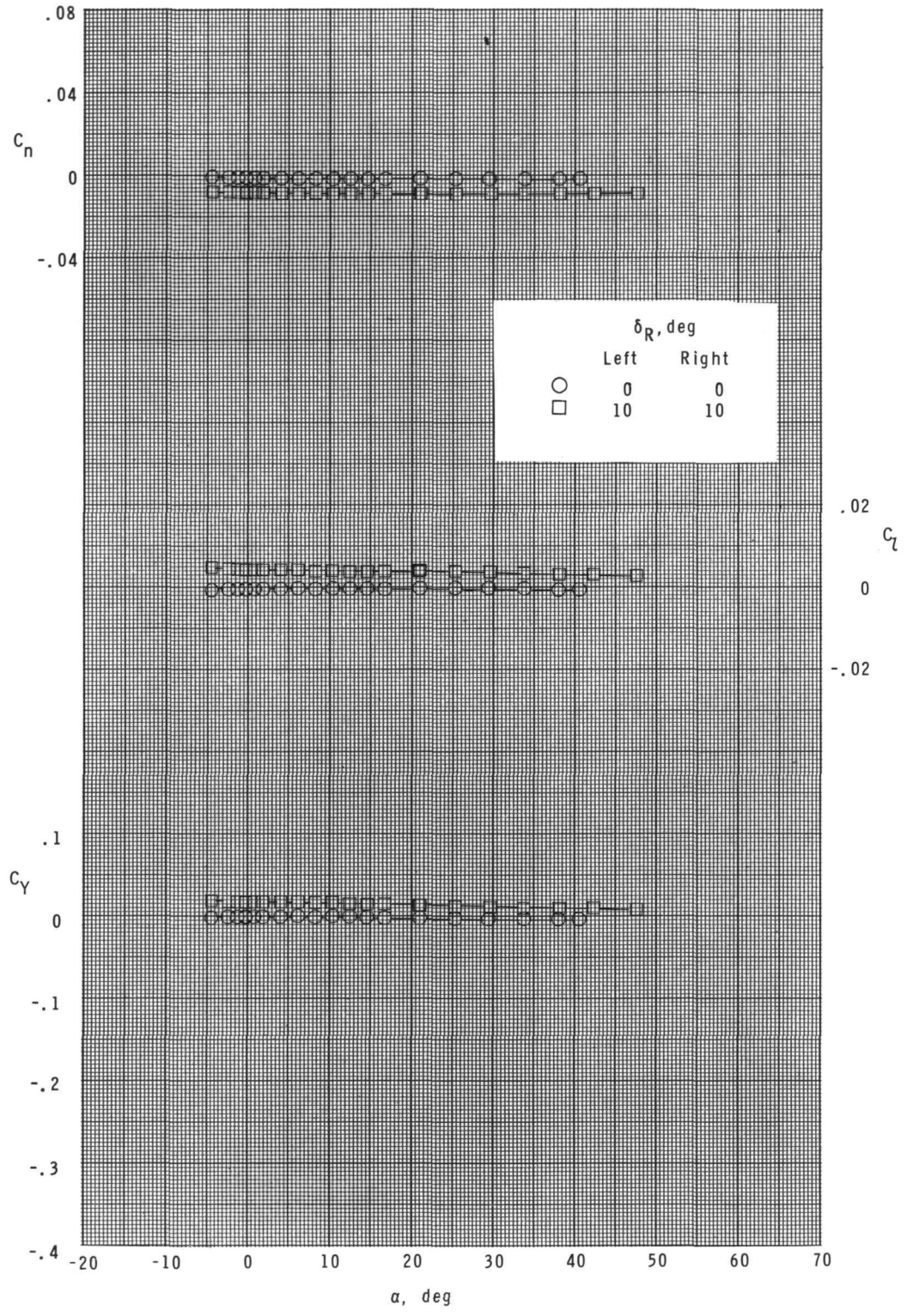

(a) M = 2.30.

Figure 18.- Effect of rudder deflection on lateral characteristics. $\delta_E = 0^o$; $\delta_F = -40^o$.

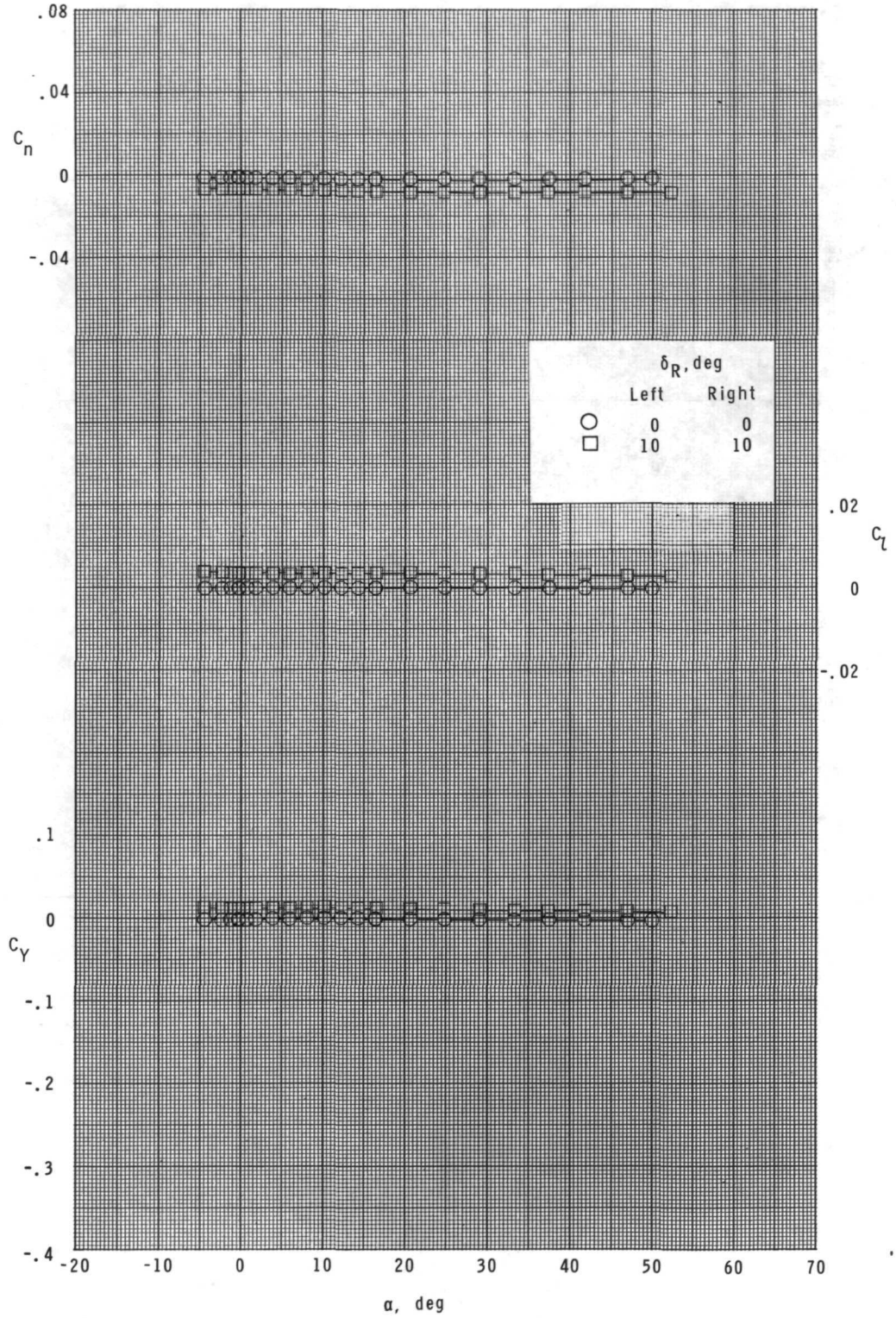

(b) M = 2.96.

Figure 18.- Continued.

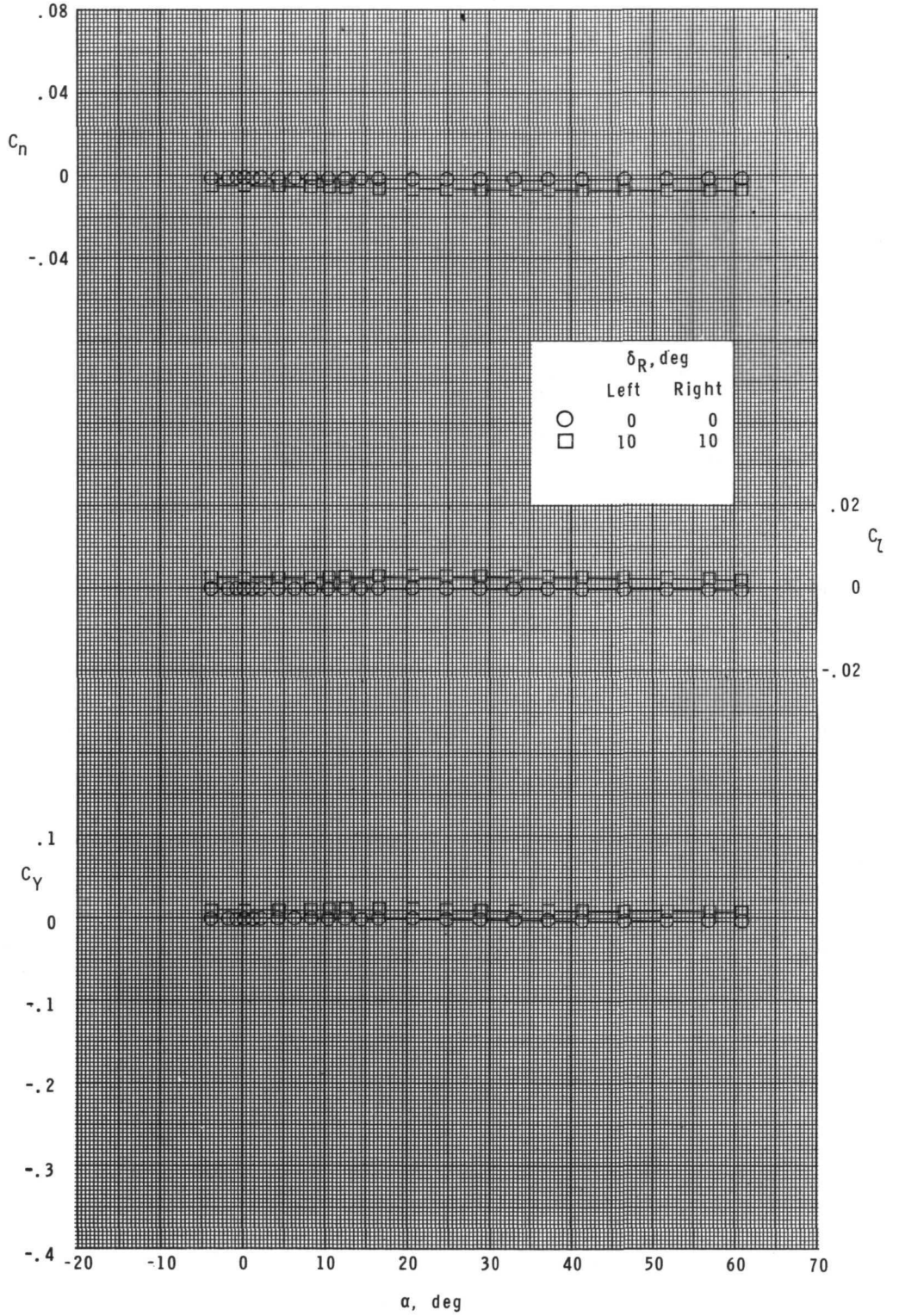

(c) M = 4.60.

Figure 18.- Concluded.

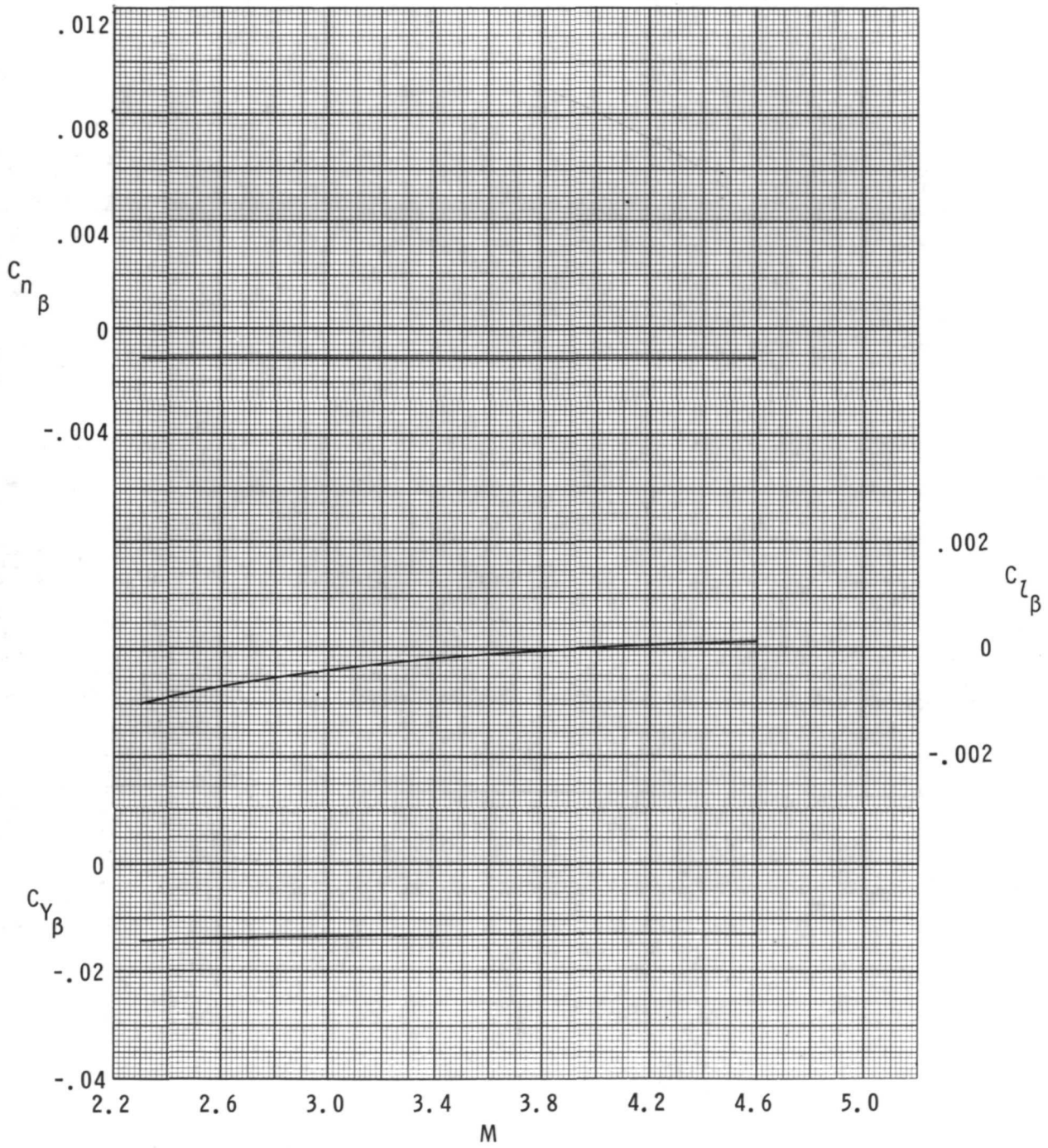

Figure 19.- Summary of lateral and directional stability parameters. $\delta_E = 0^o$; $\delta_F = -20^o$; $\delta_{R,L} = -20^o$; $\delta_{R,R} = +20^o$; $\alpha = 0^o$.

"The aeronautical and space activities of the United States shall be conducted so as to contribute . . . to the expansion of human knowledge of phenomena in the atmosphere and space. The Administration shall provide for the widest practicable and appropriate dissemination of information concerning its activities and the results thereof."

—NATIONAL AERONAUTICS AND SPACE ACT OF 1958

NASA SCIENTIFIC AND TECHNICAL PUBLICATIONS

TECHNICAL REPORTS: Scientific and technical information considered important, complete, and a lasting contribution to existing knowledge.

TECHNICAL NOTES: Information less broad in scope but nevertheless of importance as a contribution to existing knowledge.

TECHNICAL MEMORANDUMS: Information receiving limited distribution because of preliminary data, security classification, or other reasons.

CONTRACTOR REPORTS: Scientific and technical information generated under a NASA contract or grant and considered an important contribution to existing knowledge.

TECHNICAL TRANSLATIONS: Information published in a foreign language considered to merit NASA distribution in English.

SPECIAL PUBLICATIONS: Information derived from or of value to NASA activities. Publications include conference proceedings, monographs, data compilations, handbooks, sourcebooks, and special bibliographies.

TECHNOLOGY UTILIZATION PUBLICATIONS: Information on technology used by NASA that may be of particular interest in commercial and other non-aerospace applications. Publications include Tech Briefs, Technology Utilization Reports and Technology Surveys.

Details on the availability of these publications may be obtained from:

SCIENTIFIC AND TECHNICAL INFORMATION OFFICE

NATIONAL AERONAUTICS AND SPACE ADMINISTRATION

Washington, D.C. 20546